Scaled Model Wind Turbine with Active Flow Control (AFC) Technology

Team#3679

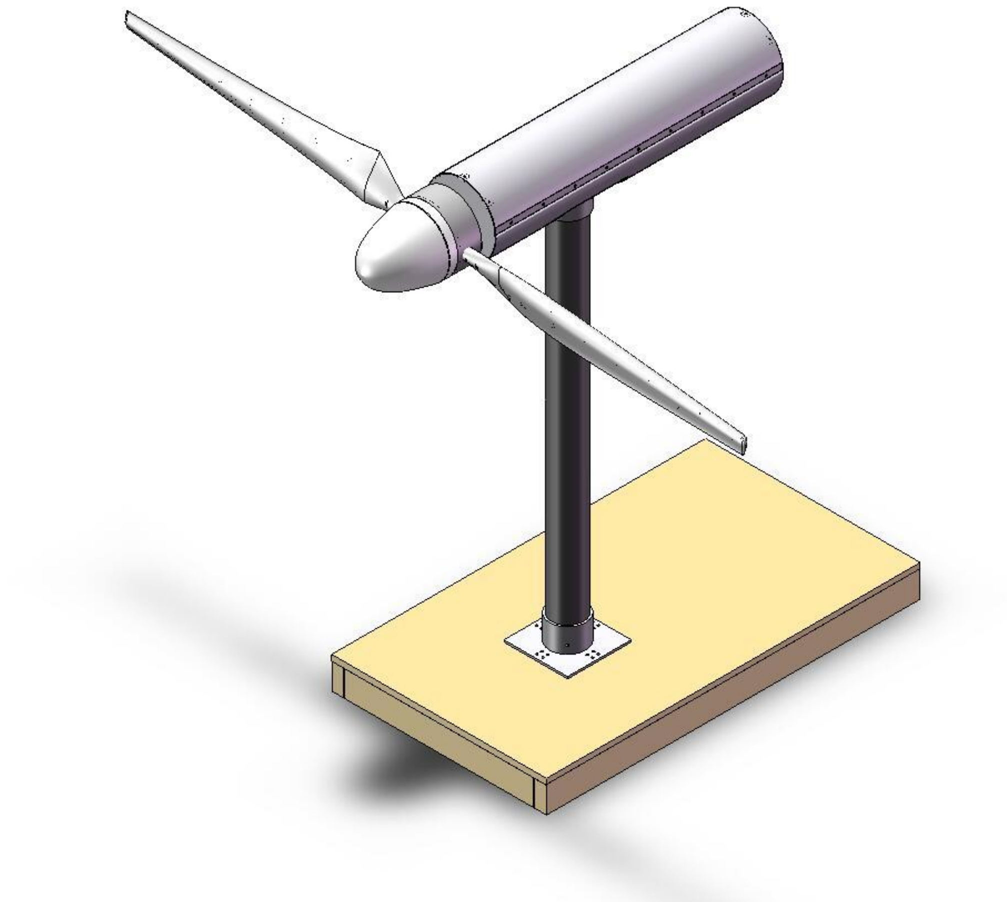

Final Report

4-29-2009

Faisal Al-Mahmoud
Khalid Mustafawi
Cory Pearman
Nathan Welborne

Abstract

The Scale Model Wind Turbine with Active Flow Control technology project aims to improve the performance of wind turbines with the use of active flow control. Current wind turbines are designed for a nominal range of wind speeds; when they operate outside of this range, performance levels drop. Another design aspect of current wind turbines is that they will not start operating until a minimum wind speed is reached. With active flow control implemented into the blades of a prototype turbine, it is possible to interact with the flow over the blades to prevent airflow separation from the blades. This will allow the wind turbine to operate at a higher performance over a larger range of wind speeds and additionally start turning at lower wind speeds, thus creating more energy.

The project has two main objectives. The first objective was to build an extruded 2D airfoil model to be tested in the large, low-speed wind tunnel located at the Aerospace and Mechanical Engineering Department at the University of Arizona. This model was used to research the effects of active flow control on lift and drag. The best results were found at 5mph wind speeds, where a large increase in lift was found with active flow control engaged. For higher wind speeds, the effects of active flow control were marginal at best. It was determined that the best case for using active flow control in wind turbines was to improve the start up wind speed.

The second objective of the project was to build a working prototype wind turbine which incorporated active flow control in the blades. The final prototype is capable of turning the generator and producing power, which is measured from a wattmeter. Unfortunately, due to issues with the testing equipment and the aerodynamic effects of using large fans to create artificial wind, the wind tunnel results could not be verified on the prototype model. With some adjustments to the experimental set up it is believed that these results could be supported.

Table of Contents

List of Figures

List of Tables

I. Introduction

A. Mission Statement

Our mission is to design and build a scale model wind turbine that incorporates cutting-edge active flow control technology, in order to increase turbine efficiency and make wind energy a more viable solution to the world's energy needs.

B. Business Case

The problem with current wind turbine today is that they are designed and optimized for a specific range of wind speeds. While this means they are extremely efficient and high performing in this nominal range of wind speeds they perform poorly when operating in wind speeds beyond this nominal range. This is why a turbines location must be known before it is designed because it is optimized for that areas specific wind patterns. Furthermore, the start of wind speeds for some wind turbines are relatively large. Some won't even start turning until a 10mph wind speed is reached.

With active flow control (AFC) technology incorporated into wind turbines these issues can be addressed. AFC can increase the nominal range of wind speeds the wind turbine can perform in. It will also decrease the minimum required wind speed to start turning the wind turbine. One additional benefit is the possible elimination of the mechanical pitch control mechanisms currently used in some wind turbines to address these issues. AFC can be changed and custom tailored to specific wind speeds a lot faster than the pitch control mechanisms.

C. Description of Active Flow Control Technology

Active flow control is a method to influence and control the behavior of the boundary layer flow over a surface. It is a time-dependent (typically periodic) disturbance introduced into the boundary layer that affects the flows behavior. For a wind turbine active flow control will be used to delay the flow separation from the wind turbine blades. Figure 1 shows wind streamlines over an airfoil in a wind tunnel experiment. In this experiment active flow control is running in the airfoil and it is easy to see that the streamlines stay attached to the airfoil for almost the entire chord length. In Figure 1 airfoil is held at the same angle of attack and the wind speed is unchanged. The active flow control is disengaged for this experiment and it is clear that the streamlines separate from the airfoil very close to the leading edge. This separation reduces the effectiveness of the airfoil severely reducing its generated lift and greatly increasing the drag.

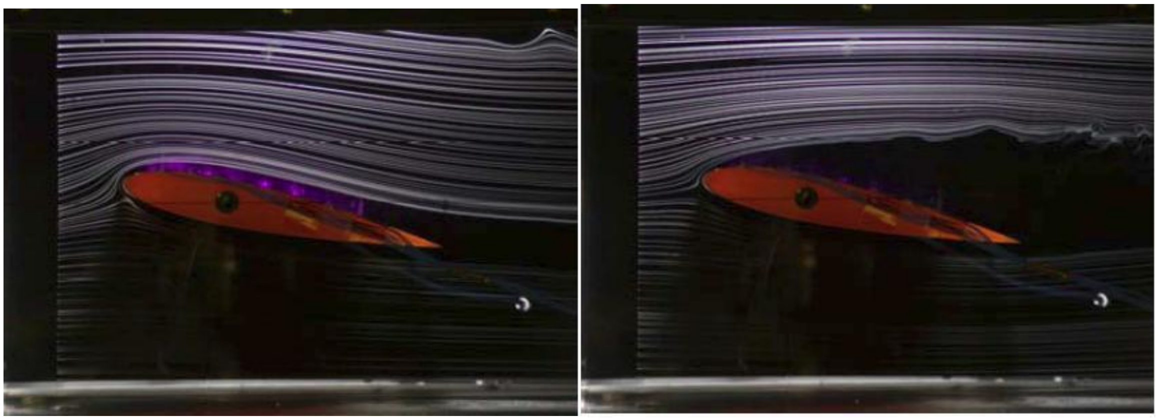

Figure 1 – Airfoil and Streamlines with AFC ON (Left) and AFC OFF (Right)

In regards to a wind turbine the separation of the wind streamlines from the airfoil means the turbine performance will be severely degraded. This separation happens when the blades are at too large of an angle of attack in reference to the wind direction or when the wind speeds are at an incorrect speed for the air flow to stay attached to the airfoil.

With active flow control implemented into the wind turbine blades the air flow can be made to stay attached to the airfoil longer over a wide range of angles and wind speeds. This has the effect of increasing the wind turbines performance for operation in wind speeds beyond its designed nominal wind speeds. It has the added benefit of making the airfoil more effective in lower wind speeds meaning that the wind turbine can start working in a lower wind speed than without active flow control.

One other note to consider is that in current wind turbines the method to address these aerodynamic performance issues is to rotate the turbine blades using a large mechanical pitch control mechanism. These have the effect of rotating the blades which increases or decreases the angle of attack of the airfoils in reference to the wind. With active flow control a similar affect can be accomplished at a faster rate. Active flow control has the ability to change quickly to be optimized for a certain wind speed while the mechanical pitch control can take a while to change the pitch of the blades.

D. Customer Needs

The customer of this project has requested that a wind turbine be constructed that has active flow control incorporated into the blades. When the active flow control is running the wind turbine should show increased performance than when active flow control is not running. Additionally the active flow control effects must be verified in a wind tunnel test by using a 2D airfoil section of the airfoil used in the wind turbine blade with active flow control incorporated into them. The wind turbine needs to be a representative of a viable solution for the large multi- Megawatt size wind turbine so some dynamic and aerodynamic properties must be scalable.

E. Voice of Customer

Constraints	
1	Active Flow Control (AFC) power must come from the electric generator run by the wind turbine
2	Funding limit of $8000
3	Blade design must be a pre-existing design
4	Generator must be COTS (Commercial Off-The-Shelf)
5	Wind Tunnel Model must fit inside Wind Tunnel

Scaling	
1	Wind Turbine Blades are geometrically scaled
2	Wind turbine power and rotation speed are dynamically scaled

Wind Tunnel Model	
1	Single 2D airfoil profile section of the blade
2	Has to incorporate AFC
3	Must be first model built
4	Must be completed and tested successfully in order to progress to the Demo Model construction
5	Wind tunnel tests will measure Lift and Drag at various angles and wind speeds

Demo Model	
1	Has to be portable (fit through doors, reasonable set up time, can fit in standard classroom)
2	No dynamic variable blade pitch, but must be capable of changing blade pitch statically
3	Has to incorporate AFC
4	Efficiency increases when AFC is used
5	AFC must be able to be turned on and off
6	Power generated must be measured and displayed
7	Conduct tests at various wind speeds and blade pitches

Table 1 – Voice of Customer

II. Functional Requirements and Constraints

System Constraints			
Constraint	**Description**		
AFC power source	Active Flow Control (AFC) power must come from the electric generator run by the wind turbine		
Blade Design	Must be geometrically scaled commercial pre-existing design		
Generator	Must be COTS		
Turbine Power	Must be dynamically scaled from the full size wind turbine		
Rotation Speed	Must be dynamically scaled from the full size wind turbine		
Measurable Constraints			
Constraint	**CTQ**	**Target Value**	
Total Project Cost	USD	<= $8000	
Constraint	**CTQ**	**Target Value**	
Wind Tunnel Model Envelope	Meters	<= 1x1.75	
2D Airfoil Profile	Yes/No	Yes	
Description	**Customer Importance**	**CTQ**	**Target Value**
Incorporates AFC	5	AFC present on blades	Yes
Constraint	**Units**	**Target Value**	
Disassembled part cross-sectional area	Meters	2.2x1	
Setup Time	Minutes	15	
Assembled model height	Meters	<2.5	
Blade Length	Meters	0.25 – 1.5	
Functional Requirements (Demo Model)			
Description	**Customer Importance**	**CTQ**	**Target Value**
Adjusts blade pitch statically	4	Angle of attack	0-180 deg.
Incorporates AFC	5	AFC present on blades	Yes
Gains efficiency when AFC is active	5	Percentage efficiency gain	>0%
Activates AFC on user command	5	User control of AFC function	Visual indication of status
Indicates power output visually	3	Output Indicated Visually	Power Output

Table 2 – System Constraints and Functional Requirement

III. Three Designs Considered

A. Plasma Actuator Active Flow Control

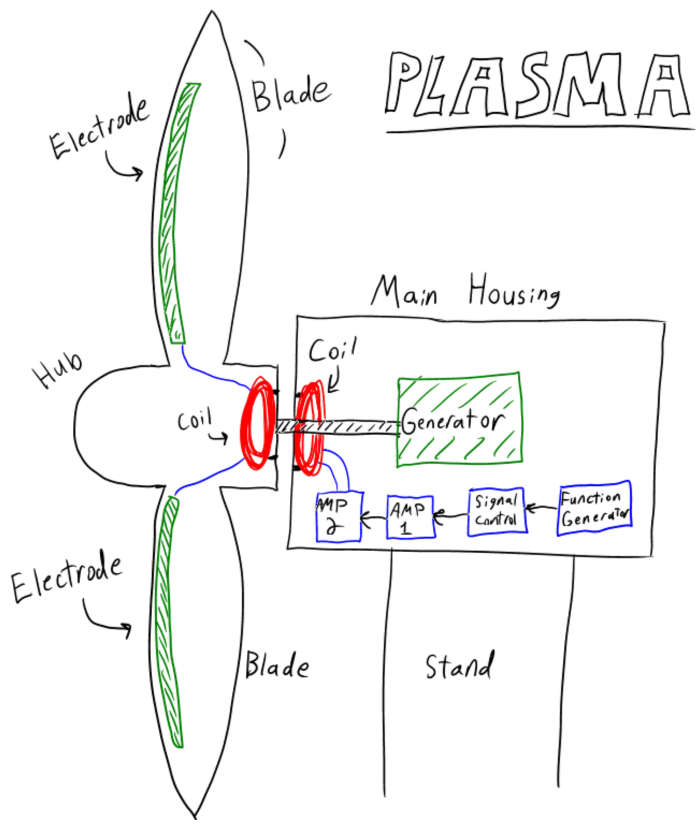

Figure 2 – Sketch of Plasma AFC Method

One possible active flow control method considered was using a plasma actuator which is pictured in Figure 2. The plasma actuator consists of two metal electrodes opposite in charges that are separated by a dielectric layer. A high voltage supply will produce voltage between 10-20 KV of alternating current (AC) voltages. The voltage is applied to both the upper electrode which is exposed to flow on the surface of the airfoil and lower electrode that is covered with the dielectric layer. The idea of the two oppositely charged electrodes is that the high voltage supplied will help in the rapidly acceleration of electrons and ions toward the lower electrode. Acceleration to the lower electrode will cause collision with air molecules that will cause the ionization of the air next to the upper electrode since the lower electrode is buried into the blade. This procedure will result in the ignition of plasma on the upper surface of the airfoil. The energy produced will add energy to the low momentum boundary layer that will cause the delay of the flow separation by keeping the air moving over the blade surface attached longer.

The circuit that will help in the generation of plasma is shown in Figure 3 and will start with a function generator that produces a high frequency and low amplitude triangular wave. These triangular waves will go to a signal control circuit that will control amplitude and the phase of the waves in case of unsteady pulsing. The signals will be amplified twice through a two stage amplifier before it is finally sent to the plasma actuators.

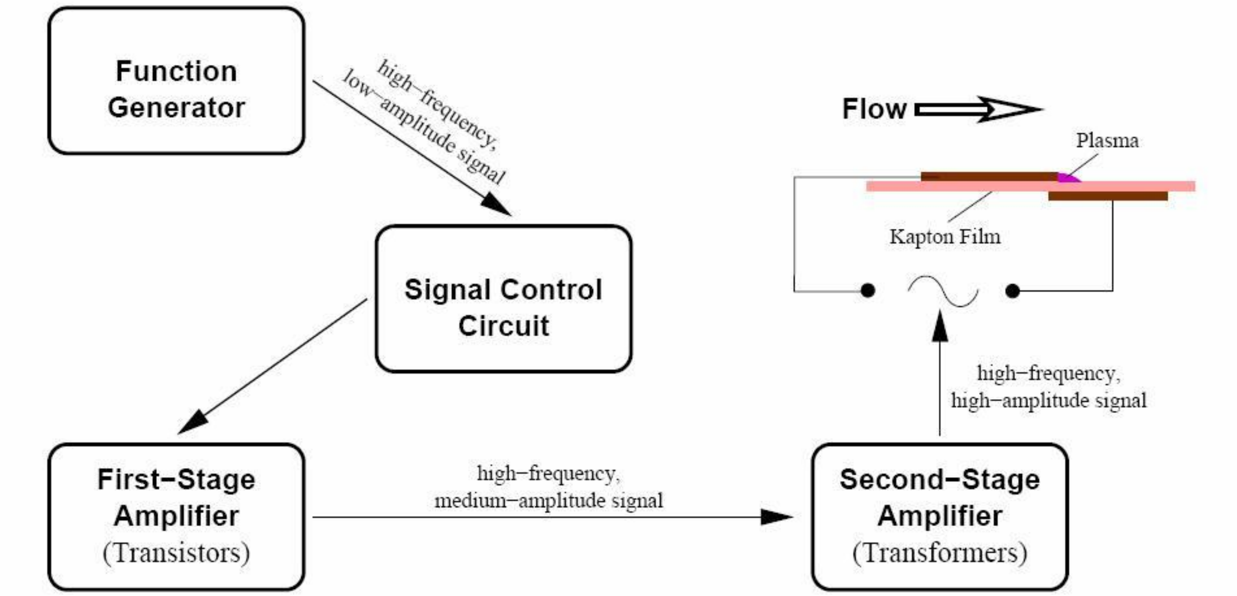

Figure 3 – Diagram of plasma actuator active flow control

To transfer the signal to the electrodes which are embedded in the rotating blades a type of open transformer will be used. The transformer would have a fixed coil mounted to the turbine housing that connects to the second-stage amplifier. The second coil will be fixed to the hub and will rotate along with the hub. The coils will have the same diameter and number of turns and since the signal being sent is AC the first coil will induce a current in the second coil and thus supply power to the electrodes.

The main advantage of the plasma actuator solution is that it has reduced size, low weight and no moving parts. It is a very simple solution using only the effects of high voltages interacting with the air to conduct active flow control.

The disadvantages and reasons this design was not chosen are that it will need to generate voltage of 10-20KV which is a huge voltage and could possibly affect its surrounding because of the electromagnetic interference it would create. Also wind turbines are exposed to the elements and the materials used in the electrodes would corrode very quickly. This would severely limit the lifespan of the active flow control method of using a plasma actuator.

		P1: AFC is present in the system	DP1.1: Plasma actuator embeded in the blade	DP1.2: Control circuitry	DP1.2.1: AC function generator	DP1.2.2: Two stage amplification	DP1.3: Transformer	P2: Hub Blade Mount	DP2.1: Teloscoping shafts	DP2.2: Set Screws	P3: User interface	DP3.1: Watt meter	DP3.2: Switch	P4: Switch	P5: Watt meter
FR0: Scaled Model wind turbine with AFC	X														
FR1: Incorprate AFC		X						O	O	O	O	O	O	O	O
FR1.1: Mechanisims in Blade			X	O	O	O	O	O	O	O	O	O	O	O	O
FR1.2: AFC controller			O	X			O	O	O	O	O	O	O	O	O
FR1.2.1: Frequency control			O		X	O	O	O	O	O	O	O	O	O	O
FR1.2.2: Amplitude control			O		O	X	O	O	O	O	O	O	O	O	O
FR1.3: Rotating Connection			O	O	O	O	X	O	O	O	O	O	O	O	O
FR2: Adjusts blade pitch statically		O	O	O	O	O	O	X			O	O	O	O	O
FR2.1: Rotate Blade		O	O	O	O	O	O		X	O	O	O	O	O	O
FR2.2: Secure Blade		O	O	O	O	O	O		O	X	O	O	O	O	O
FR3: Measure efficiency		O	O	O	O	O	O	O	O	O	X			O	O
FR3.1: Record Power measurment		O	O	O	O	O	O	O	O	O		X	O	O	O
FR3.2: Turn AFC off and on		O	O	O	O	O	O	O	O	O		O	X	O	O
FR4: Activates AFC on user command		O	O	O	O	O	O	O	O	O	O	O	X	X	O
FR5: Indicates power output visually		O	O	O	O	O	O	O	O	O	O	X	O	O	X

Table 3 – Design Matrix for Plasma Actuator

Matrix Explanation:
In Table 3 the system has coupling at any point where there is an 'X' on both side of the diagonal across the matrix. The design is uncoupled but still has some linked design parameters. These are the 'Wattmeter and Switch' column, the wattmeter has a relation with the 'indicates power output visually' in the Functional Requirements and the Switch with the 'Activates AFC on user command'.

B. Compressed Air

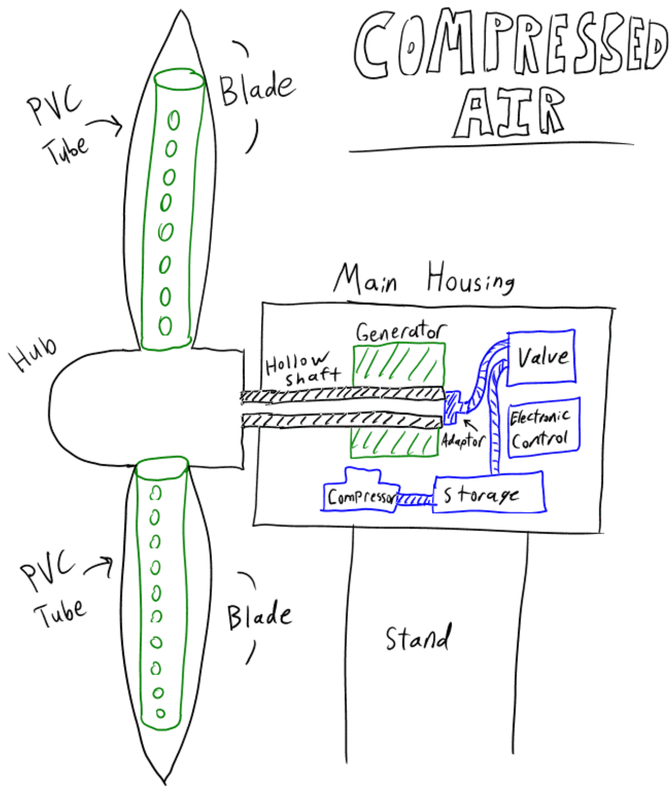

Figure 4 – Sketch of Compressed Air active flow control

Another active flow control method considered was using compressed air to perform active flow control shown in Figure 4. This method uses a compressor to compress air which is then pulsed to the turbine blades through a compressed air system. The pulsing of the air is controlled by an electronic valve whose opening and closing frequency is controlled by an electronic control circuit. The pulsing air is transferred to the rotating through an adaptor which attaches to the end of a hollow shaft. The entire hub assembly is sealed and PVC tubes are installed in the blades with holes drilled through the blade surface and PVC tubes which allow the pulsed air to influence the boundary layer flow.

The advantages of using compressed air are that it has proven its effectiveness in aircraft applications and that the source of the air pulse will be in the main housing that is the air compressor. Also the pressure in the system can be small with good results from previous testing from 5psi to 30psi.

The disadvantages of the design are numerous. The design will potentially have large energy losses due to the air compressor requiring a large amount of power to run. That is a big problem because the whole point of the wind turbine is to generate maximum power. Additionally, this is a system with a lot of components requiring air tight seals and having any air leaks will affect the efficiency of the design. The sealing of the design causes another problem when manufacturability is considered. Building a completely sealed system from air compressor to blades is a tough task. Any small leaks after fabrication is complete will quickly grow into major leaks that will limit this method of active flow controls lifespan.

	DP0:	DP1: AFC is present in the system	DP1.1: Numatic pulse actuator	DP1.2: Control circuitry	DP1.2.1: Valves	DP1.2.2: Compresor	DP1.3: Sealed air passege way	DP2: Hub Blade Mount	DP2.1: Sealed Teloscoping shafts	DP2.2: Set Screws	DP3: User interface	DP3.1: Watt meter	DP3.2: Switch	DP4: Switch	DP5: Watt meter
FR0: Scaled Model wind turbine with AFC	X														
FR1: Incorprate AFC		X						O	O	O	O	O	O	O	O
FR1.1: Mechanisims in Blade			X	O	O	O	O	O	O	O	O	O	O	O	O
FR1.2: AFC controller			O	X			O	O	O	O	O	O	O	O	O
FR1.2.1: Frequency control			O		X	O	O	O	O	O	O	O	O	O	O
FR1.2.2: Amplitude control			O		O	X	O	O	O	O	O	O	O	O	O
FR1.3: Rotating Connection			O	O	O	O	X	O	O	O	O	O	O	O	O
FR2: Adjusts blade pitch statically		O	O	O	O	O	O	X			O	O	O	O	O
FR2.1: Rotate Blade		O	O	O	O	O	O		X	O	O	O	O	O	O
FR2.2: Secure Blade		O	O	O	O	O	O		O	X	O	O	O	O	O
FR3: Measure efficiency		O	O	O	O	O	O	O	O	O	X			O	O
FR3.1: Record Power measurment		O	O	O	O	O	O	O	O	O		X	O	O	O
FR3.2: Turn AFC off and on		O	O	O	O	O	O	O	O	O		O	X	O	O
FR4: Activates AFC on user command		O	O	O	O	O	O	O	O	O	O	O	X	X	O
FR5: Indicates power output visually		O	O	O	O	O	O	O	O	O	O	X	O	O	X

Table 4 - Design Matrix for Compressed Air

Matrix Explanation:

In Table 4 it can be seen that the coupling is at any point where there is an 'X' on one side of the diagonal in the matrix. The design is uncoupled but still has some linked design parameters. These are the 'Wattmeter and Switch' column, the wattmeter has a relation with the 'indicates power output visually' in the Functional Requirements and the Switch with the 'Activates AFC on user command'.

C. Loud Speaker

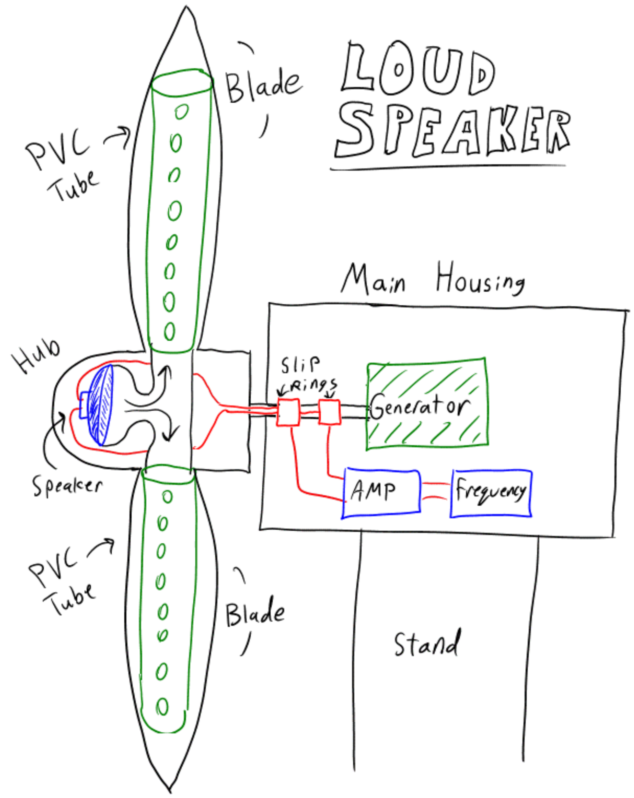

Figure 5 – Sketch of Loud Speaker active flow control design

The chosen design for incorporating active flow control into the wind turbine is the loud speaker method. A loud speaker is the main element in the design that will be used to pulse the air inside the hub and blades through the holes to the boundary layer flow. The method requires a speaker able to work in the low frequency ranges (around 100Hz) so a small "tweeter" type speaker would be insufficient. The larger diameter loud speaker will be located in the center of the rotating hub so that its large mass has little effect on the inertia of the blades. The speaker will run at a specific frequency and generate the pulsing air through two mechanisms. These mechanisms are discussed in greater detail in section IX and will be briefly discussed here. Firstly a chamber will be sealed from the front of the speaker to the end caps on the PVC pipes located in the blades. The lengths of the tube are critical because they need to be tuned to the desired frequency. The sound waves produced by the speaker will resonate down the tube and cause pressure waves which result in air pulsing out of the holes drilled into the PVC pipes and blade surface. The second method is the pulsing of the actual speaker diaphragm. Because the chamber is sealed the movement of the speaker diaphragm will cause further pressure waves which will add to the air pulses.

To control the speaker a frequency generator will control the frequency and an amplifier will control the speaker's amplitude. To transfer the signal to the rotating hub a slip ring will be used to make a rotating electrical connection on the main shaft.

There are many advantages to this system. The first is that the actual air pulse source is located in the rotating hub with the blades. Additionally there is a single moving part which is the loud speaker and the amplitudes required to run the speaker are very low so the power consumption of the system will be low. This allows the most energy to be generated by the wind turbine. Furthermore, this method is affected the least by any defects in the system allowing for acceptable operation of the active flow control over a large range of defects to the system such as cracks and broken seals.
The disadvantages to this system are that it requires the most mounting of components in the rotating hub and the slip ring contacts can produce high frequency noise. The noise is not a concern because the loud speaker will be unresponsive to high frequency signals so no filtering after the slip rings will be required.

	DP0:	DP1: AFC is present in the system	DP1.1: Loud speaker actuator	DP1.2: Control circuitry	DP1.2.1: Frequency generator	DP1.2.2: Amplifier	DP1.3: Sliiperings	DP2: Hub Blade Mount	DP2.1: Teloscoping shafts	DP2.2: Set Screws	DP3: User interface	DP3.1: Watt meter	DP3.2: Switch	DP4: Switch	DP5: Watt meter
FR0: Scaled Model wind turbine with AFC	X														
FR1: Incorprate AFC		X						O	O	O	O	O	O	O	O
FR1.1: Mechanisims in Blade			X	O	O	O	O	O	O	O	O	O	O	O	O
FR1.2: AFC controller			O	X			O	O	O	O	O	O	O	O	O
FR1.2.1: Frequency control			O		X	O	O	O	O	O	O	O	O	O	O
FR1.2.2: Amplitude control			O		O	X	O	O	O	O	O	O	O	O	O
FR1.3: Rotating Connection			O	O	O	O	X	O	O	O	O	O	O	O	O
FR2: Adjusts blade pitch statically		O	O	O	O	O	O	X			O	O	O	O	O
FR2.1: Rotate Blade		O	O	O	O	O	O		X	O	O	O	O	O	O
FR2.2: Secure Blade		O	O	O	O	O	O		O	X	O	O	O	O	O
FR3: Measure efficiency		O	O	O	O	O	O	O	O	O	X			O	O
FR3.1: Record Power measurment		O	O	O	O	O	O	O	O	O		X	O	O	O
FR3.2: Turn AFC off and on		O	O	O	O	O	O	O	O	O		O	X	O	O
FR4: Activates AFC on user command		O	O	O	O	O	O	O	O	O	O	O	O	X	O
FR5: Indicates power output visually		O	O	O	O	O	O	O	O	O	O	O	O	O	X

Table 5 - Design Matrix for Loud Speaker

In Table 5 it can be seen that the coupling is at any point where there is an 'X' on one side of the diagonal in the matrix. The design is uncoupled but still has some linked design parameters. These are the 'Wattmeter and Switch' column, the wattmeter has a relation with the ‘indicates power output visually’ in the Functional Requirements and the Switch with the ‘Activates AFC on user command’.

D. TRIZ of Speakers

Using Acclaro it was found that there was a contradiction between the speaker frequencies vs. the speaker size. The initial idea was to use multiple small speakers in the blades to perform the active flow control. The design requires low frequency actuation which is not easily produced by small speakers. The larger speakers required to produce the correct frequency were large and heavy which caused problems when placed on the blades. The large masses far away from the center of rotation would increase the minimum start up wind speed for the wind turbine to start operating and thus have a negative effect on the project’s goals.

TRIZ was used to solve the contradiction. The improving feature was the loss of information in that with the larger speaker the ability to produce the low frequencies accurately increases. The worsening feature was weight of the moving object since the larger speakers weighed more. TRIZ stated that preliminary action could solve the contradiction. That idea was used in coming up with moving the speaker to the center of the hub so that a large speaker could be used and it would have little effect on the turbines ability to rotate since the larger mass is located and centered around the axis of rotation.

E. Method to select DP’s

The three methods were analyzed using a Pugh Analysis technique and comparing their various pro’s and con’s. In the Pugh analysis the three designs were ranked on a scale of 100 in various criteria that had different weights. The speaker method came out as the best choice with a score of 90 over the other scores of 76 and 79. Additionally the pro’s and con’s Table 6 states some of the big reasons that the speaker method was chosen. This being mainly that the disadvantages to this method were miniscule compared to the other two disadvantages.

Pugh Analysis

Alternatives	Baseline	Speakers	Plasma	Compressed air	GE
Criteria					
Incorporates AFC	50	50	50	50	0
Cost	10	7	5	6	9
Quality	10	7	6	4	9
Manufacturability	5	3	2	1	4
AFC Efficiency	15	14	9	11	0
Customer Acceptance	10	9	7	4	0
Score:	100	90	79	76	22

Table 6 – Pugh Analysis

	Loudspeakers	Plasma Actuators	Pulsed Air
Pro's	•Air pulse source is contained in spinning hub •One single speaker/woofer •Low amount of moving parts •Low power cost	•Reduced size and weight •Absence of moving parts •Increased reliability	•Proven effectiveness in aircraft applications •Air pulse source is contained in main housing
Con's	•Slip rings induce a lot of electrical noise •Requires most modification to hub	•Needs high Voltage (10kV) •Electromagnetic interference •Corrosion of the electrodes	•Potentially high energy loss due to air compressor •Air leaks decrease efficiency •Manufacturability

Table 7 – Pros and Cons of Designs

IV. Speaker and PVC Tube Experiment

One of the keys to successful implementation of Active Flow Control via loudspeaker actuation is acoustic tuning. Acoustically tuning the sound chamber within the turbine blade will allow the loudspeaker to operate most efficiently in the frequency range required for AFC. In short, any resonance chamber (in this case, the hollow PVC tubing inside the turbine blades) will resonate best at certain natural frequencies, which are determined by the length of the chamber. By selecting a chamber length that is optimized to the range of frequencies required by Active Flow Control, the volume of air pulsed out of the blades for a given sound level can be greatly increased.

For any given frequency, the wavelength of the sound wave of that frequency may be determined from Equation (1) below:

$c = \lambda \cdot f$ **(Equation 1)**

Where *(f)* is the frequency, *(c)* is the local speed of sound in air, and *(λ)* is the wavelength. As suggested by the project Sponsor, active flow control functions best for flow field disturbances occurring at approximately 100Hz. In conjunction with a local speed of sound of approximately 345 m/s, the length of a sound wave at this frequency may easily be computed to be 3.45m. For a closed-ended, cylindrical resonance chamber, such as the one that may be found in the turbine blades (see Figure 20), the required length of a resonant chamber for a given frequency may be found using Equation (2) below:

$L = \frac{n}{4}\lambda$ **(Equation 2)**

Where *(L)* is the required length, and *(n)* is a constant, positive, odd integer (*n=1,3,5…*) representing the mode of resonance in the chamber. Using the above wavelength of 3.45m for AFC resonance and a value of *n*=1 (the first-order resonance), the required chamber length for resonance is 0.8625m. Coincidentally, this compares favorably with the geometrically scaled blade length of 1.0m for the demonstration wind turbine, meaning that a tube running almost the entire length of the turbine blade will resonate best at approximately 100Hz.

However, this does not guarantee that the Active Flow Control will work as intended. The actual frequency for optimum flow smoothing must be empirically determined in a wind tunnel (testing scheduled for January / February 2009). Additionally, this frequency may change slightly depending upon prevailing wind speed and the turbine's rotation rate. Consequently, the Active Flow Control may not necessarily be able to operate at the resonance frequency at all times. Therefore, in order to verify the viability of acoustically-actuated Active Flow Control for a range of frequencies, a set of preliminary tests was conducted.

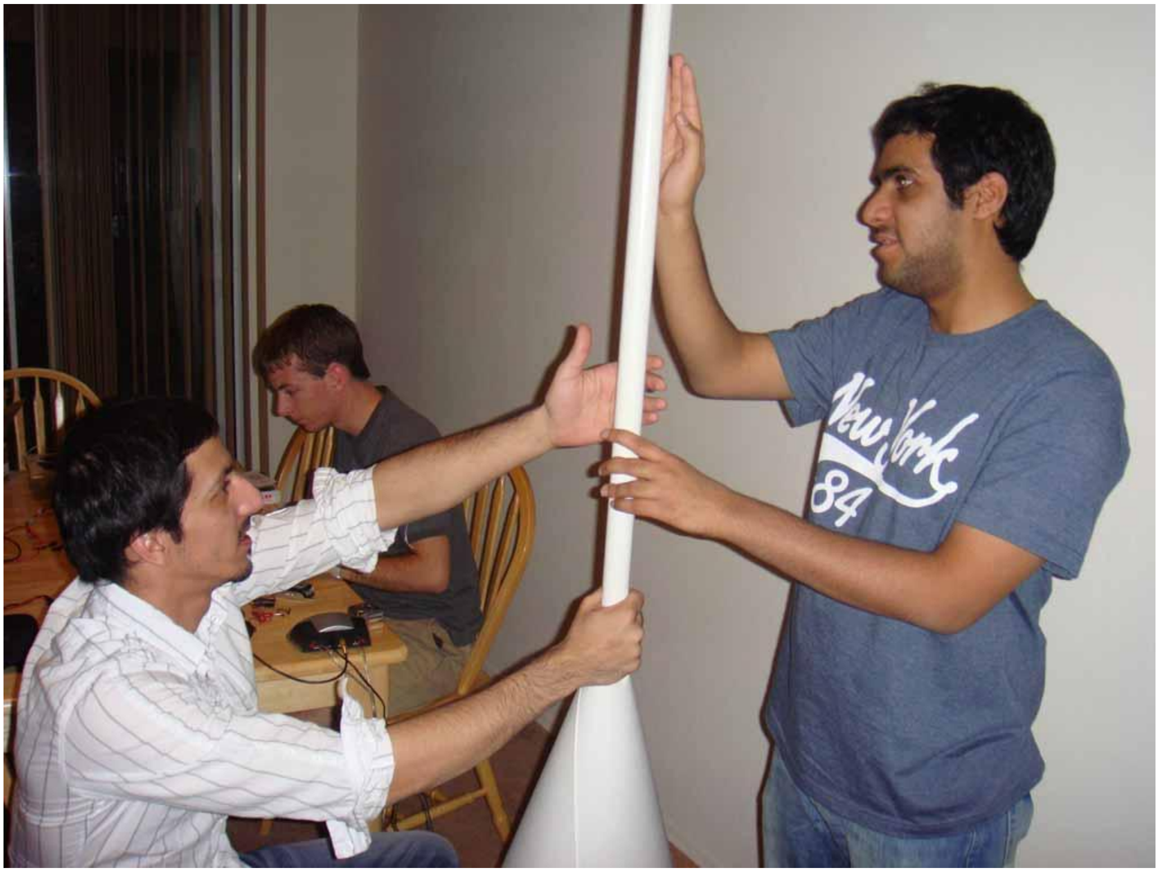

Figure 6 – Khalid and Faisal feeling air flows and Nathan controlling the speaker

These tests were designed to simulate the speaker-and-acoustic chamber as it would be implemented on the turbine. As such, a PVC tube of 1" diameter (approximately the maximum diameter that could be utilized in the scaled turbine blade) was sealed on one end, and a number of 1/16" diameter holes were drilled into its surface at 4cm intervals. This was then affixed to a loudspeaker via an adapter, and a frequency generator and amplifier were used to achieve the desired waveform. The volume of air moved through the tube openings was then measured. This measurement was accomplished by finding the approximate maximum distance away from the tube's surface that air disturbances or flow could be felt by an observer (see Figure 6). Although this system of measurement is decidedly prone to inaccuracy, it was deemed acceptable because numerous tests performed in the Aerospace and Mechanical Engineering Department have shown that even a tiny surface disturbance over an airfoil is enough to realize the benefits of AFC. Therefore, it is reasonable to assume that if disturbances could be felt at distances from the tube of an inch or greater; the loudspeaker actuation method could reasonably be predicted to function as desired in the final product.

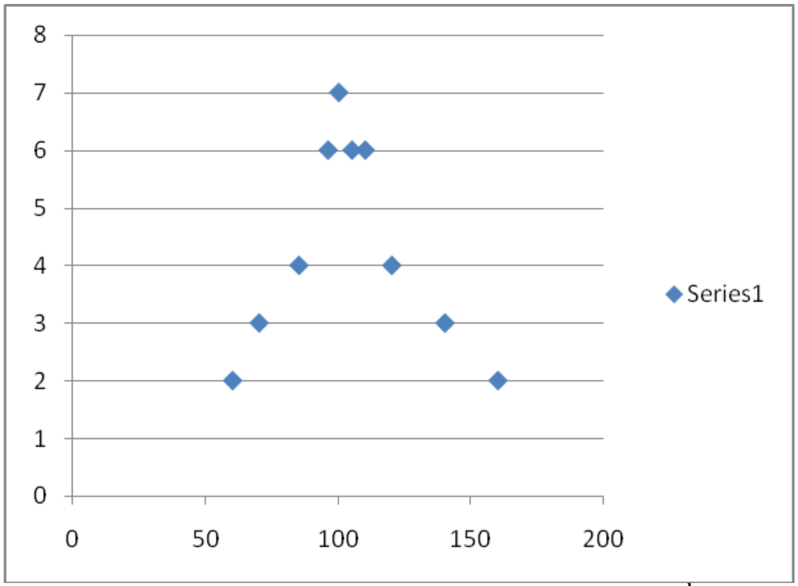

Figure 7 - Frequency versus airflow distance (in) for 2nd test

Figure 8 – Khalid, Cory and Nathan testing the 10 inch subwoofer

Figure 9 – Nathan, Cory and Faisal testing the T-shaped splitter enclosure

The preceding procedure was repeated for a number of speaker, chamber, and adapter types, as well as a range of frequencies. The results of one such test have been plotted in Figure 7. The validity of resonance theory is immediately clear from the shape of the graph, which exhibits a peak in flow disturbance distance at the resonance frequency of 100Hz. However, the gradual slope of the data away from the peak resonance frequency indicates that the chamber still resonates quite well for a range of frequencies near the resonant frequency. More importantly, at frequencies far from the resonance frequency (the "tails" of the graph), flow disturbances could still be felt at a distance of about two inches from the surface of the tube, more than sufficient for proper operation of AFC. These results were typical for both 6 and 10 inch speaker diameters, as well as for enclosures as varied as subwoofer cabinets (Figure 8), conical nozzle enclosures, and T-shaped splitter enclosures (most similar to the final product's configuration, (Figure 9), and amplifiers ranging in power from 10 watts to over 100 watts. As such, these tests unequivocally indicate that AFC can be successfully implemented using a loudspeaker. This result bodes well for the success of the final design, and serves as a solid foundation for design activities surrounding the acoustic chamber within the wind turbine blades.

V. Wind Tunnel Model

A wind tunnel model will be built to perform an experiment to verify the active flow control effects on the chosen wind turbine airfoil. The wind tunnel experiments were performed to observe the reaction of the airfoil to different wind speeds with different angle of attack. Active flow control was then engaged and disengaged during the experiments to measure the forces generated by the airfoil section in each case. Since the optimum location for the active flow control holes to be placed on the airfoil had not yet been determined, two rows of holes at two chord locations will be tested. The first row was located near the leading edge, and the second at roughly 40% chord (the maximum thickness of the airfoil). The wind tunnel experiments were to determine the best place to locate the active flow control holes. Figure 10 shows a view of the initial design concept for the wind tunnel model.

Figure 10 – Wind Tunnel 2D airfoil section

A. Design

The Wind Tunnel model is an extruded 2D airfoil section of the airfoil used in the turbine blade. The NREL wind turbine was chosen, which uses the NREL S809 airfoil. The active flow control method is incorporated into the model to allow for the study of its effect on the airfoil performance.

The first step in the design process was to decide upon the size of the model. Because of the aerodynamic effects of having a finite wing in the wind tunnel, it is desirable to get as close to the outer walls of the test chamber as possible. This eliminated or reduced the effect of tip vortices which can influence the measurements. The AME Low Speed wind tunnel test section is 4 feet across. The models span was chosen to be 3.75 feet to allow about 1/8 inch of clearance on either side. Due to the large size of this airfoil and the turbulent flow it will experience, some rocking of the model is expected and there can be no interference caused by the walls of the wind tunnel.

The other size requirement was to determine the chord of the model. The testing would take place over a large range of wind speeds and needed to accurately simulate the various speeds the turbine blades would see. As the turbine blades spin, the father away from the center axis of rotation a blade section is, the faster that portion of the blade is moving. A chord of 12 inches was chosen because it is right in the middle of the Reynolds numbers expected to be seen by the turbine blades. These Reynolds numbers may be found in Appendix D.

Figure 11 - Wind tunnel model design CAD

The next consideration was how to incorporate active flow control into the wind tunnel model. Because active flow control has almost been exclusively tested for aircraft wings, not much testing has been done at low Reynolds numbers. The project sponsor advised to have two rows of active flow control that could be toggled on or off to test the effects at different chord locations. It was thought that there might be leading edge separation at the high angles of attack and trailing edge separation at the lower angles of attack. This was verified by performing xfoil analysis on the airfoil, available in Appendix A, which shows that separation primarily occurred at 56% chord on the trailing edge and 15% chord at the leading edge. The active flow control must be working in an area where the flow is still attached to the airfoil, so 10% and 45% chord was chosen for the two rows. An added benefit of this configuration was that both rows could be tested at once, which is another area where little research had been conducted.

The loud speaker method was selected to actuate the active flow control as this was the most relevant to the project. The speaker would be mounted outside of the wind tunnel and the sound waves and air pulses would be carried to the wind tunnel through a series of tubes through the bottom of the test chamber and into the model. PVC pipes at the desired locations would run the length of the airfoil section. Once glued to the fiberglass skin, holes would be drilled to provide the access the active flow control needs to interact with the flow around the airfoil. The tubes leading from the speaker connect in the middle of the model at a PVC T-connector. This also simulates how the prototype will be built. The tubes were cut to specific lengths to tune them to a certain frequency that the active flow control should work well at when operated in low Reynolds numbers.

A standard mount was provided by the project sponsor, which interfaces nicely to the central pylon in the wind tunnel. To ensure maximum strength and rigidity a 1 inch square steel tube was used as the main spar in the model. Thick ½ inch plywood ribs were placed every 5 inches and the skin was made from 8 ounce fiberglass.

The active flow control holes were determined to be 1 mm in diameter with a spacing of 10 mm initially. If the active flow control was found to be ineffective, more holes could be drilled between the holes due to the large spacing.

The design can be seen in Figure 11.

B. Build

The construction of the wind tunnel model was a long, multistage process that took well over 200 man hours to complete. The first step was to make the molds of the airfoil. Using the CNC foam cutter in one of the project sponsor's labs, the team cut large positive plugs of each half of the airfoil. This process is shown in Figure 12.

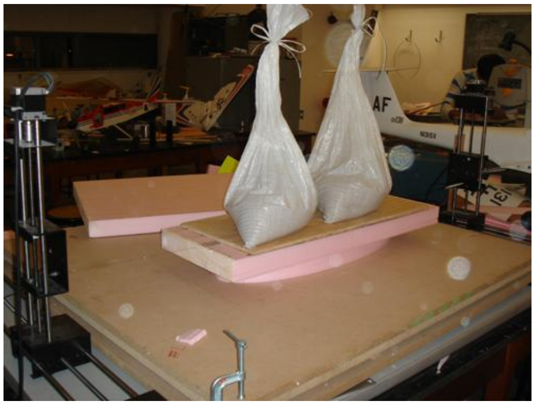

Figure 12 - Foam Cutter

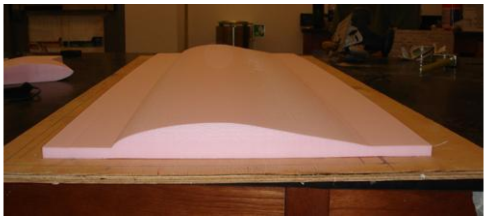

Figure 13 - Foam Plug

These delicate foam plugs (Figure 13) were sanded smooth and a thin plastic covering was carefully applied to the surface. This created a smooth surface that the molds could be made from.

After prepping the plugs with wax and other releasing agents, a large amount of heavy 8 ounce fiberglass was applied to the plugs. This was dried overnight and checked the next day. Stiffeners were added to the fiberglass molds' back sides to ensure that no torsion would happen and that they would sit flat on the table. Once the stiffeners were in place the molds were pulled off of the plugs. There were some imperfections found to the surface of the molds which were repaired. Once the molds were ready and prepped the skin of the wind tunnel model was laid up in the molds. Again, lots of heavy 8 ounce fiberglass was used. This is shown in Figure 14.

Figure 14 - Fiberglass Molds

Once the skin dried, the plywood ribs, steel spar, PVC tubes and pylon mount were attached to the top skin which is shown in Figure 15. This was because there needed to be a nice seal between the PVC pipe and the skin of the airfoil. Holes would later be drilled into the surface through the PVC pipe to allow the active flow control to work. Any cracks or empty spaces would reduce the effectiveness of the active flow control. Once everything was glued to the top skin, the two molds were closed together with a large bead of glue running where the seam would be.

Figure 15 - Interior Work Wind Tunnel Model

After the two skin halves dried, the molds were pulled open and the finishing work began. Hours upon hours of sanding, along with other finishing touches, was required. The bottom surface was cut open to allow access to the active flow control tubes and pylon mount. The last touches were to paint the surface and drill the holes.

Figure 16 shows the completed wind tunnel model.

Figure 16 - Wind tunnel model in Wind Tunnel

C. Testing

The tests performed in the wind tunnel included a large amount of variables. It was calculated that an immense amount of testing would be required to test every combination. Additionally each test must be run multiple times to verify the results. Each test would run the model through a range of angles of attack. Between each test the other variables would be set, these included the active flow control row, frequency, amplitude and the wind speed the wind tunnel was set at.

This table shows the experiment matrix. The test was divided into five blocks. The goal of this matrix is to focus on which combination will produce the best results. Each of the blocks is used to determine a best setting for a given variable which is then in turn used in the next block. The first block shows the baseline tests that were used to compare the performance increases when active flow control was used. Block 1 to 5 shows different tests for different active flow control configurations, different frequencies and different amplitudes. Both rows were used individually and together. There was little research to indicate that two rows in the blade can be used in AFC, but it was advised by the project sponsor to see what effect the two rows have. Block five was used to find the best results in all of the tests done to get the best setting possible for AFC.

Table 8 - Wind Tunnel Testing Design Matrix

Block	Block Test No.	Total Test No.	Wind Speed (mph)	AFC Status	Frequency (Hz)	Amplitude (% of full volume)	Angle of Attack (deg)
Baseline	1	1	5	Off	Off	Off	-6.4 to 24.3
	1a	2	5	Row 1	150	30	-6.4 to 24.3
	2	2	10	Off	Off	Off	-6.4 to 24.3
	3	3	15	Off	Off	Off	-6.4 to 24.3
	4	4	20	Off	Off	Off	-6.4 to 24.3
	5	5	25	Off	Off	Off	-6.4 to 24.3
1	1	6	15	Row 2	150	13	-6.4 to 24.3

	2	7	15	Row 2	150	25	-6.4 to 24.3
	3	8	15	Row 2	150	38	-6.4 to 24.3
	4	9	15	Row 2	150	50	-6.4 to 24.3
	5	10	15	Row 1	150	63	-6.4 to 24.3
	6	11	15	Row 1	150	75	-6.4 to 24.3
2	1	12	15	Row 2	75	Best of Block 1 (13)	-6.4 to 24.3
	2	13	15	Row 2	100	Best of Block 1 (13)	-6.4 to 24.3
	3	14	15	Row 2	125	Best of Block 1 (13)	-6.4 to 24.3
	1	15	15	Row 2	150	Best of Block 1 (13)	-6.4 to 24.3
	2	16	15	Row 2	225	Best of Block 1 (13)	-6.4 to 24.3
	3	17	15	Row 2	300	Best of Block 1 (13)	-6.4 to 24.3
	4	18	15	Row 2	1050	Best of Block 1 (13)	-6.4 to 24.3
	5	19	15	Row 2	1900	Best of Block 1 (13)	-6.4 to 24.3
3	1	20	5	Row 1	Best of Block 2	Best of Block 1 (13)	-6.4 to 24.3
	2	21	15	Row 1	Best of Block 2	Best of Block 1 (13)	-6.4 to 24.3
	3	22	25	Row 1	Best of Block 2	Best of Block 1 (13)	-6.4 to 24.3
4	4	23	5	Row 1 & 2	Best of Block 2	Best of Block 1 (13)	-6.4 to 24.3
	5	24	15	Row 1 & 2	Best of Block 2	Best of Block 1 (13)	-6.4 to 24.3
	1	25	25	Row 1 & 2	Best of Block 2	Best of Block 1 (13)	-6.4 to 24.3
5	3	26	20	Row 1	Best of Block 2	Best of Block 1 (13)	-6.4 to 24.3
	4	27	5	Row 2	Best of Block 2	Best of Block 1 (13)	-6.4 to 24.3
	5	28	25	Row 2	Best of Block 2	Best of Block 1 (13)	-6.4 to 24.3
	6	29	20	Row 2	Best of Block 2	Best of Block 1 (13)	-6.4 to 24.3
	7	30	10	Row 1 & 2	Best of Block 2	Best of Block 1 (13)	-6.4 to 24.3
	9	31	20	Row 1 & 2	Best of Block 2	Best of Block 1 (13)	-6.4 to 24.3

VI. Final Design

A. Overall Description

The final design, deemed the Demo Model, consists of a small wind turbine which is designed to be a good representation of a typical full-scale wind turbine. It can be shown that the behaviors demonstrated by this Demo Model could be replicated in the larger wind turbines for equal performance increases.

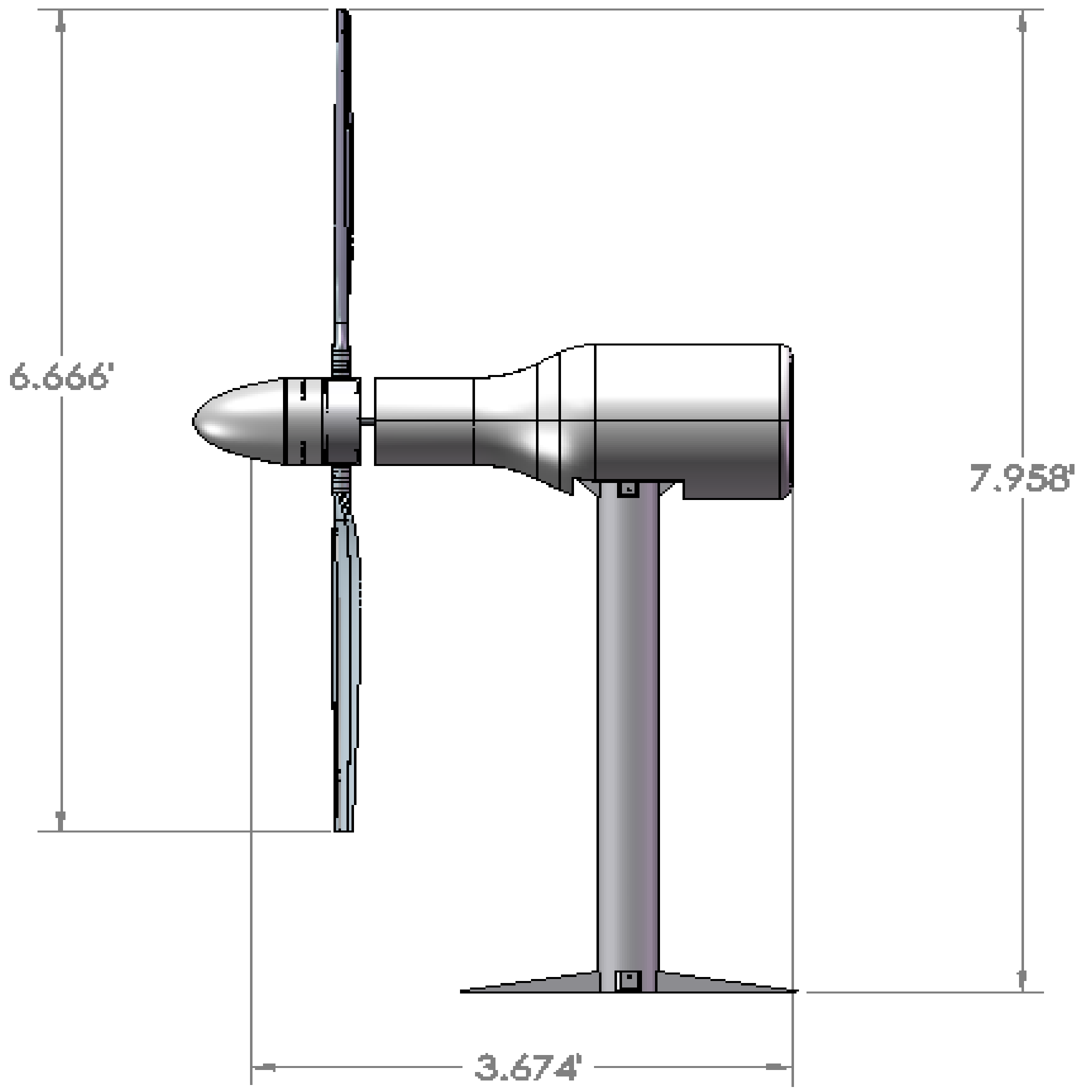

Figure 17 – Demo Model overall dimensions

The Demo Model is small wind turbine with geometrically scaled turbine blades modeled after the NREL 10 meter wind turbine which is discussed further in section X.B. The loud speaker active flow control method was selected based on the criterion discussed in section VIII. The loud speaker is mounted in the rotating hub which connects and transfers power to the main housing through the main shaft. In the main housing the turbine generator is run through a planetary gear box to generate power. The electronics system that controls the active flow control is also located in the main housing and is connected to the rotating speaker through a slip ring mounted on the main shaft.

The entire tower is mounted on a support tower giving it a total projected height of around eight feet. Normally a wind turbine would be mounted on a tall tower to escape any ground effects introduced into the wind and gain access to the general higher wind speeds located at larger heights above the Earth's surface. For this project an artificial wind generator such as a large diameter fan will be used to accurately and controllably produce wind for experimental testing. Thus the rotor disk can be mounted close to the ground making the experiments easier to conduct while producing accurate results.

B. Details of Blade

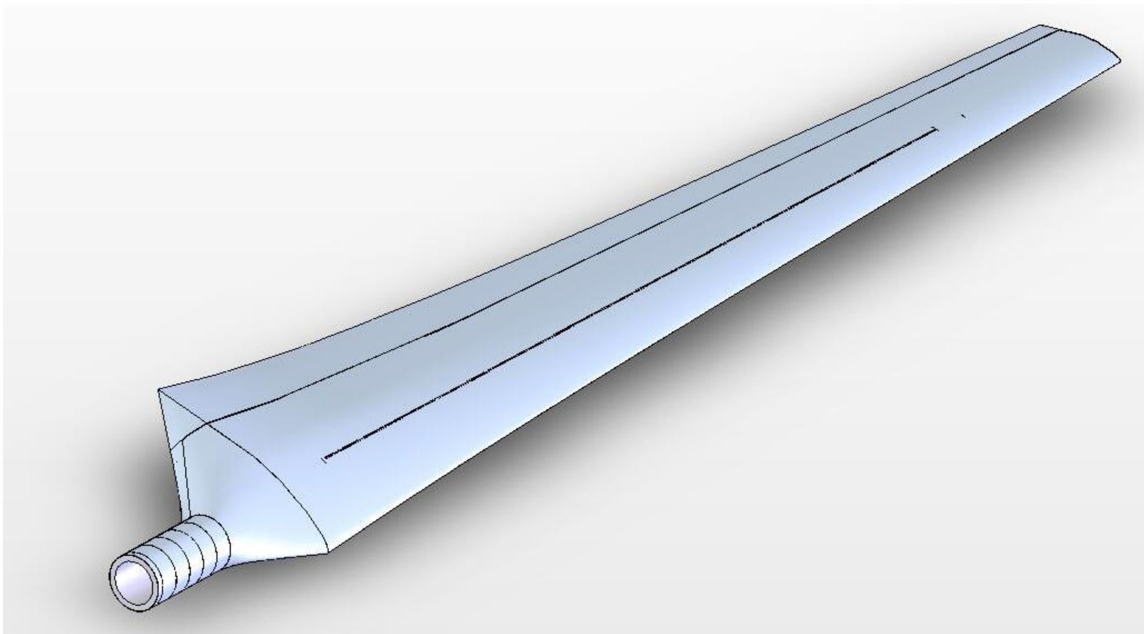

Figure 18 – Scaled Wind Turbine Blade

The wind turbine blades are the most important element in the design. Not only do they provide the power to turn the turbine they provide the Demo Model with aerodynamically similar behaviors of the large wind turbine. This is accomplished by exactly geometrically scaling the turbine blades of a larger wind turbine. The NREL 10 meter wind turbine was selected as the wind turbine the project would scale down because of the plethora of experimental testing data available to the public. The NREL wind turbine was used in an experiment at the NASA AMES wind tunnel in the year 2000 to research the accuracy of CFD computations of wind turbines. As a result all details of the experiment and an incredible amount of information were available to this project to use as was not the case with the larger GE multi-megawatt wind turbines.

The airfoil used in the NREL blade is the S809 airfoil which can be seen in appendix A. The airfoil was analyzed using an Xfoil program to compute the C_L versus Alpha curves used in the scaling equations. These graphs can be seen in appendix A. Using Froude scaling equations and dimensionless analysis the following equation can be used to scale the rpm needed to be reached by the Demo Model to accurately behave like the full scale blades would behave.

$$\omega_m = \frac{\omega_F}{\sqrt{n}}$$ **(Equation 3)**

Where (ω_m) is the model rotation speed, (ω_F) is the full scale rotation speed and (n) is the scaling factor. To decide on a scaling factor the team simply took the target blade length of 1 meter and divided by the NREL 5 meter blade length giving a scaling factor of roughly 1/5th.

The scaling calculations can be seen in appendix B.

One issue faced by the design team was in calculating the lift and resulting rpm that could be expected to be produced by the Demo Model scaled down turbine blades. The issue with this is that because the blades are spinning around a center axis there is a different effective wind speed seen at every radius position along the length of the blade. The farther away from the center of rotation the faster the blade section travels. This is shown in appendix B in the Reynolds number calculations section.

The Reynolds number equation is given where (ρ) is the density, (V) is the air velocity, (D) is the characteristic length which is the blade chord length and (μ) is the kinematics viscosity.

$$\mathrm{Re} = \frac{\rho V D}{\mu}$$ **(Equation 4)**

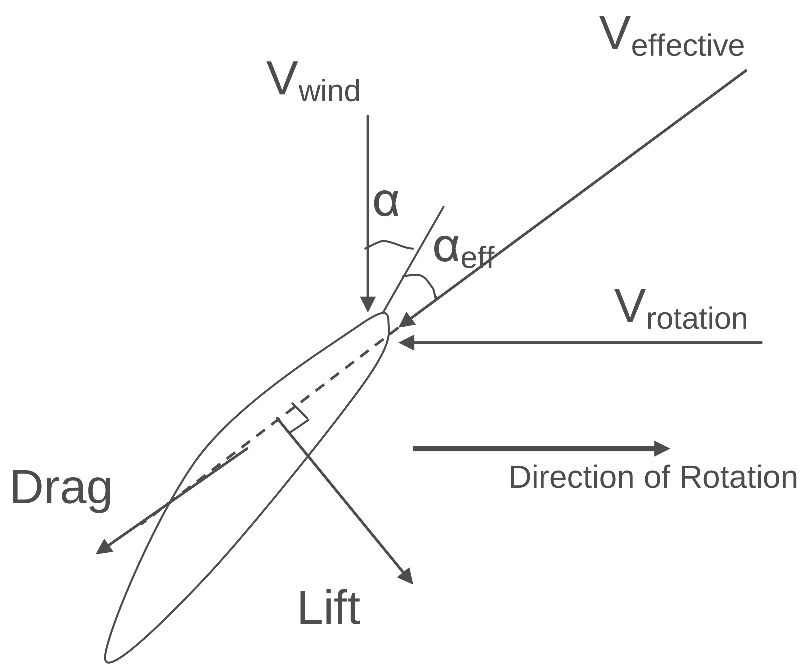

Figure 19 – Forces acting on wind turbine airfoil

The forces acting on a given airfoil section on the blade are shown in Figure 19 where it can be seen that the lift acts perpendicular to the effective wind speed seen by the airfoil. This effective wind speed is a combination between the wind speed and the rotational speed of the turbine blade. Only the component of the lift and drag along the direction of rotation effect the rpm speed.

The computation of this lift value and direction requires advanced scripting used in conjunction with an Xfoil type program to analyze the lift for the entire length of the blade. This calculation was deemed outside of the scope of this project and with the help of the project sponsor an estimation of these values is used. From the NREL 10 meter turbine information on lift and rpm values can be used to estimate the scaled model lift and rpm as being around 80 lbs and 80 rpm. These were used in structural calculations for various parts of the wind turbine and also for selecting the generator.

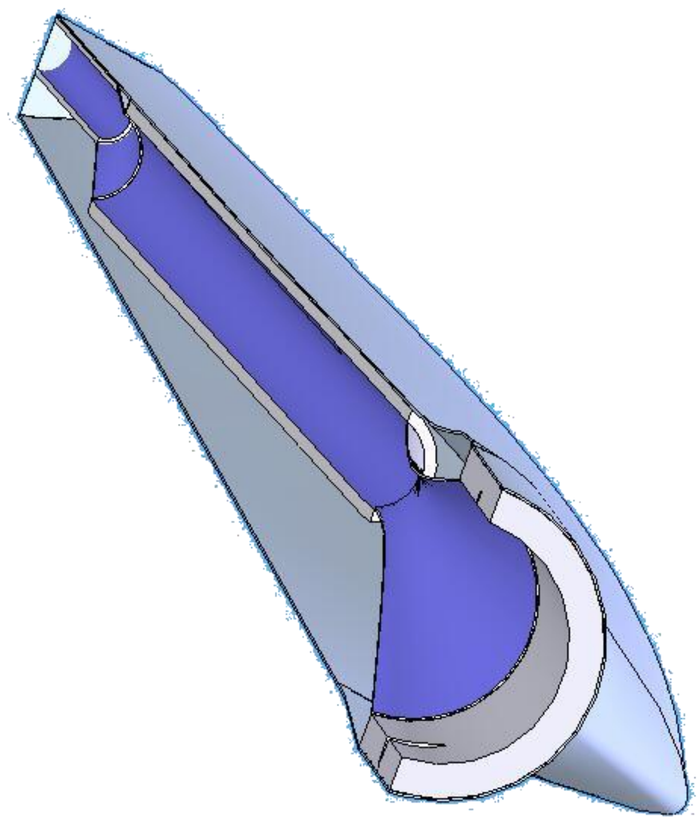

Figure 20 – Cross section view of turbine blade

Blade Description

The turbine blades will consist of a fiberglass skin with the interior components mounted inside the hollow center to perform structural support and implement the active flow control method. The main feature of the blade construction is the air passage way seen in Figure 20 that allows the sound waves and pulsing air to travel down the length of the blade. The air tubes start out at around 1inch at the blades root and transitions down to a .5inch PVC tube in order to have the longest stretch of unchanged tube diameter along the blade length. The blade section this tube covers is also estimated to be the most strongly affected section from active flow control. Along the length of this air passage way 1mm holes are drilled through both the blade surface and air passage way walls every 2 – 3mm to allow the pulsing air to affect the boundary layer flow over the blades surface which are shown in Figure 21.

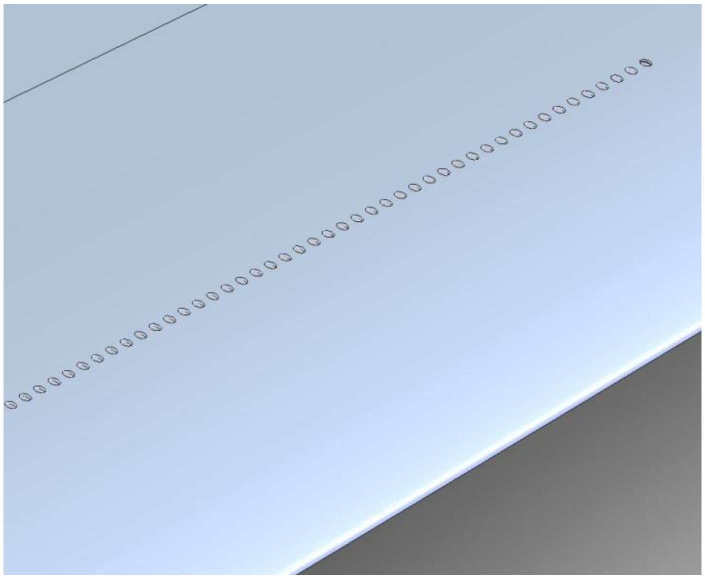

Figure 21 – AFC holes on blade surface

The air passage way must be specifically tuned to a certain frequency that the speaker will be run at. This calculation is discussed in section IX. The air tubes will be cut to the specified length and multiple diameter step downs might be needed as the blades thickness decrease as the radius increases.

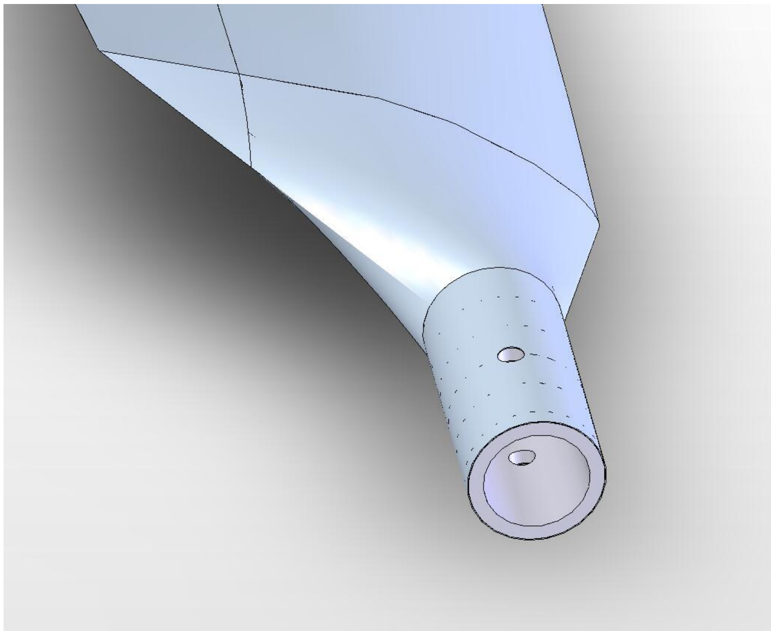

Figure 22 – blade root

A fiberglass laminated balsa wood spar will be mounted underneath the air passage way to add structural rigidity to the turbine blade. At the root of the blade is a 1.25inch aluminum tube that will serve dual roles as the mounting mechanism to the turbine hub and used to set the blade pitch. This is shown in Figure 22. To mount to the hub a telescoping 1inch aluminum tube will be attached to the hub and fit inside the tube mounted in the blade. There will be around 3-4 inches of contact between the tubes. Two 1/4inch set bolts will be screwed down through the threaded holes on the side of the tube mounted in the blade. These will serve to secure the blade to the hub and set the pitch angle of the blade.

A disk will be mounted on the hub that has angle measurements that correspond to a tab on the blades which will be used in positioning the pitch. Additionally a safety cable will be attached to the blade that will attach to a second location on the hub. Over all pitch angles this safety cable will prevent the blade from sliding off the hub tube and in the event of the hub tube breaking will keep the blade attached to the turbine.

The composite blade construction requires the skin to be laid up in blade molds which will be custom built in house by the project team. The mold will consist of two halves and the internal components will be mounted to the top half blade skin first. Then the two halves will be closed together and the interior components will then be mounted to both halves as the two halves join together. Once the blade is pulled out the active flow control holes will be drilled and the blades will be finished.

C. Details of Hub

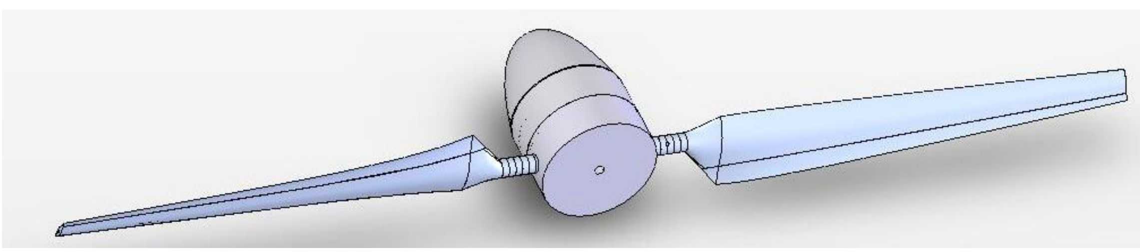

Figure 23 – Hub assembly with blades attached

The hub's main functions are to support the turbine blades, transmit the torque generated by the blades to the main shaft to drive the generator and mount the speaker so that active flow control can be initiated in the blades. Figure 23 shows the outside view of the hub assembly and Figure 24 shows the hub cap and main hub components as transparent showing the internal parts.

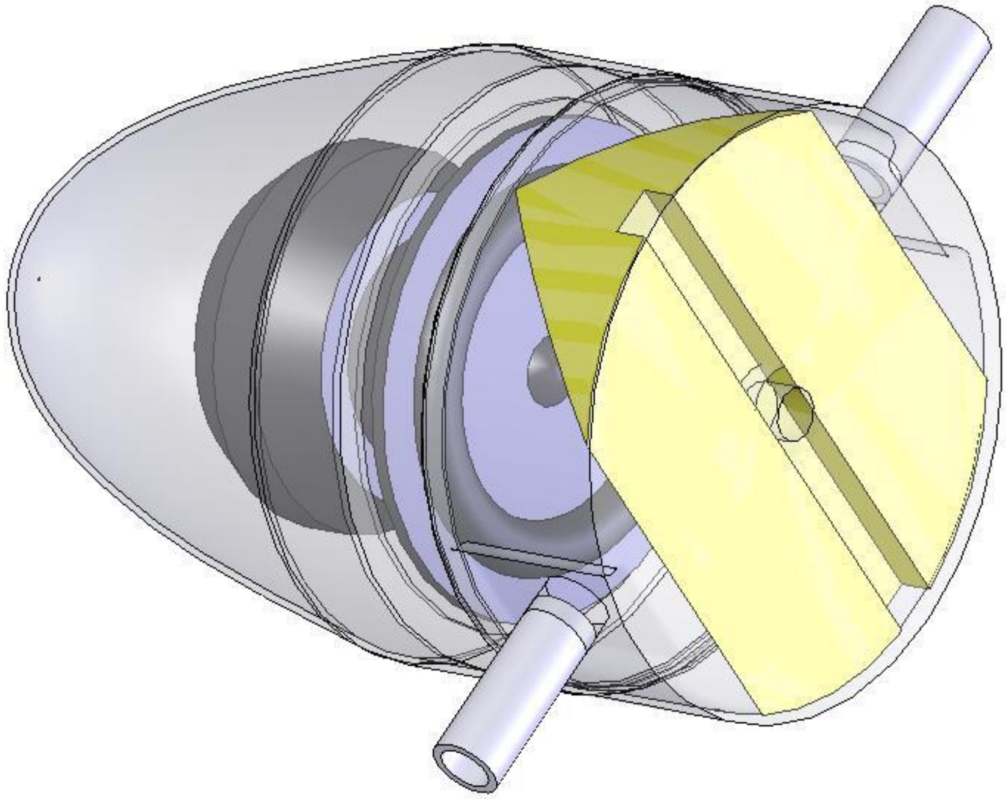

Figure 24 – Transparent outer casing of hub assembly

The hub cap is made of fiber glass skin and has the mounting hardware for the loud speaker. The speaker used is 6inch mid bass speaker with and extra large magnet which allows the diaphragm deflection distance to reach 8mm instead of the average 3mm. This provides a high amount of air movement during the speakers operation. Special consideration was given to the hub cap shape to ensure that the air flow around the hub was as smooth as possible. Originally it was designed to be spherical but it was learned that the spherical shape would produce separation effects of the air flow around the hub and degrade the turbine performance. The hub cap will be removable to allow access to the main shaft connection point for assembly and disassembly purposes.

Inside the main hub will be sound-absorbing foam will be used to help guide the air flow and reduce any sound wave reflections that would degrade the performance of the loud speaker. The best shape for the absorbing foam is still being determined and the foam is very easy to shape into a wide range of shapes. The current foam shape is shown in Figure 25.

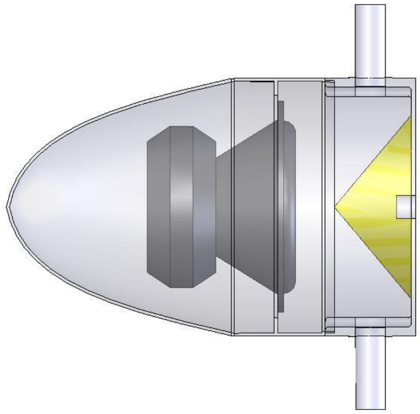

Figure 25 – Side view of transparent hub assembly

The main hub will support the entire weight of the hub assembly on the main shaft attachment as well as support the blades. The difficulty is that the center of the hub must be hollow to allow airflow and sound to travel to the blades. This meant that any structural parts that would be internal in the hub had to be small and that a majority of the loading would be handled by the exterior hub structure. Initially multiple parts were going to be used to connect all the pieces together but concerns over strength lead to the decision to machine the 8inch diameter main hub piece out of a solid block of aluminum. The blades as discussed in section X.B will mount to the hub via a 1inch hollow telescoping tube which allows the sound waves and air to flow from the hub into the blades. These tubes are shown in Figure 26 and will be welded to the main hub. The main hub was designed to have high strength in the needed areas and lightweight with minimal structure in the interior. The hub assembly will mount to the main shaft through the mounting structure machined into the main hub and fixed there by a removable pin that will be slid through the main shaft.

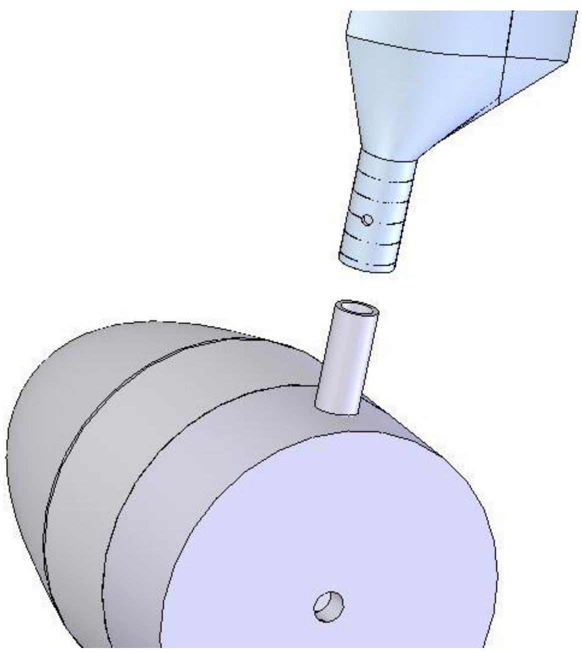

Figure 26 – Hub assembly and blade mount

D. Details of Housing

The Housing Assembly is a critical component of the wind turbine. It contains the entire turbine powertrain and Active Flow Control (AFC) system, supports the Hub Assembly, and interfaces with the Tower Assembly. Figure 27 shows the Housing Assembly with all major internal components.

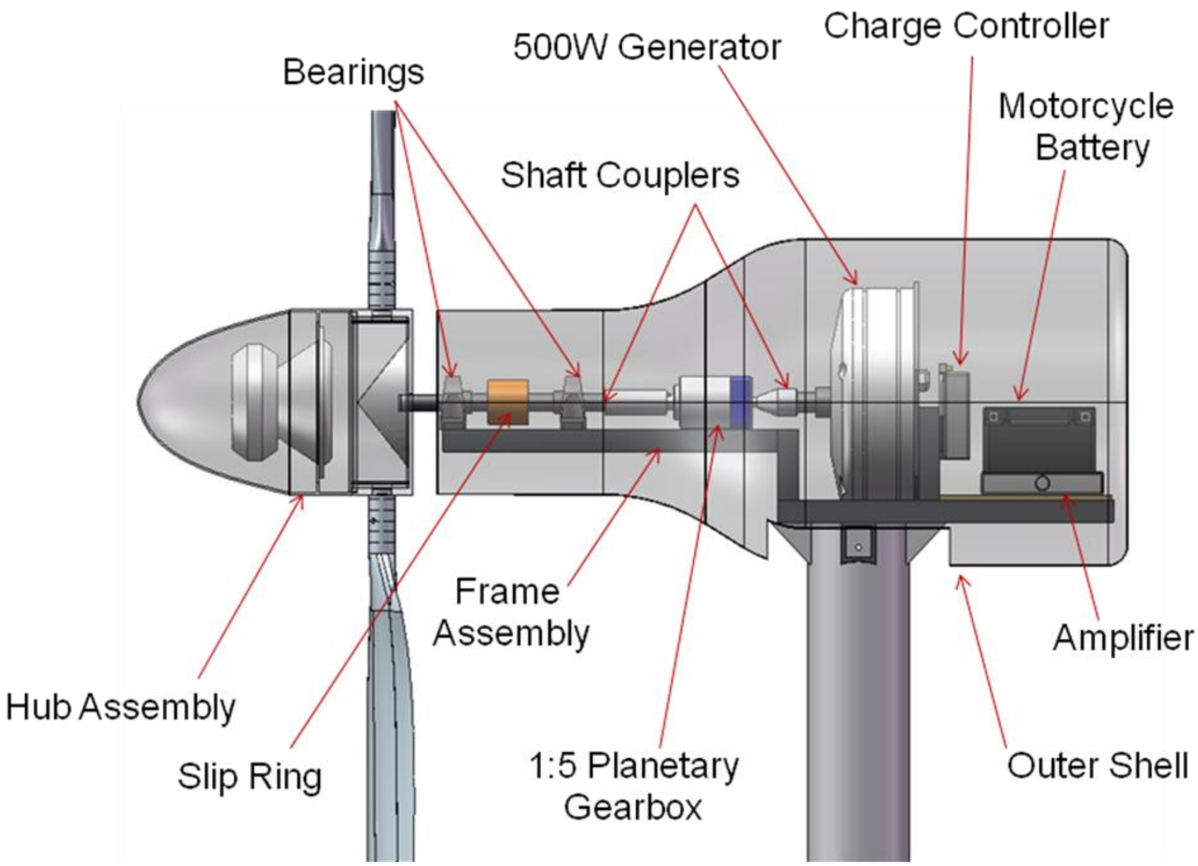

Figure 27 – Housing assembly component view

The most important component of the Housing Assembly is the Frame subassembly, shown in Figure 28. The Frame Assembly must transfer the load due to the weight of all of the Housing and Hub Assembly components to the Tower Assembly. As such, it must be strong and rigid. For these reasons, the Frame Assembly was designed to be constructed from 1”x1” square tube steel, with a wall thickness of 0.12”. While best engineering judgment has been applied in selecting a tube size that will be able to support the weight of the Housing and Hub Assemblies, it is important to note that finite element analysis (FEA) is not feasible in this case. This is because no reliable approximation for welded joints can be made in FEA software, and the complexity of the Frame Assembly exceeds the limited capabilities of the COSMOSExpress FEA package. However, the design team is confident that this tubing will result in a frame which is easily to able to support large loads, provides a flat mounting surface for components, and is also simple to fabricate and construct.

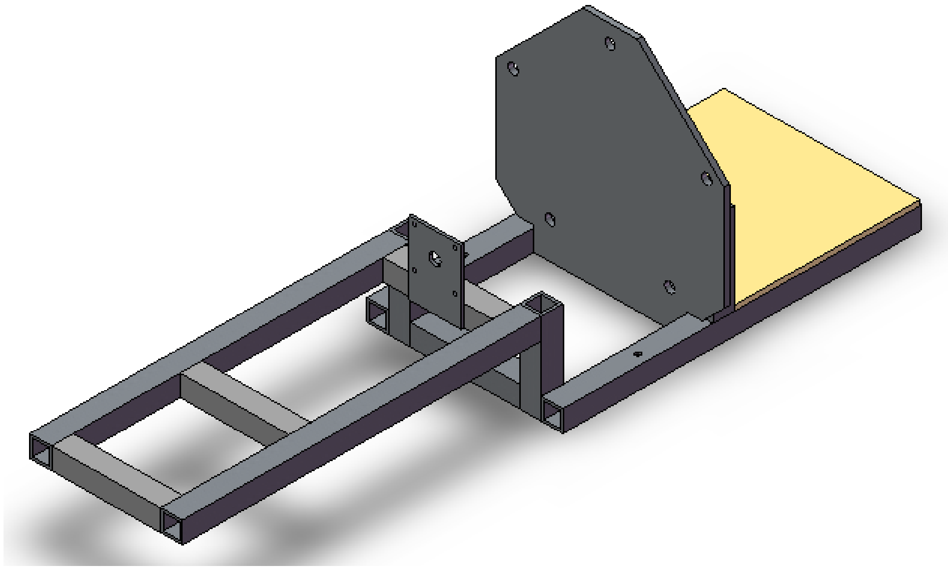

Figure 28 – Frame assembly isometric view

In addition to the tube frame, the Frame Assembly contains two mounting brackets, and a mounting shelf created from 0.25” plywood. The Shelf serves as a mounting location for electrical components, such as the Battery, Amplifier, and fuses. Plywood is an ideal material for this, because it is strong enough to support these relatively light components, and yet lighter and less expensive than a steel or aluminum plate of comparable size and thickness.

The two mounting brackets support two critical components of the drivetrain: the Gearbox and Generator. Both components are mounted via bolts which run parallel to the turbine axis of rotation, and as such a mounting bracket must be installed to support them. The Generator Mount Bracket and Gearbox Mount Bracket are shown below in Figure 29.

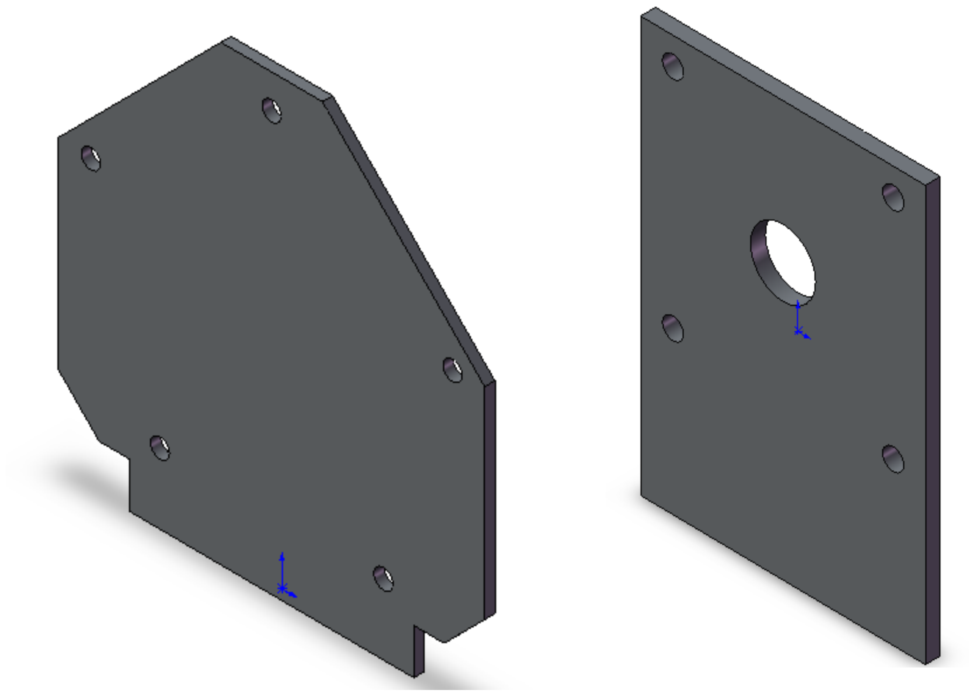

Figure 29 – Generator (left) and gearbox (right) mount bracket

The strength of each mounting bracket was analyzed using the COSMOSExpress finite element software package. The loads and constraints for each bracket are shown in Figure 30 and Figure 31. Each bracket may experience both a vertical load *F*, due to the weight of the component it is supporting, and an axial load *P*, which results from the axial lift and drag force components on the turbine blades. The load *F* is simply the weight of each component, and takes values of 2.43lb and 28lb for the Gearbox and Generator, respectively. The axial force *P* is not precisely known at this point, but a rough approximation of 85lb has been made. This is a best estimate resulting from data for the full-size NREL turbine. See appendix C for details on this approximation. Note that *P* is taken as having the same magnitude for both brackets.

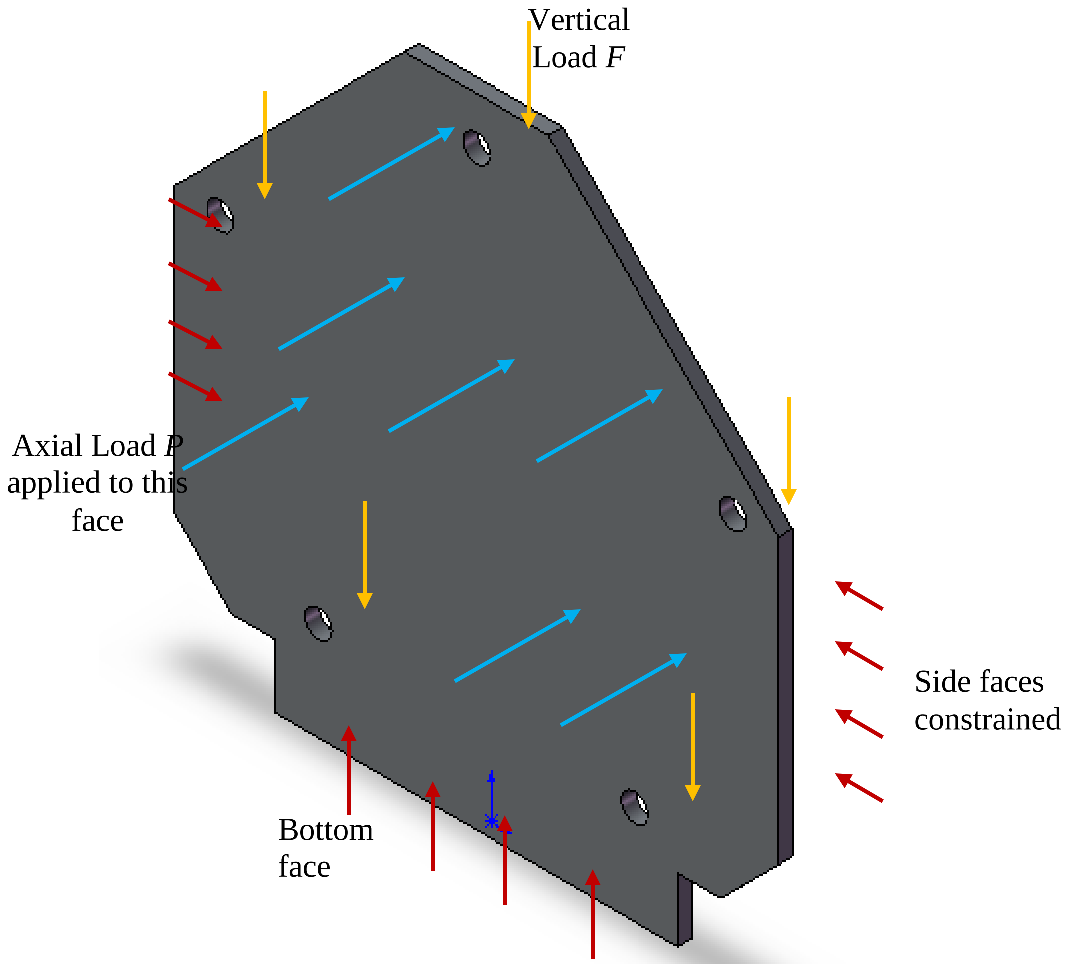

Figure 30 – Loads and constraints for generator mount bracket

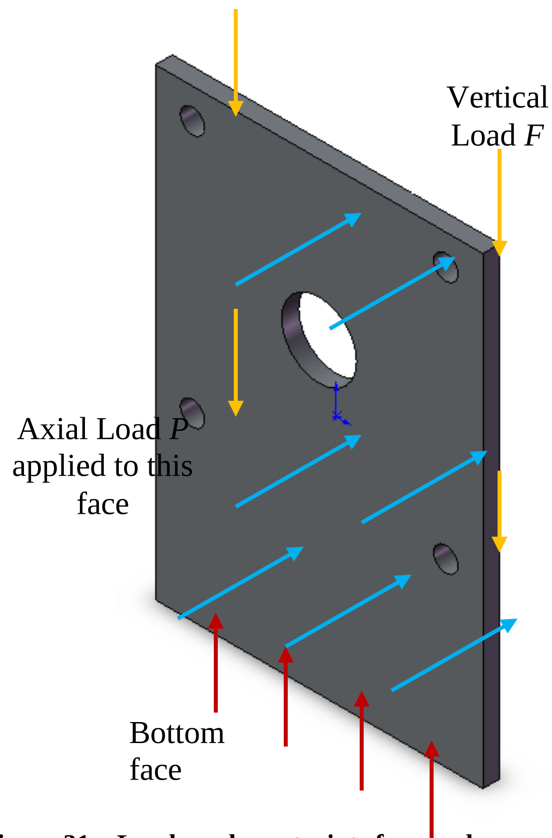

Figure 31 – Loads and constraints for gearbox mount bracket

The stress distributions in each bracket are shown in Figure 32 and Figure 33 below. It is important to note that the stress distribution will certainly be lower in the actual installation, because the brackets are welded over a much larger area than that simulated in the analysis. Consequently, the maximum stress in the Gearbox Mount Bracket was developed at the base of the bracket, where it is welded to the frame, as would be expected. In the Generator Mount Bracket, the maximum stress was developed at the bolt holes nearest the welds to the upright supports, which is a result of the conservative set of constraints. The maximum Von Mises stress for each bracket and factor of safety is shown in Table 9. From the Table, it is clear that both brackets will easily support the axial and vertical loads described.

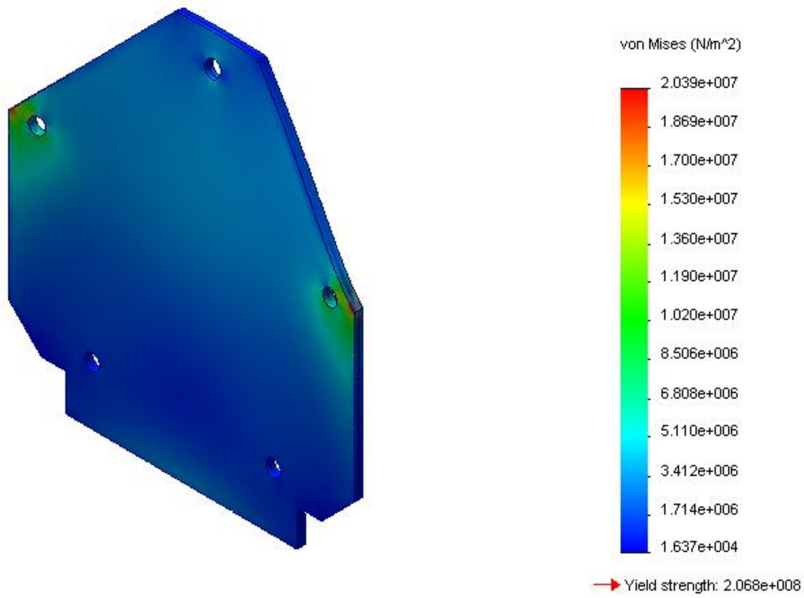

Figure 32 – Generator mount bracket stress distribution

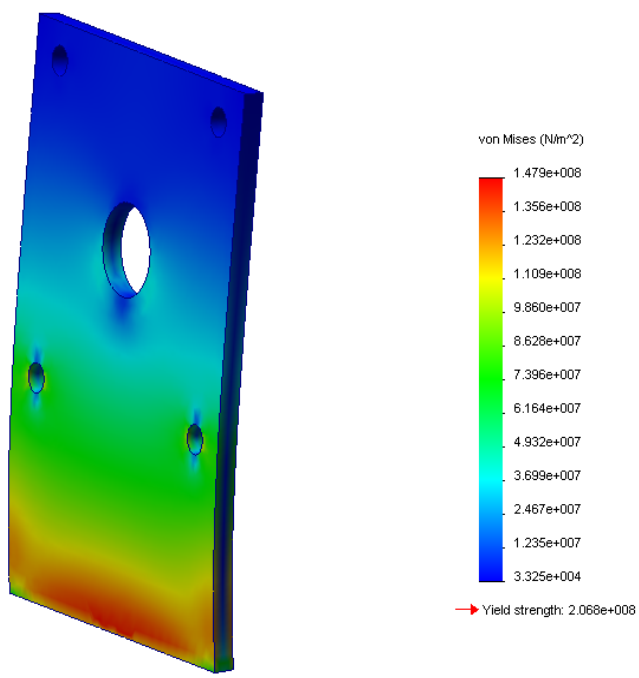

Figure 33 – Gearbox mount bracket stress distribution

Component	Maximum Von Mises Stress (MPa)	Yield Strength (MPa)	Factor of Safety
Bracket, Gearbox Mount	147.9	360 (AISI 4130 Steel)	2.43
Bracket, Generator Mount	20.39	360 (AISI 4130 Steel)	17.7

Table 9 – Summary of the safety factors

The Frame Assembly and all internal components are encased by the two Shell pieces. The primary functions of the Shell are to protect the internal components from water and contaminants, provide an aerodynamic surface for airflow after it passes through the turbine blades, divert some airflow to the Generator for cooling purposes, and lend an aesthetic appearance to the turbine exterior. Additionally, the Shell should be lightweight and able to separate into two pieces, to allow access to the enclosed components.

Both Shell pieces are shown together in Figure 34. The Shell has a circular cross section, which changes in diameter along the length of the Shell. The diameter at the Hub (front) end of the Shell is the same diameter as the Main Hub, at 8.0”. This prevents any separation bubbles in the flow as it flows from the Hub to the Shell. The Shell then smoothly widens in diameter as it progresses rearward, to a maximum diameter of 15.0”. This allows clearance for the Frame Assembly and Generator without introducing any abrupt changes in the surface, which would disrupt the flow. It is important to minimize such flow disruptions, because they can affect flow upstream, potentially to include the flow both through and before the turbine blades, and therefore potentially reducing efficiency. As a final feature, the bottom Shell piece incorporates a cutout to allow access for attachment of the Tower Assembly, as shown in Figure 35.

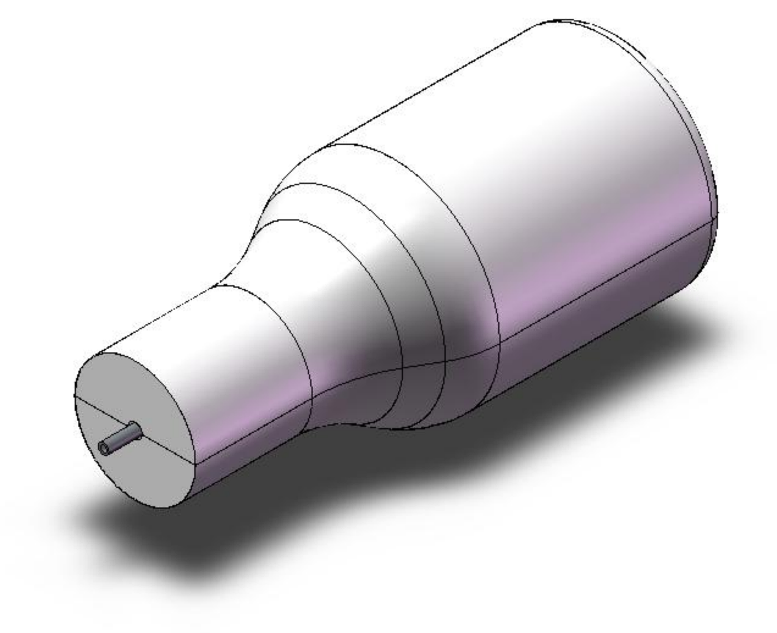

Figure 34 – Complete shell isometric view

Figure 35 – Frame assembly access cutout

Two potential materials are under consideration for the Shell. One possibility is to fabricate the Shell from fiberglass. This would require construction of a foam mold, and then applying fiberglass over the mold. The mold itself would be of a single half of the cylindrical Shell, and would be reused to create both halves of the Shell. The advantage to this method is the relative ease of creating the mold and applying fiberglass over it, which is a common and proven method of fabrication. However, this method is also extremely time-consuming in both the construction of the mold and the application of the fiberglass. Additionally, the availability of an outside shop for this type of fabrication is questionable, meaning the Shell would have to be constructed in-house.

The second material candidate is very thin (.020") aluminum sheet. This has the advantage of being lighter than fiberglass (because of the thinner wall). In addition, the fabrication may also be outsourced to an experienced sheet metal shop, which would result in a higher-quality product, as well as reduce the number of components which must be produced in-house. However, the disadvantage to sheet metal is the uncertainty surrounding its producibility. The Shell would need to be split into several smaller forms, which would then be fastened together to reach the final shape. Consequently, the cost of production for sheet metal will almost certainly be higher than that for fiberglass, although the savings in man-hours during the project fabrication phase may well outweigh this. The design team intends to seek feedback from local sheet metal shops on the manufacturability of the current Shell shape as well as its procurement cost, and make a final decision in conjunction with the project Sponsor at that time.

The majority of the mechanical components internal to the Housing Assembly belong to the turbine powertrain. These include the Bearings, Drive Shaft, Slip Ring, Planetary

Gearbox, Generator, and two Shaft Couplers. Of these, the Drive Shaft is the primary power transmission device. Its only functions are to support the weight of the Hub Assembly, provide a routing path for the speaker wires, and transfer the mechanical power generated by the turbine blades to the rest of the powertrain. The component selected for this function is an off-the-shelf commercial linear motion tubular shaft, with an outer diameter of 0.75", an inner diameter of 0.44", and is precision-ground from AISI 52100 steel.

The stress analysis for the bending load on the Shaft due to the Hub Assembly is detailed in Appendix F. From this analysis, it is expected that this shaft will exceed the strength required to support the Hub Assembly, with a maximum vertical deflection of 0.003", well within the angular deflection tolerance of the Bearings. Additionally, the Shaft will experience a torsional load at start-up, but this is expected to be trivial in comparison to the bending load generated by the Hub Assembly.

The Drive Shaft is supported at both ends by the main Bearings. These Commercial, Off-the-Shelf (COTS) roller ball bearings (see Figure 36) facilitate smooth power transmission (up to 10,000rpm), as well as transfer some of the bending load in the Drive Shaft to the Frame Assembly. The wind turbine will operate in an outdoor, windy, dusty environment, and as such, dust contamination is a very real possibility. Therefore, when selecting the Bearings, it was important that the chosen component be sealed on both sides of the race. Finally, the selected Bearing must be able to support both the vertical (radial) load developed by the weight of the Hub Assembly, as well as any axial loads generated by the turbine blades. The chosen bearing is rated for a maximum radial load of 2,860lb, far in excess of the load generated by the Hub Assembly.

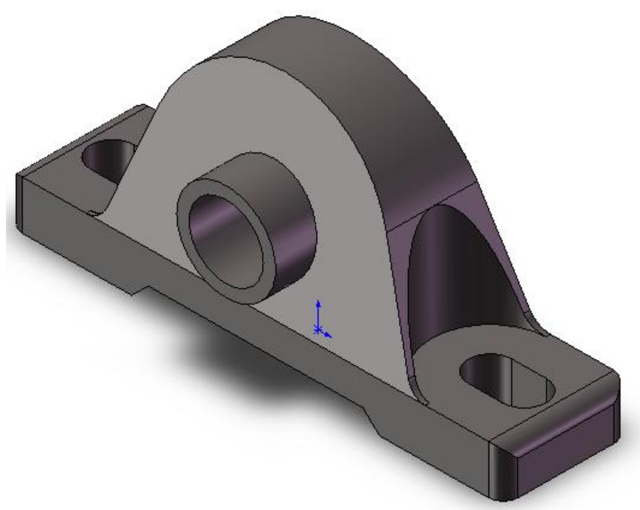

Figure 36 – Steel Ball Bearing isometric view

After the mechanical power developed by the turbine blades passes through the Drive Shaft, it is transferred to the Gearbox via a shaft coupler, and then from the Gearbox to the Generator by a second shaft coupler. Both of these couplers will be machined in-house to fit the various diameters and attachment mechanisms of the Drive Shaft, Gearbox, and Generator. Both components will be machined from 6061 aluminum alloy. The Gearbox Shaft Coupler and Generator Shaft Coupler are shown in Figure 37:

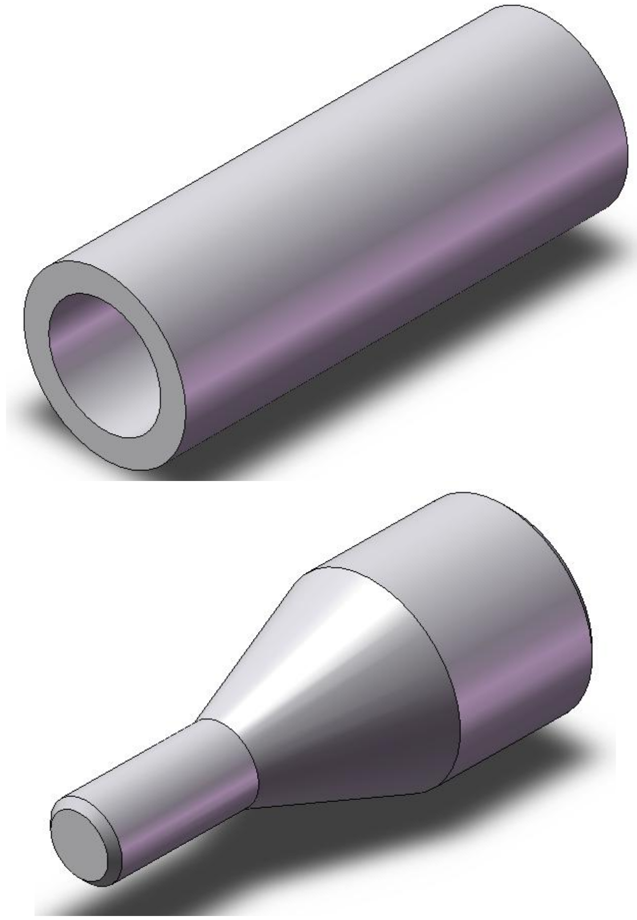

Figure 37 – Gearbox (top) and Generator (bottom) shaft couplers

The Gearbox Shaft Coupler is a simple female-female design, with ¾-10 threads on one end (to connect to the Drive Shaft), and a keyed 16mm-diameter hole on the opposite end, to mate with the keyway on the input shaft of the Gearbox. In contrast, the Generator Shaft Coupler is a male-female coupler, with a 0.50" male shaft on one end, to mate to the output coupler on the Gearbox. The other end of the coupler is a tapped M24 hole, to mate to the threads on the input shaft of the Generator. Between these two ends is a gently tapered midsection, to reduce any torsional stress concentrations developed within the part.

The primary loading mechanism for both couplers is a torsional load experienced at start-up, at the time when the turbine blades begin producing torque, but the Generator has not yet started to turn. However, as noted above, this load is expected to be trivial, and furthermore cannot be adequately quantified until the Generator has been purchased and measurements of start-up torque have been made. At that time, any increases in coupler thickness or changes in geometry may be made if necessary.

The Planetary Gearbox, mated to a shaft coupler on either end, serves to increase the rotation speed of the Generator with respect to the turbine blades. This allows the

Generator to operate in the RPM range where it is most efficient, thereby producing more electrical power. A planetary gearbox also features concentric input and output shafts, which permits the Generator to remain in line with the rest of the drivetrain, and consequently allows for a more streamlined housing design.

The gearbox selected for the demonstration wind turbine is manufactured by Anaheim Automation, a trusted maker of DC motors and gearboxes (see Figure 38). It offers a 1:5 speed increase from the input to output shafts, and can accept axial loads of 136lb, as well as radial loads up to 189lb. Both of these ratings are significantly greater than the estimated axial and radial loads of 50lb and 85lb, respectively. Furthermore, the Gearbox is rated for an output torque of up to 38 ft-lb. While the start-up torque of the Generator is not currently known (see above), it is likely to be considerably less than this rating. Therefore, it is expected that the chosen Gearbox will be able to adequately transmit power to the Generator over the entire lifespan of the wind turbine.

Figure 38 – Planetary Gearbox photograph

The final powertrain component is the Generator, pictured in Figure 39. The chosen generator is of the permanent magnet variety, which is particularly suited for wind turbines, and many such generators are in use in small commercial wind turbines the world over. The electrical operation and specifications of the Generator are discussed in detail in Section X.F. From a mechanical standpoint, the most significant aspect of the Generator is its weight; at 28lb, it is the heaviest single component in the wind turbine. However, the Generator is securely mounted to a bracket within the Frame Assembly, and the strength of this bracket has been verified in Figure 32.

Figure 39 – Permanent Magnet Generator

Heat generation is the other significant consideration in the operation of the Generator. Unfortunately, at this time, the generator specifications (efficiency, maximum operating temperature, etc.) necessary for a complete thermal analysis are not available. For now, the wind turbine design will accomplish thermal management of the Generator via cooling ducts, to be implemented on the final design of the Shell. When the Generator has been procured, efficiency testing will be conducted to determine the data necessary for a complete thermal analysis, including sizing and placement of the Shell ducts.

E. Details of Tower

The Tower Assembly, pictured in Figure 40, serves as the primary support structure for the Housing and Hub Assemblies. It must support the weight of the Housing and Hub, as well as absorb any horizontal loads generated by wind or the operation of the turbine itself. These horizontal loads create a tipping moment at the top of the Tower, and so it must be stable enough to resist this moment. As a final requirement, the Tower must be separable from the Housing Assembly, to facilitate transportation of the turbine.

Figure 40 – Turbine tower assembly isometric view

The initial iteration of the Tower design used a support truss of square footprint (see Figure 41), rather than a circular tube such as that shown in Figure 40. It was initially judged that a truss of tube steel would be easiest and least expensive to construct. However, Housing Frame, to which the Tower Assembly must mount, has an overall width of only 9”. This does not allow for a sufficient ground footprint without mounting the legs at an angle to the vertical axis. However, it was also determined that the legs must be angled in to support the tower in two directions, which created the unsightly splayed-legs configuration shown in Figure 42. In addition to its lack of aesthetic appeal, this design was determined to be insufficiently stable without a significant amount of support members (a truss configuration such as that found in bridges or building rafters). These would be difficult to construct at the proper angles and would add significantly to the amount of cutting, grinding, tube-fitting, and welding required for construction.

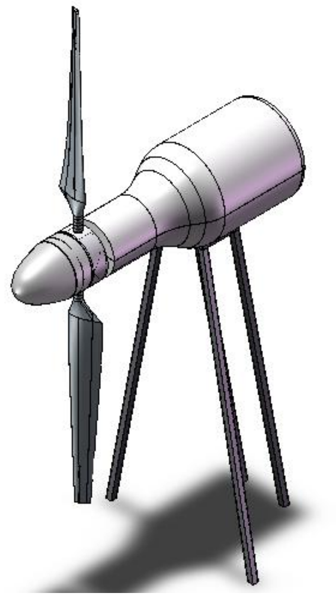

Figure 41 – Wind turbine with Truss-style tower

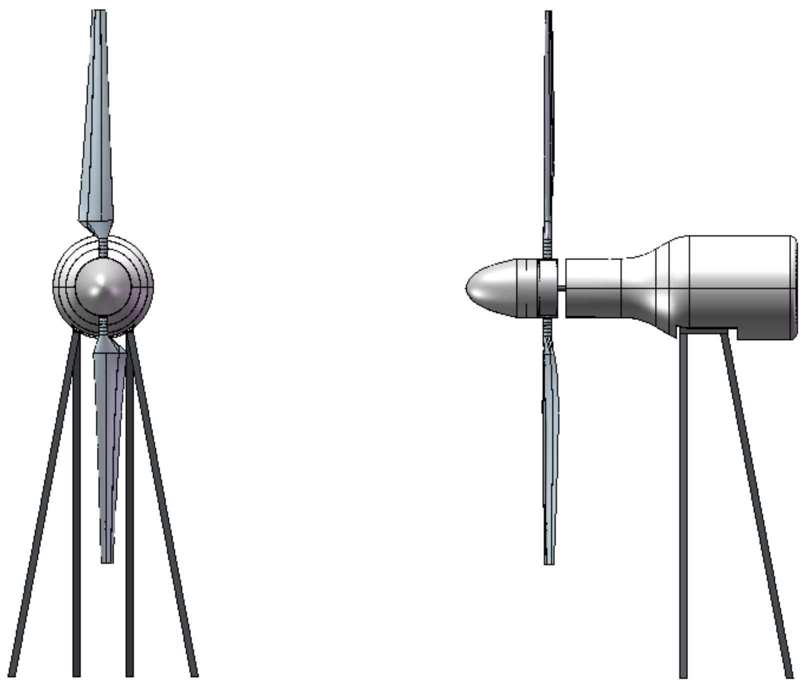

Figure 42 – Truss style tower Front and Right Views

As a result of these factors, the Tower was redesigned to incorporate a single circular support column, supported by right angle brackets at the top, and long, flat feet at the base. This drastically increased both the aesthetic appeal and the ease of fabrication of the Tower Assembly. The Support Column, shown in Figure 43, is an aluminum tube of 5" outer diameter, 0.25" wall thickness, and overall length of 50". Aluminum was selected because it is considerably lighter than steel, easy to machine, and is still much stronger than the maximum compressive stress developed by the weight of the Housing and Hub Assemblies, based on preliminary calculations. A similarly-sized length of plastic (PVC or similar) plumbing piping is also a candidate for selection, and this determination will be made once the maximum operating blade and wind loads have been determined for the turbine.

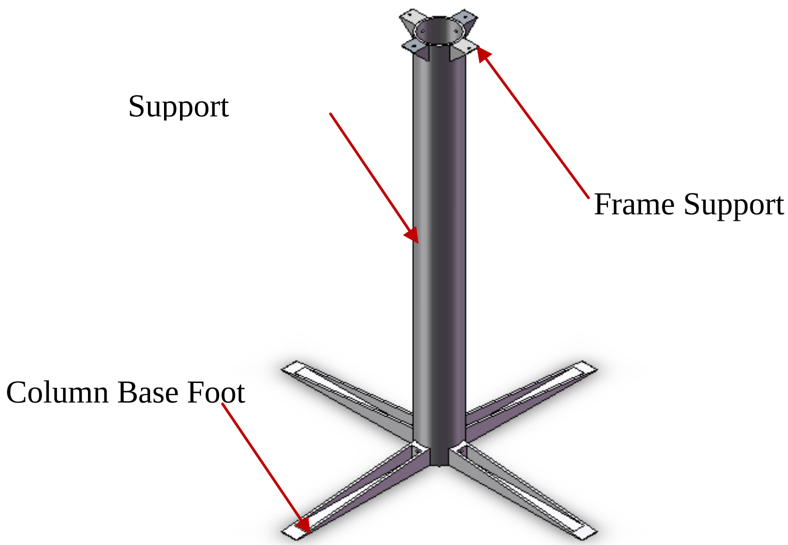

Figure 43 – Column-style tower assembly components

The four Frame Support Brackets, bolted to the top of the Support Column, are designed to transfer the load of the Housing and Hub Assemblies from the Housing frame to the Support Column. They will be machined in-house from 2024 Aluminum Alloy (or similar). The Bracket, shown in detail in Figure 44, features two ¼" through holes at right angles to each other, for attachment to the Support Column and Housing Frame. One end of the Bracket (see Figure 45) has a concave radius machined to match the outer diameter of the Support Column, so that the bracket will mount flush to the surface of the column.

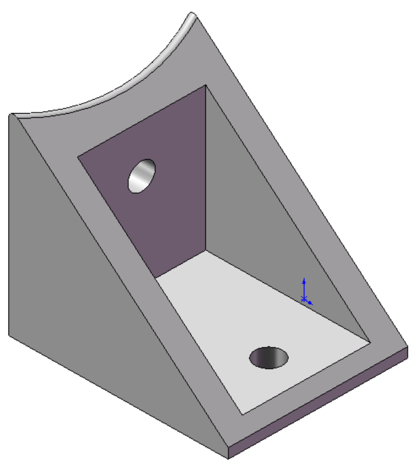

Figure 44 – Frame support bracket isometric view

Preliminary finite element analysis (FEA) of the Frame Support Bracket was conducted using Solidworks 2007 and COSMOSExpress. The component was constrained at the through hole for mounting to the Support Column, and the applied load of 120 lb was applied to the top face of the component, as shown in Figure 45. This load is an overestimate of the total weight of the Housing and Hub Assemblies, which currently weigh approximately 107 lb, as a best estimate. Nevertheless, this load was chosen for the purposes of conservative estimation and to allow room for future weight increases if necessary.

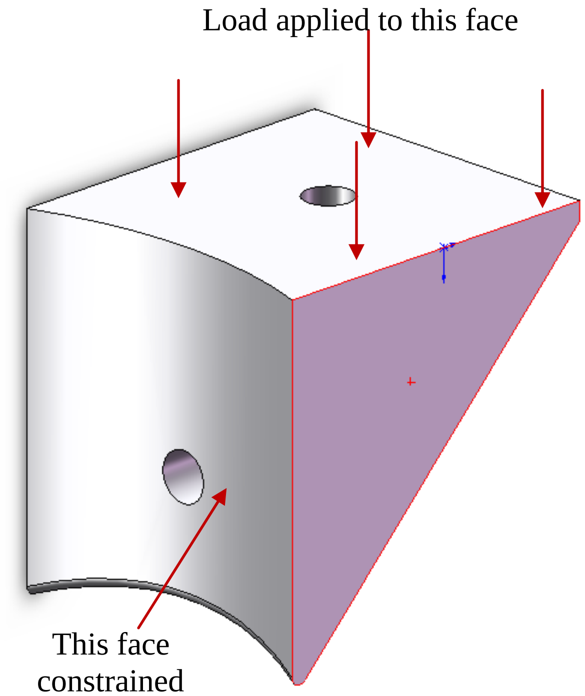

Figure 45 – Loads and restraints used in COSMOSExpress

The stress distribution in the model, as a result of the FEA, is shown in Figure 46. The maximum Von Mises stress predicted by the analysis occurs near to the Column mounting through hole, as expected, and has a magnitude of 41.69 MPa. With a yield stress of 324 MPa for 2024-T351 aluminum alloy, this stress results in a safety factor of 7.8. This result was deemed reasonable because of the considerable thickness of the part in the region of the Column mount bolt hole, as well as the selection of a high-strength aluminum alloy. As such, it is believed that this component will be able to withstand any reasonable loading from the Hub and Housing Assemblies, while still allowing room for fatigue strength reduction during the wind turbine’s projected lifetime.

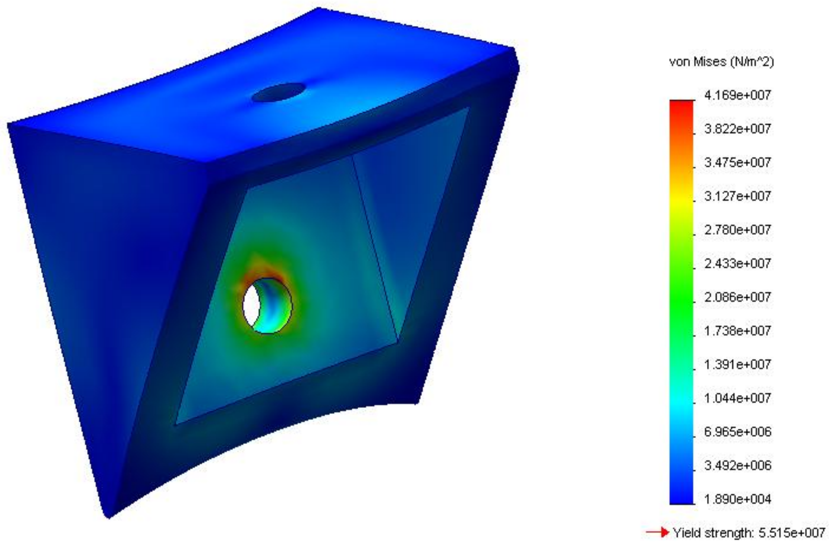

Figure 46 – FEA Results – Stress distribution in Frame Support Bracket

The Column Base Foot is the final component of the Tower Assembly. Its primary function is to resist the tipping moments generated by wind and turbine operating loads on the Housing and Tower. The current design, shown in Figure 47 below, is geometrically very similar to the Frame Support Bracket, with the exception that its base has a length of 18”.

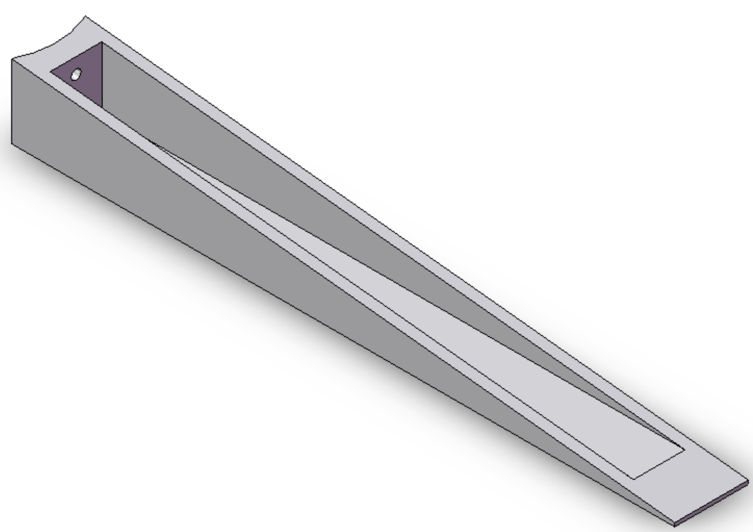

Figure 47 – Column Base Foot isometric view

This component was analyzed to ensure it would not fail in its primary function of resisting tipping moments in freestanding as well as fixed installations. The free body diagram of the Tower Assembly under load is shown in Figure 48, along with the relevant dimensions (in inches).

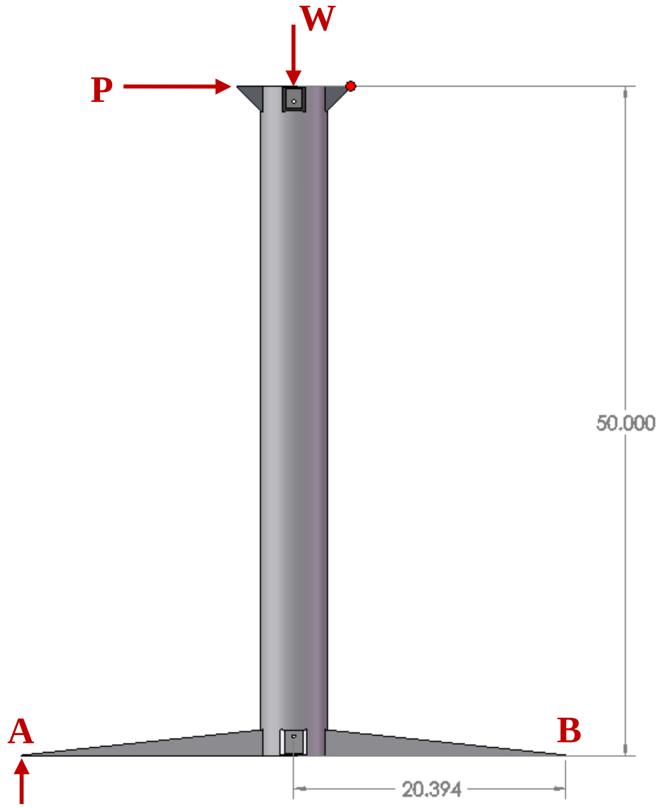

Figure 48 – Tower assembly loading and dimensions

The load W is the weight of the Hub and Housing Assemblies, estimated as 107 lb. The horizontal load P is not precisely known at this point. However, it has been estimated that this load will not exceed 85 lb, using data from the full-size NREL 10m wind turbine. To calculate the load P_{tip} (located at point P), a simple sum of the moments acting around point B may be taken, with the condition that at the tipping point, load A=0. This sum of moments results in the following expression:

$$(107lb)(20.4")-P_{tip}(50")=0$$

From this equation, the tipping load *P* can be computed to be 43.7lb. This does not satisfy the condition that P_{tip}>85lb for a freestanding structure. However, when the wind turbine is in use, it will be bolted to a fixed surface (such as the lab floor) at or near point A. An axial tensile load of 85-43.7=41.3lb is trivial for a mounting bolt of diameter 0.25" or larger, therefore, it is not expected that tipping will be an issue for a fixed installation. If the turbine is operated in a freestanding installation (such as for a temporary demonstration), the tipping load may be neutralized by using a counterweight (such as a sandbag) at point A. Additionally, an alternative, longer Column Base Foot may be considered, pending sponsor approval. This would likely be fabricated from wood to reduce raw stock costs, and would be approximately 40" long. At this time, however, the Tower assembly, in a fixed installation, will withstand any reasonable tipping moment without question.

F. Electrical Design

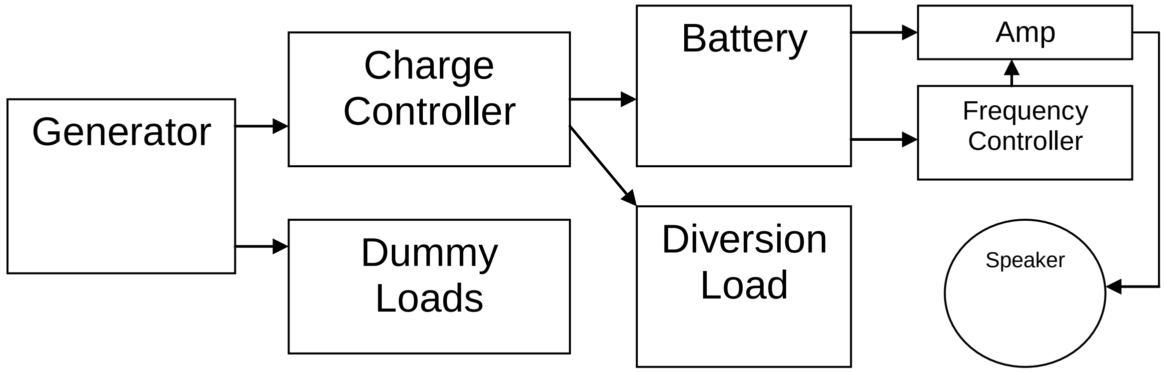

Figure 49 – Electrical Circuit Diagram

The AFC must be powered by internal sources which is kept charged by the generator run by the wind turbine. The selected generated is the GL-PMG-500A 3-phase AC permanent magnet generator produced by the Ginlong corporation. This generator is capable of generating 12 volts at around 100 rpms. Connected to the generator will be a wind turbine charge converter.

The charge converter is simply a DC-DC converter and will regulate the voltage down to 12 volts that will be connected to the AFC components. Excess power will be used to power dummy loads for demonstration purposes. Additionally a wattmeter will be used directly attached to the generator to visually show how much power the wind turbine is measuring.

Also connected to the charge converter is a diversion load that the charge converter will switch power too once the battery is fully charged to prevent over-charging. Once again, the diversion load will consist of demonstration components such as light bulbs, etc.

The battery that powers the AFC components is charged by the charge converter. The function generator and speaker amplifier are directly connected to the battery. To transfer the electrical signal to the speaker which is housed in the rotating hub a one circuit slip ring will be mounted on the main shaft. The amplifier will connect to the slip ring and the slip ring will connect to the speaker. There may be some small amount of noise introduced into the signal because of the physical contact of the brushes on the slip ring, but due to the nature of the speakers inability to pick up extremely high frequencies it was deemed unnecessary to filter the signal after the slip ring connection.

The speaker is a mid bass 6 inch speaker with an extra large magnet. This allows it to deflect up to 8mm during operation instead of the normal 3mm most speakers are capable. This speaker's nominal frequency range is right around the targeted 100Hz which means it will perform well for the active flow control device.

VII. Redesign

A. Blades

From the wind tunnel testing the unexpected discovery that dual rows of active flow control performs better than either of the single row cases led to a blade redesign. Additionally a superior construction technique was found which would reduce the complexity and manufacturing time.

The separation was found to be at around 15% chord and 55 % chord depending on if it was leading edge separation or trailing edge separation. For the active flow control to have an effect it must interact with the flow over the airfoil that is still attached. This means the active flow control must be set at a location before the separation occurs. The team chose to set the leading edge row at 10% chord and the second row at 45% chord. The blade design now needed two sound chambers at these locations which complicated the construction. These sound chambers are shown in Figure 50.

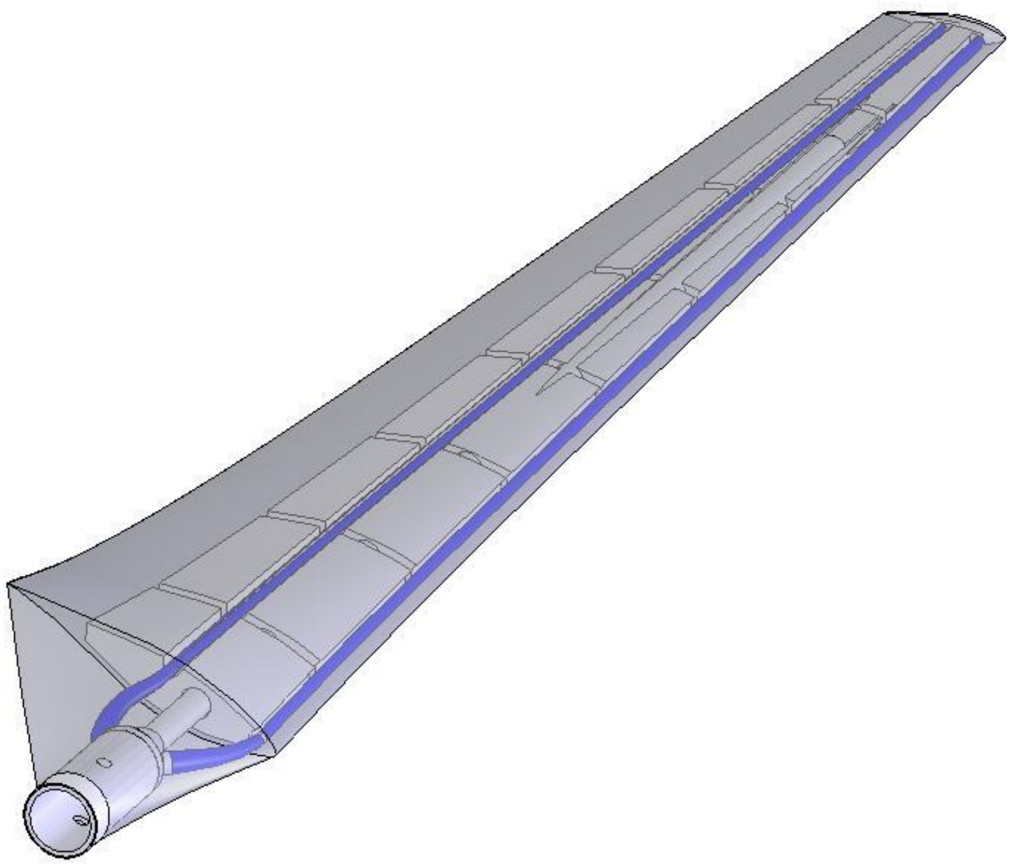

Figure 50 - Sound Chambers (blue)

The problem was simplified by changing the construction method used. The team decided to have the blades printed out using a rapid prototype machine which lays down a thin layer of ABS plastic using a computer controlled printer head to create the shape. This allowed us to have almost unlimited complexity of the internal structure of the blade. This meant the team was able to build in the sound chambers into the blade and have them printed out.

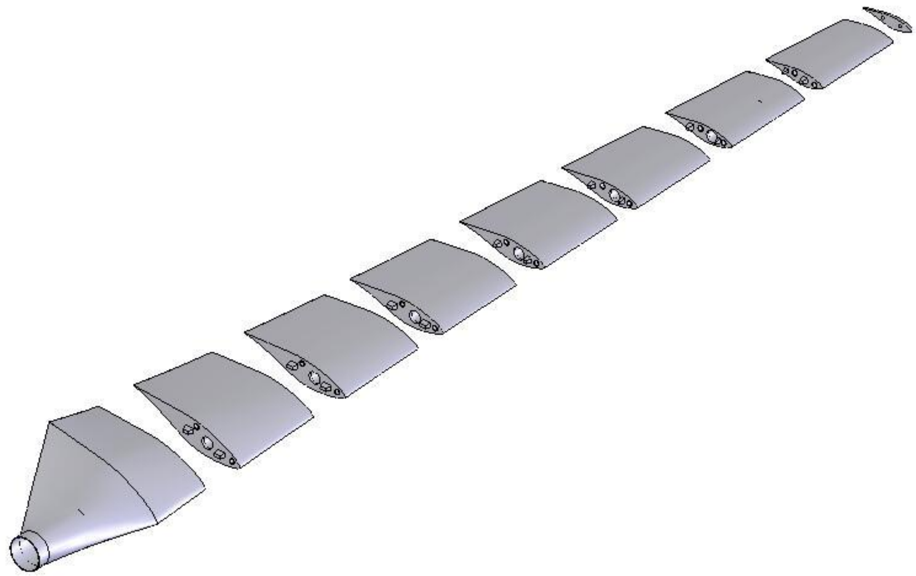

Figure 51 - Blade sections broken up

One problem with this method is the maximum size a part that could be printed in the machine. It was not capable of printing the entire blade out in one piece. Also the machine only has eight inches of travel in the vertical direction. This forced us to cut up the blade into a total or nine sections shown in Figure 51 that the team would have to attach to each other later. The team proceeded to build in locating features into each section that would help in lining up the various sections when they were being attached to one another.

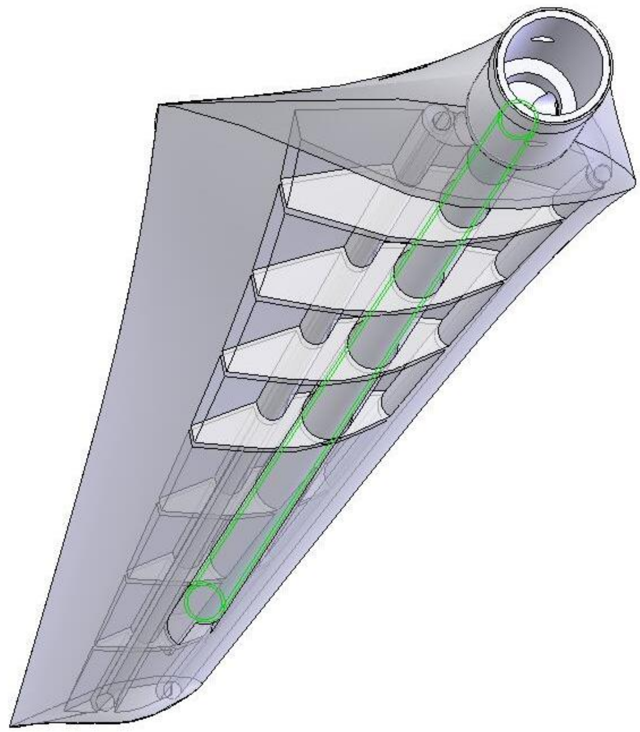

Figure 52 - Blade Spar (in green)

The strength of the blade was a large concern as none of the members have had any experience working with the ABS plastic. A carbon fiber spar was designed to run almost the entire length of the blade. This is shown in Figure 52. It has the additional benefit of helping with the blade sections alignment during construction because each section could be slid onto and glued to the spar one at a time. The forces the spar would absorb had to be transported to the blade mount for maximum strength and rigidity. This was a complication because whatever part was designed would still need to allow the sound and air to travel from the internal tube at the root of the blade, but into the two active flow control rows that ran the length of the blade.

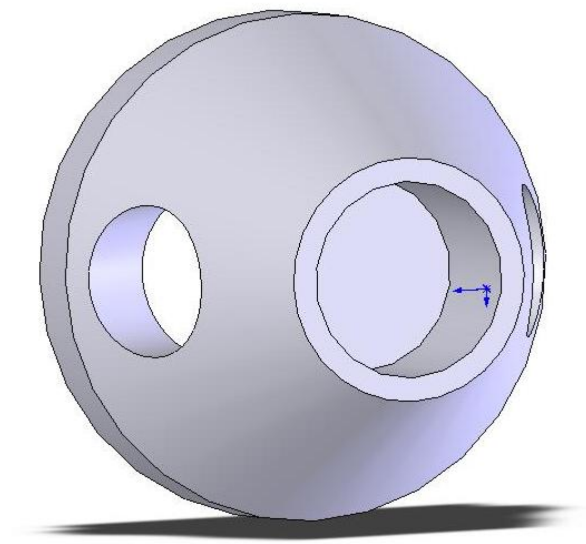

Figure 53 - Spar Coupler, front view

This led to the design of the spar coupler seen if Figure 53. This spar coupler attached to the spar at one end and also closed the spar off from any sound or air injected into the blade for use by the active flow control tubes. Then the spar coupler would attach to the root tube of the blade which would effectively transfer the loads experienced by the spar to the blade mount. The center portion of the spar coupler would be hollow with two holes drilled in the side at angles which connected up to the built in chambers of the blade.

Additionally a slight change in how the blades were secured to the hub happened as well. Instead of having the set screw on the outside of the blade, it would be on the back of the hub and secure the blade by pressing on the tube which slides into the hub holders. The newly designed blade would be easier to build and be more accurate to the CAD design since there is less room for human error. The price of the blade would be comparable to the original price expected.

B. Generator Change

Figure 54 - Wind Blue DC-520 Generator

It was requested that a generator with a smaller diameter be chosen by the project sponsor due to fears of aerodynamic inefficiencies caused by the originally selected 12-inch diameter generator. With a smaller diameter generator the outer shell of the turbine could be redesigned to maintain the same diameter as the turbine hub. This would allow for the best aerodynamics. The Critical Design Report was written in December and since then a graduate student working with the project sponsor had calculated the expected rpms and torque from the blades designed for this project. Figure 55 shows the expected rpms for various wind speeds. These values led to the selection of the Wind Blue DC-520 PMA High Speed generator. This new generator is shown in Figure 54.

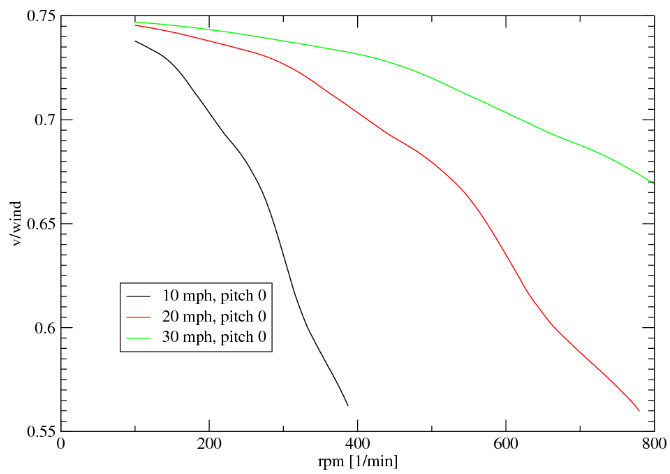

Figure 55 - RPM vs. Wind

Since the generator changed the method it is attached to the frame had to be changed as well as the shape of the frame could change. The new generator would be attached to the frame by two brackets shown in Figure 56.

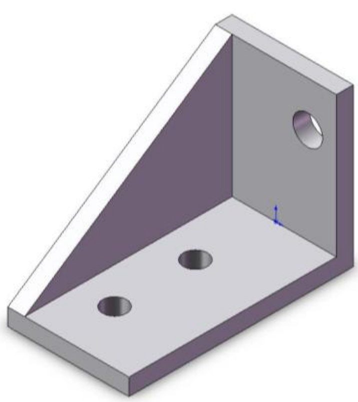

Figure 56 - Bracket for generator mount

C. Outer Shell

Two major changes were made to the Shell from the original design at CDR (Critical Design Review). Most importantly, the Shell was re-shaped to a smaller diameter. Because the Generator was changed to a much smaller unit post-CDR, the Shell could be shrunk to a uniform diameter, shown in Figure 57 below. The change in Shell diameter was the primary reason for the change to the smaller WindBlue generator. The new Shell is also more easily manufactured because it is a less complex shape. The second major change in the Shell design was the decision to fabricate the Shell from sheet metal. The new, less complex design meant that local sheet metal shops had the ability to produce the design. This was considered advantageous for several reasons, primarily because of the labor savings versus hand-laid fiberglass, as discussed earlier.

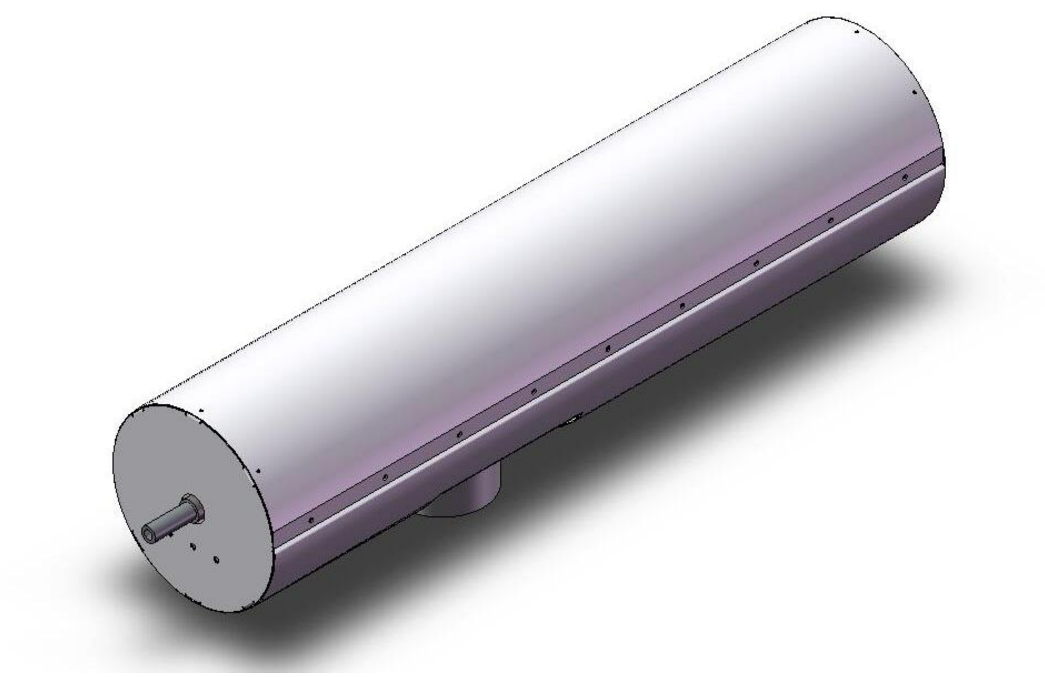

Figure 57 - Shell Assembly Isometric View

The current Shell Assembly is split into four pieces: two end caps, a top panel, and bottom panel. The four panels are fastened using PEM brand sheet metal nuts and screws, allowing for easy assembly with only a simple screwdriver. A detail view of the Shell assembly method is shown in Figure 58 below. The modular design and PEM fasteners allow the operator to remove the top panel at any time, as seen in Figure 59, allowing for easy access to the turbine's internal components. All Shell Assembly panels are fabricated from 0.040" thick aluminum sheet (5052 aluminum alloy), which is both strong and light, and all panels were designed in accordance with sheet metal best practices, ensuring tight fit without interference.

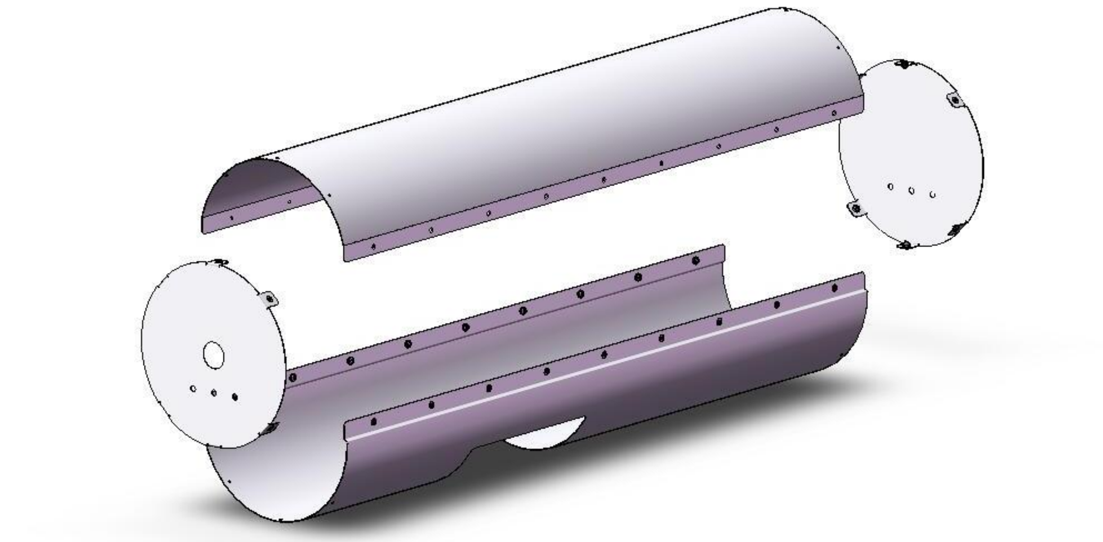

Figure 58 - Shell Assembly Method

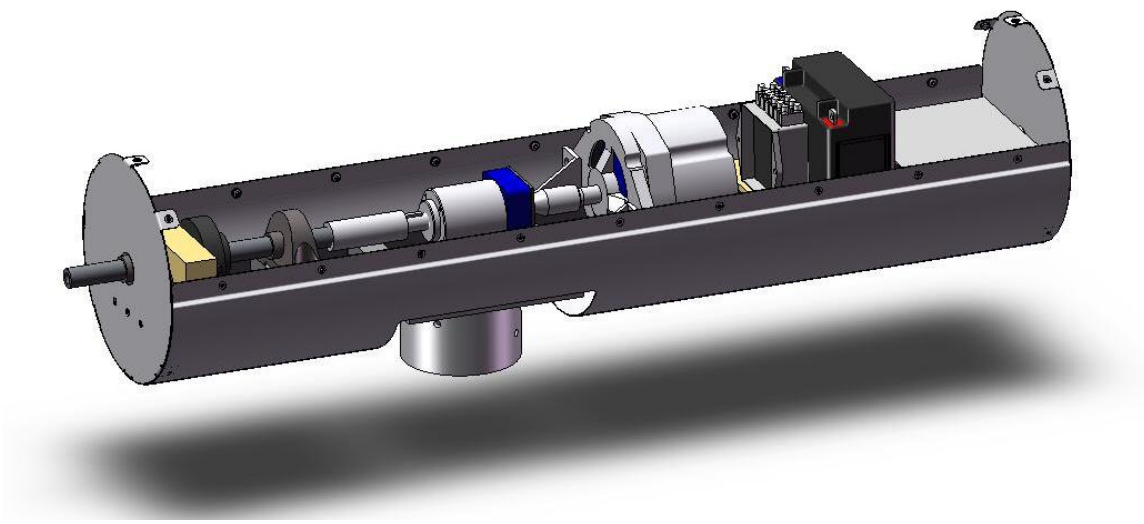

Figure 59 - Shell Assembly, Top Panel Removed

D. Tower and Base

Once the turbine project had passed the CDR milestone, the design of the Base and Tower were re-evaluated. The brackets which fasten the Tower to the Frame Assembly were deemed too difficult to manufacture in-house, and outside machining was similarly considered too expensive. Therefore, a new bracket was created, which would still serve the purpose of fastening the Frame Assembly and Tower, but which would also be simple to fabricate.

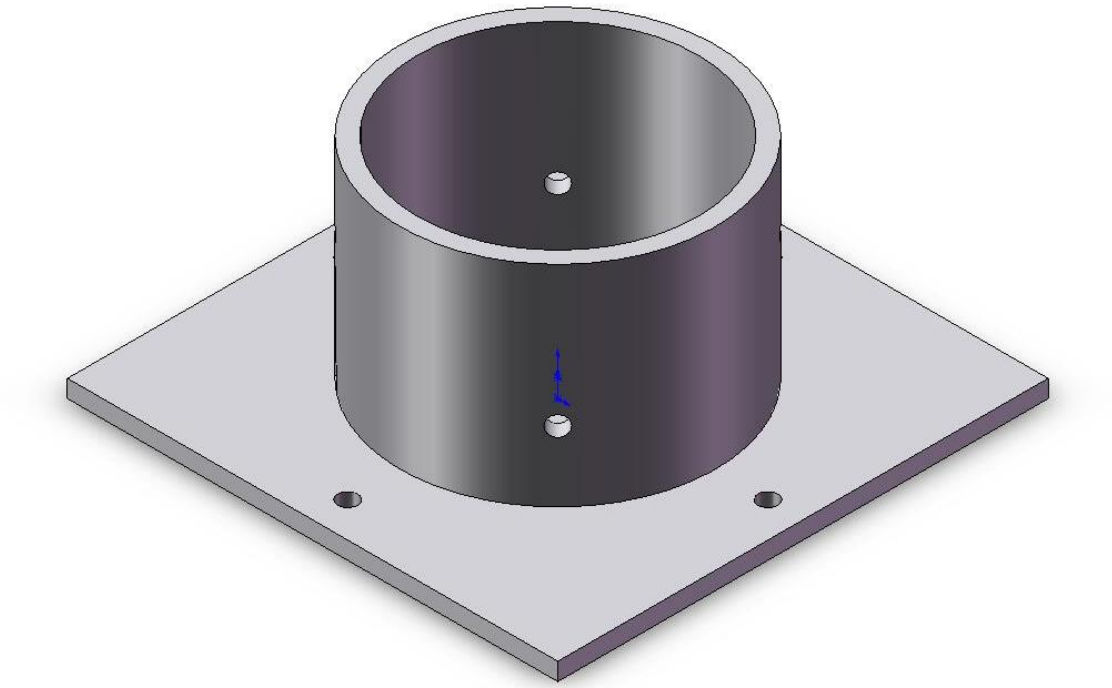

Figure 60 - Redesigned Tower Mount Bracket Isometric View

The new Tower Mount Bracket may be seen in Figure 60 above. It consists of an aluminum tube, honed to an inside diameter just larger than the Tower outside diameter. This tube is welded to a square plate. Both the plate and tube have through holes for fasteners. The Tower Mount Bracket is fastened to the Frame Assembly using the holes on the plate, and the Tower is then inserted into the tube. Carriage bolts are then inserted into matching holes on the tube and Tower, which prevents the Tower from rotating inside the tube. Because the Tower Mount Bracket is constructed from two separate pieces of aluminum and then welded into the final part, it is easily fabricated using standard machining processes and welding methods.

The turbine's supporting legs were redesigned for the same manufacturability reasons as the Tower Brackets. In addition, early testing of four-legged designs proved to be too unstable for reliable operation. As a result, the legs were replaced with a single Base created from MDF (Medium-Density Fiberboard) and other woods. The new Base is shown fastened to the Tower in Figure 61 below.

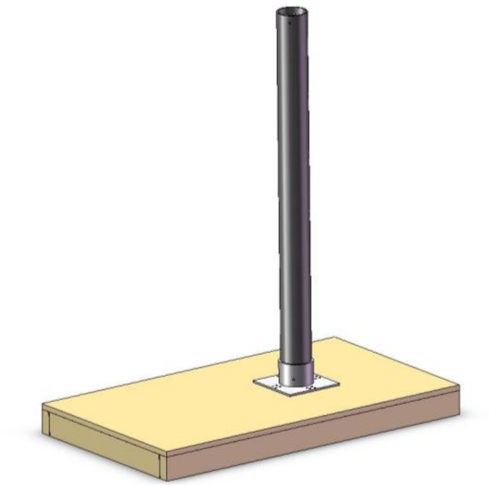

Figure 61 - Isometric View of Tower with Redesigned Base

In the Figure above, the Base is fastened to the Tower using a second bracket, the Base Bracket. This bracket is nearly identical in design to the Tower Mount Bracket. The only difference between the two brackets is the type of holes drilled on the flat plate. The Base Bracket has an array of 16 countersunk holes on the plate, which are aligned with a similar array of through holes on the Base. This ensures that the Tower is securely mounted to the Base, and reduces the chance of individual bolts pulling through the wooden Base. An isometric view of the Base Bracket is provided in Figure 62 below for reference.

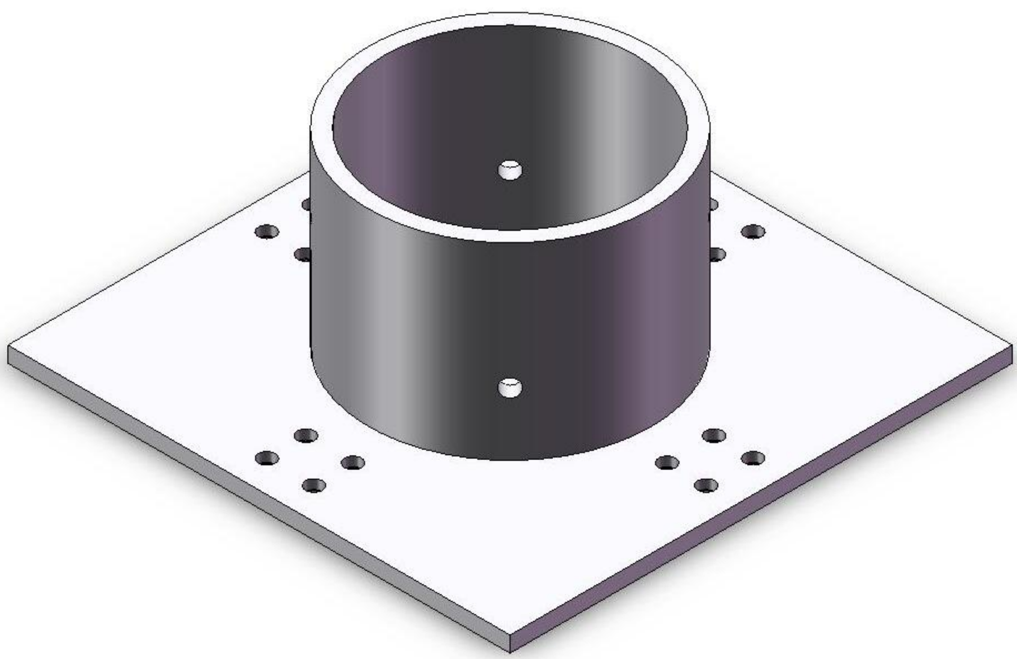

Figure 62 - Isometric View of Base Bracket

E. Frame

Due to the change in generators discussed in Section VII.B, the Frame was redesigned post-CDR. The WindBlue generator is much smaller in diameter than the former generator; therefore, the Frame was re-sized to accommodate it. The forward section of the Frame (everything from the Gearbox Mount Plate forward) is essentially the same. However, the "step" that existed to contain the Generator in the old Frame design has been removed, and the Frame is now a simple ladder design, as seen in Figure 63 below. This has benefited the turbine design in numerous ways. The new Frame is now much stronger in bending, because the elimination of the step in the Frame has eliminated a stress concentration. Overall, it is now expected that the Frame will be more resistant to bending moments than the old design. Additionally, the new Frame requires seven fewer tubes than the old design, greatly decreasing the assembly time.

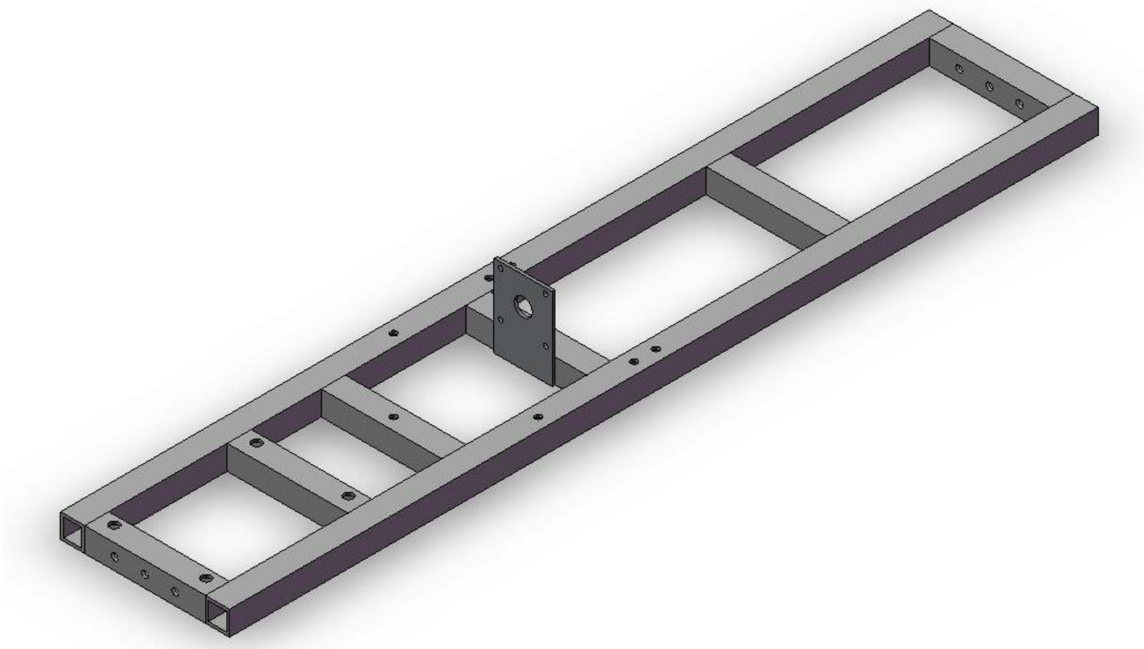

Figure 63 - Redesigned Frame Isometric View

F. Electrical

The goal of the prototype turbine's electrical design differs from that of most commercial wind turbines. In commercial turbines, the primary objective is the generation of power for consumer use. In the prototype turbine, however, the primary objective is generating enough electricity to charge a small battery, which is then used to power the Active Flow Control system. Therefore, the electrical system was redesigned to focus on this objective. The primary system components are outlined in Table 10 below:

Table 10 - Summary of Electrical System Components

Component	Manufacturer/Part No.	Function
Generator	WindBlue Power/DC-520	Generate electrical energy from blade rotation
Diode	WindBlue/REC-DEL	Convert AC current to DC
Charge Controller	SES Flexcharge/NC-25A	Regulate DC voltage to charge Battery
Battery	Generic	Store energy for AFC consumption
Power Meter	Annex Depot/HB404	Measure power produced by Generator
Amplifier	Sonic Impact/5065	Amplify sound signal and relay to speaker
Speaker	Tang Band/W6-1721	Generate sound waves for AFC operation

The selected generator is described elsewhere in this report. The WindBlue generator's output is a three-phase AC signal, which greatly reduces the size of the current carrying wires. However, the AC current must be converted to a DC current before it can be used to charge the battery. This task is performed by a three-phase bridge rectifier diode, shown below in Figure 64. The selected diode, while sold by WindBlue, is actually an aftermarket replacement for the diode contained in Delco brand automotive alternators. This means that the diode has a proven record of durability and performance. In addition, the diode is rated to 150 amps, which is in far excess of the maximum current produced by the generator.

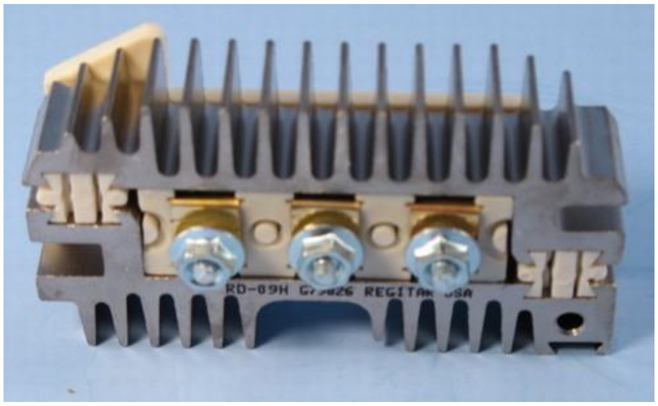

Figure 64 - Three-Phase Bridge Rectifier Diode

After the electrical current is converted to DC by the diode, it is fed to the charge controller. The charge controller, shown in Figure 65, regulates the voltage from the diode to one that is suitable for battery charging. In the case of this system, the battery is a 12V model, and the charge controller is therefore set to charge it at a nominal voltage of 14.4V. If the potential created by the turbine is less than this value, then the charge controller opens the circuit, allowing the generator to rotate freely. This is important because with no load on the generator, it is able to accelerate more quickly to a rotational rate which is suitable for battery charging. However, if the voltage created by the generator exceeds 14.4V, or when the battery is fully charged, the charge controller diverts any additional voltage to a “divert load”, which in this system is a simple resistor. This mode of operation ensures that the battery is not overcharged, thereby eliminating any possibility of fire or explosion.

Figure 65 - DC-DC Charge Controller

Connected to the negative (or ground) side of the diode is a DC power meter (see Figure 66 below), which is used to measure the power output of the wind turbine. Because the charge controller opens the circuit when the generator voltage is less than the charging voltage, the watt meter must be located on a separate circuit from the charging circuit. This ensures that power measurements can be made even when the turbine is not charging the battery. However, it is important to note that the watt meter will not give accurate power readings if the charging system is active, and so the charging and power measurement circuits are best used one at a time.

Figure 66 - DC Power Meter

Connected to the system's 12V battery is the Active Flow Control (AFC) circuit, which consists of an amplifier and speaker. The amplifier, a Sonic Impact 5065 digital amplifier was chosen because of its high sound quality in a small, power-efficient package. Efficiency was the key selection criteria, because any power consumed by the amplifier lessens any efficiency gained by the use of AFC. Similarly, the speaker was selected primarily with efficiency in mind. An efficient speaker would not only produce clean sound, it would also lessen the electrical power required for a given volume.

The amplifier is fed a sine wave signal from a frequency generator. Originally, the frequency generator was to be a standalone unit. However, this was changed to a software frequency generator, NCH Tone Generator, which may be installed and used by any Windows-based PC with a sound card. This represented a large cost savings, as the software is free, and any of the Sponsor's existing computers may be employed for this task. The software is available from http://www.nch.com.au/tonegen/index.html.

The integration of the electrical system was a fairly straightforward task. Since wiring diagrams were available for most of the major components, a master wiring diagram was compiled for the entire electrical system. In addition, fuses and other necessities were added in accordance with best practices for safety and system protection. This diagram is available in Appendix N – Electrical System Diagram.

VIII. Build

The construction of the prototype model was a long process requiring months of the project teams time. Many challenges were overcome in the building of this wind turbine and the experience and knowledge of the team members has increases significantly. Each individual section of the prototype models construction method is described in the sections below.

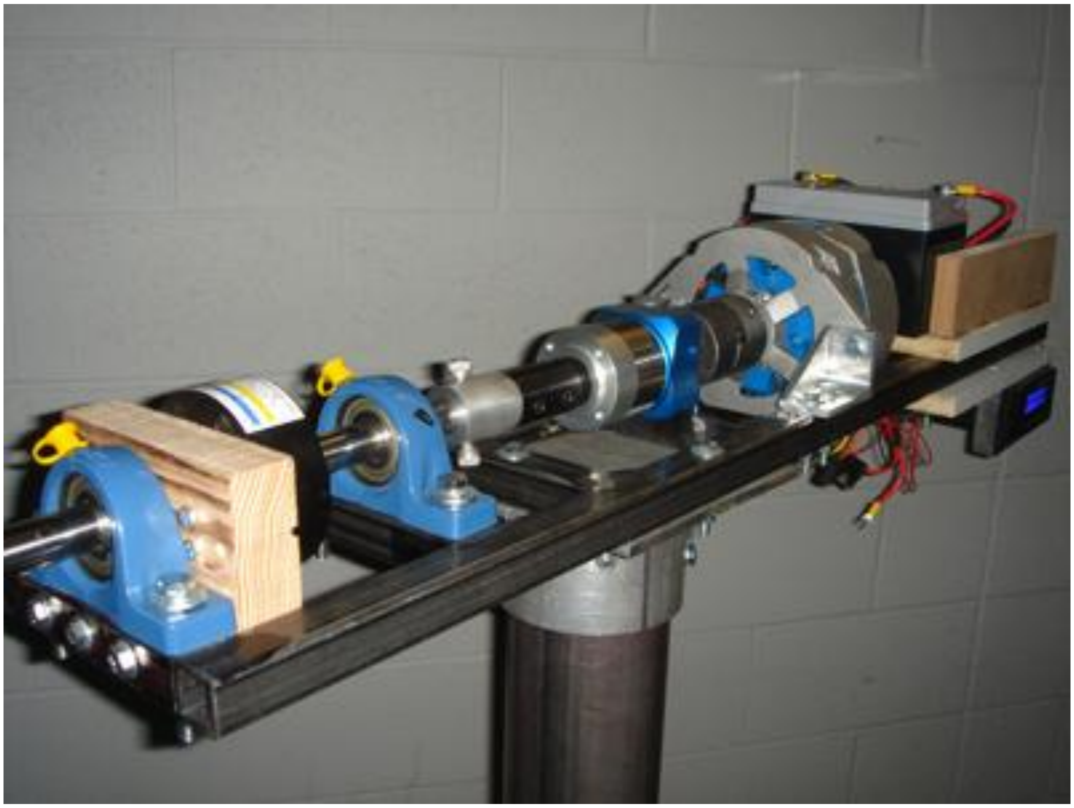

Figure 67 - Frame/Housing

A. Frame/Housing

The frame assembly consisted of two 36 in square tubes parallel to each other that had 6 small square tubes perpendicular to them that acted as supports to help mount different components of the design. The first two square tubes were designed as a mount for the two bearings that was used to support the shaft. Also a wooden block was placed after the first square tube supported by three screws as a mount for the slip ring. A gearbox mount was welded in the third square tube that had the gearbox facing the hub connecting to the shaft

There were two couplers used for the gearbox. The first is the gearbox –shaft coupler that was originally a circle rod which was drilled with the same diameter of the shaft and mounted by using two set screws. The other side of the coupler was turned down using a lathe to fit the gearbox coupler. Second is the gear box –generator coupler that is a circular rod coupler was machined using a lathe to narrow down the diameter to fit in to the gearbox which had a hole in the mount that gives it access to the gearbox. Also that was used to fit to the generator coupler.

Two generator mounts were machined from a 2.5in x 1.35in x 1.75 in aluminum block that was milled using a milling machine from the inside with two holes that connect to the frame and one hole that attaches to the generator to make sure that it's stable and not moving. The last two square tubes were set to have the all the electrical components.

B. Blades

The blade construction happened just as the design dictated. The rapid prototype machine accurately printed the blades to the exact exterior dimensions expected. The locating pegs build in for ease of construction where incorrectly printed which lead to some initial problems. The extruding pegs had to be cut in half and sanded down to fit into the slots. This required minimal effort and was done quickly. After this slight modification the blade sections fit well together and slid over the carbon fiber spar with ease.

The internal aluminum pieces such as the root tube and spar coupler were machined in AME's machine shop. The root tube was a simple lathe operation to turn down the stock tube to the 1.2 inches required to fit snuggly inside the blade. The spar coupler was much more complicated to make. The biggest problem with this piece was drilling the holes into the slanted cone surface at the required angle. At one point the drill bit jittered and caused the hole to be abnormal. This should not affect its performance because it still matched up with the hole in the blade section since the jittering caused the hole to be larger.

The first step in the actual fabrication process was JB welding the spar coupler to the root tube. The spar coupler has a lip machined into it which the root tube slid over. The JB weld takes over 6 hours to reach full strength so this step should be done at night and left over night to dry. After this part was made it was then glued into the bottom blade section. Special care was taken to align the holes in the spar coupler to the holes in the blade section. Additionally the spar was glued to the spar coupler and blade section.

The next eight sections were attached one at a time allowing for the glue to dry between each step. They were slid onto the spar, the locating pegs were slid into the locating slots and everything was glued together.

The additional steps after this main assembly were to patch up the cracks between the blade sections with a filling agent. Then the blades needed to be sanded smooth because the rapid prototype parts do not come perfectly smooth. And the junctions between all the various blade sections had excess glue. After the surface of the blade was the desired smoothness the active flow control holes were drilled. These consist of 1 mm holes drilled every 5 mm along the length of the blade. Special care is taken to ensure that the holes are drilled normal to the blade surface. The finished blades are shown in Figure 68.

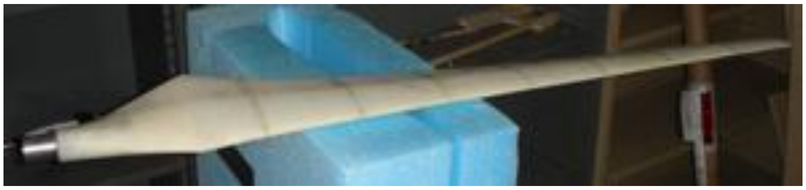

Figure 68 - Completed Blade

It should be noted that the project sponsor requested not to paint the blades so that future work could be conducted to improve upon the surface quality attained by hand sanding.

C. Tower

The tower is a 50 in steel tube supported on the top and the bottom with base brackets support. The top base bracket was used to attach the steel tubes of the frame. The bracket consists of a short circular tube that was machined using a lathe to enable it to fit snugly around the steel tube. A square aluminum plate was cut and welded to the tube. This plate has through holes which are used to bolt the bracket onto the frame which can then be attached to the steel tower.

On the bottom side of the tower there is another bracket which was machined in a similar way. Instead of having four holes it has 16 countersunk holes that were drilled to insure that the wind turbine would stand flat and stable. The feet used to stabilize the wind turbine was replaced due to the instability that the feet showed during testing. They were allowing vibrations and swaying to happen while pushing the wind turbine. Instead of having the original feet a wood rectangle was cut from ¾ inch MDF board. This was in turn raised off the fly by wooding boards which added to the strength and allowed enough space underneath to bolt the bracket to the wooden plank. Since the wind turbine showed most its weight on the back side it was mounted with more space in the back side than the front side that insured that it was balanced.

D. Hub

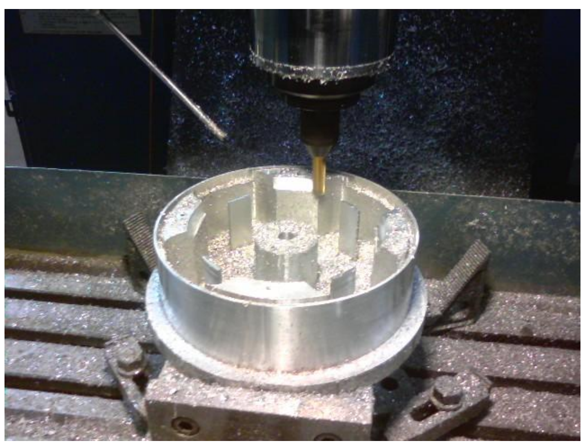

Figure 69 - Hub on CNC machine

The hub was by far the most difficult and time consuming part to make in this entire project. This part was quoted by other machine shops with CNC capabilities to cost over $2200.00 to make. With the help of Joe Hartley, the AME machine shop supervisor, the team was able to cut this part on the CNC machine in a little over a week and a half. The process was long, grueling and not recommended for future projects.

The original stock piece of metal was a solid 9-inch diameter, 3 inch thick disk. Before this was put on the CNC machine a test program was written and a small piece of wood was used to cut the shape of the hub. Once all the necessary features required to be cut using the CNC machine were made on the wood block it was giving the go ahead for cutting the metal piece. Using a 1-inch diameter end mill and taking twenty-thousandths deep cuts, the machine slowly cut away. The CNC machine was used to cut the complex clover shape which allowed the hub to be structurally strong while being as light as possible. The circles for the shaft mount, outside diameter and ridge for the nose cone were interpolated by the CNC machine as well. The bolt circle for the speaker to mount to was drilled into the top of the hub and finally the edges of the hub were marked by the CNC machine.

The hub was then taken to the lathe and the bottom half of the hubs outside diameter was cut and the ¾ inch hole for the shaft was drilled into the back side of the hub. The 1-inch holes for the blades to slide into were then cut using a manual mill. The remaining holes were match drilled to the various hardware that attaches to the hub, and the required holes were tapped for bolt threads.

Originally the hub weighed a little over 30 pounds and after the machining was completed it weighed 4.6 pounds. It took over 100 man hours to complete and cost over $150.

E. Electronics

A wooden shelf was divided to half by using a table saw both shelves were drilled with counter sink holes to make the surface straight for the battery and amplifier. The shelves were mounted on the upper and lower of the frame with all electrical components mounted to the shelves. Two plywood square blocks were set up to prevent the batteries and amp to fall sideways. A plastic cover was made using the band saw and mounted to the lower shelf for the multimeter that slipped inside it reading power and current from the side. Also the charge controller was mounted to the lower shelf with screws.

IX. Testing Prototype Model

Figure 70 - Wind Turbine Assembled

A. Verification

FR 1.0 Incorporate AFC

FR1.1: AFC Mechanisms in blade: The chosen AFC method requires a series of holes which run the length of the blade. The holes need to be at a certain spacing and chord position. Preliminary calculations and recommendations from the project sponsor indicated that holes approximately 1mm in diameter and spaced 10mm apart would provide optimal performance. See Figure 71 - Turbine Blade with AFC holes for an example of AFC holes on the turbine blade. It was found from the wind tunnel testing that two rows of active flow control worked best. This has been incorporated into the current turbine blades. When the blades are installed in the turbine and the speaker is running and generating a sinusoidal pattern of a set frequency air pulses can be felt initiating from the holes in the blade. This is the active flow control and works while they turbine is spinning.

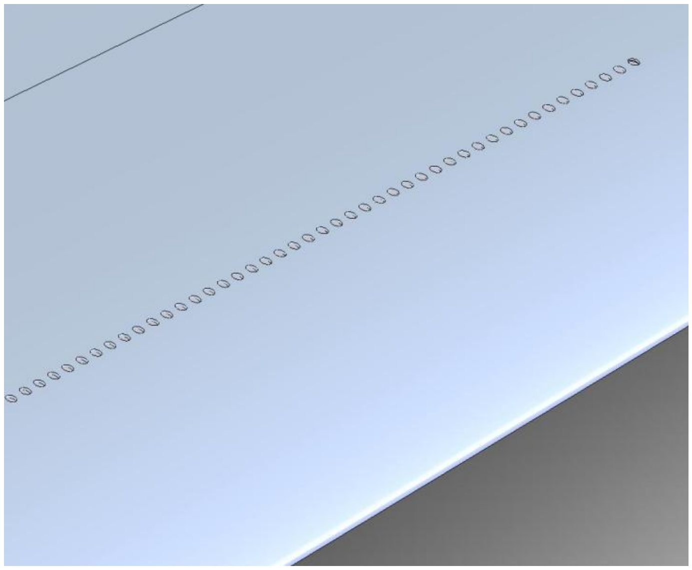

Figure 71 - Turbine Blade with AFC holes

FR1.2: AFC Controller: The chosen active flow control regime necessitates a system for controlling the frequency and amplitude of the sound waves emitted from the speaker. These sound waves and air pulses caused by the speaker's diaphragm moving back and forth create the active flow control used on the blades.

FR1.2.1: Frequency Controller: For cost reasons, the simplest and most effective frequency controller is PC software, which may be run on any Windows PC. The chosen software package is *NCH Tone Generator* (http://www.nch.com.au/tonegen/index.html). Active flow control requires the use of a sine wave with a frequency in the range of 50-300Hz. The chosen software may generate sine waves with a frequency from 1-22000HZ, so the software is expected to meet FR1.2.1. The signal is sent to the speaker in the turbine via the standard speaker port on the computer.

FR1.2.2: Amplitude Controller: Large-amplitude sound waves are not necessary to create the effects of active flow control. Therefore, a small speaker amplifier will adequately deliver the necessary power, expected to be about 10W to the speaker. The amplifier chosen is the Sonic Impact 5065 T-Amp (http://www.parts-express.com/pe/showdetl.cfm?Partnumber=300-958). This amplifier is able to deliver 15W per channel at 4 Ohms impedance. Therefore, it is expected that this amplifier will satisfy FR1.2.2.

FR1.3: Rotating Connection: In order for the speaker to be installed in the turbine's rotating hub, a slip ring is necessary to provide a rotating electrical contact for the sound signal. A copy of the specification drawing for this slip ring may be found in Appendix K. As shown on the specification sheet, the slip ring is rated for a maximum of 50W (50V*10A), far in excess of the 10-15W it will conduct. In addition, its dimensions fit the specifications and tolerances required for the turbine's driveshaft. Finally, though the current specification sheet shows a maximum of 180rpm, the team has contacted the vendor, and is currently in the process of obtaining a specification sheet for an identical slipring, but which is able to handle up to 1000rpm, which is greater than the expected maximum of about 950rpm. Therefore, the slipring is expected to meet the requirements of FR1.3.

FR2.0: Adjusts blade pitch statically

FR2.1: Rotate blade: In order to achieve static blade pitch adjustment, the blades must be capable of rotation when the turbine is not in motion. This is achieved using a system of telescoping tubes, one on the turbine hub, and the other on the blade root. The blade root will fit snugly inside the hub opening while simultaneously permitting the blade to rotate on its pitch axis. Then a large 5/16 inch set screw is tightened down locking the blade in place. This system allows an infinite number of angles be chosen, thereby satisfying FR2.1.

FR2.2: Secure blade: Once the blade has been rotated to the desired pitch angle, it must be fixed to that angle during turbine operation. One set screws per blade will fasten the blade to the hub, which is sufficient to fix the blade under normal operation. Under abnormal or excessive loading, safety cables will be employed to ensure the blade stays fastened to the hub in case of set screw failure. The combination of safety cable and dual set screws will provide safe and reliable operation of the turbine while maintaining the desired blade pitch, thereby satisfying FR2.2.

FR3.0 Measure Efficiency

FR3.1: Record power measurement: A watt meter will be directly attached to the generator to accurately and visually measure how much power the wind turbine is producing. The chosen watt meter maximum voltage range will be up to 500 VAC and the maximum current range up to 300 Amps, both well within the operating limits of the generator. In addition, it stores up to 10,750 points for current and voltage and has a sample rate from 1 second to 18 hours. Data can be uploaded to a computer for graphing and analysis. This will allow the performance increases realized by AFC to be accurately logged and analyzed, thereby meeting the requirements of FR3.1.

FR3.2: Turn AFC off and on: The active flow control can be turned off in numerous ways. The way used most often during testing was to turn the amp on and off. Additionally the sound on the computer which is serving as the frequency generator can be turned on and off.

Table 11 - Verification Results

Verification method	Accomplishment
FR1.0:Incorporates AFC	
FR1.1: AFC Mechanisms in blade	Yes
FR1.2: AFC Controller:	Yes
FR1.2.1: Frequency Controller:	Yes
FR1.2.2: Amplitude Controller	Yes
FR1.3: Rotating Connection:	Yes
FR2.0: Adjusts blade pitch statically	
FR2.1: Rotate blade	Yes
FR2.2: Secure blade	Yes
FR3.0 Measure Efficiency	
FR3.1: Record power measurement	Yes
FR3.2: Turn AFC off and on	Yes

Verification Results:

FR 1.0 Incorporate AFC

FR1.1: AFC Mechanisms in blade:
Active flow control was verified to be incorporated in the blades. The combination of the speaker, amp and frequency generator sending the sound waves and air pulses to the chambers in the blade resulted in air pulsed on the blade surface.

FR1.2: AFC Controller: The speaker was installed and tested on the wind turbine. It was found to be fully functional and adequate to create active flow control.

FR1.2.1: Frequency Controller:
The PC software used was verified by checking it produced the different frequency ranges, more specifically the frequencies that active flow control was designed to work at. Active flow control requires the use of a sine wave with a frequency in the range of 50-300Hz. The chosen software may generate sine waves with a frequency from 1-22000HZ so the software was verified to include all the ranges of frequencies that are needed for that purpose.

FR1.2.2: Amplitude Controller:
The amplifier was tested using an audio check as well as a volt meter which measured the voltage applied to the speaker. As the volume was increased or decreased both the sound level and voltage would change accordingly.

FR1.3: Rotating Connection:
The slip ring that was used to allow the transmission of power and electrical signals from a stationary to a rotating structure was verified by using the multimeter that indicted that the voltage is flowing through the slip rings during slow rotation. The speaker was heard making sound to test the slip ring at faster rotations.

FR2.0: Adjusts blade pitch statically

FR2.1: Rotate blade:
The blades were tested and verified to be able to rotate freely in all angles needed using the system of telescoping tubes, one on the turbine hub, and the other on the blade root. All pitch angles required by the experiments were verified.

FR2.2: Secure blade:
Blades were verified to be secured by tightening the set screws on each blade. They could not rotate and slip out freely. A load of over three times the expected centripetal force felt by the blades was applied and no slippage or rotation occurred.

FR3.0 Measure Efficiency
FR3.1: Record power measurement:
Power measurement was verified by the watt meter onboard. When the hub was rotated manually the watt meter indicated the power measurement. When the blades turned in a configuration where they were capable of turning the generator the power generated was measured and displayed by the wattmeter.

FR3.2: Turn AFC off and on
The active flow control could be turned on and verified it was on by running a hand over the blade surface and feeling the air pulses. When the active flow was turned off the air pulsing stopped.

B. Validation

Validation Methods:

A series of tests were conducted on the model at different wind speeds to determine the wind turbine's performance over the range of wind speeds. Additionally, tests to validate parts of the wind turbine design were conducted in a static state to determine if they fulfill the customer requirements.

D. Adjusts blade pitch statically – the customer will be shown how to change the blade pitch while the wind turbine is not in operation. It will either be acceptable or unacceptable.
E. Incorporates Active Flow Control (AFC) – the wind turbine AFC will be turned on while the turbine is not in operation and the customer will be able to feel the AFC working by feeling the air pulses being projected from the blade surface. As long as there is some airflow that the customer can feel with their hands the AFC is working.
F. Gains efficiency when AFC is active – A series of test at various wind speeds will be performed with AFC operational and not in operation. The power generated by the wind turbine will be measured and recorded. During the comparison the wind turbine is expected to generate more power when the AFC is operating than

when the AFC is not operating. Any increase is power generated will validate this FR.

G. Activates AFC on user command – While the wind turbine is not operating the team will show the customer the switch which turns the AFC on and off.

H. Indicates power output visually – The team will perform a demonstration test with the wind turbine to show the customer how it operates. During this demonstration the team will show the customer the watt meter which will have an electronic display showing the power being generated by the wind turbine.

Table 12 - Validation Results

Validation Results	Accomplishments
Adjusts blade pitch statically	Yes
Incorporates Active Flow Control (AFC)	Yes
Gains efficiency when AFC is active	No
Activates AFC on user command	Yes
Indicates power output visually	Yes

X. Results

A. Wind Tunnel Testing Results

The wind tunnel testing took place in early February and produced some very promising results. These results immediately caused some redesigns of parts of the project. Sampled here are some of the important discoveries made during the testing. For the data of the 120 plus tests conducted please see the attached files to this report.

Figure 72 is the lift coefficient graph of the S809 airfoil at 5 mph. The active flow controls were set at 50 Hz with amplitude of 50% power. It can be seen that in the low angles of attack the active flow control provides a large increase in lift. The actual lift measured by the force balance in the wind tunnel was found to increase by 500%. From the graph the baseline actually has a negative coefficient of lift which means it would actually produce negative lift. With any active flow control running there is a performance increase. The different rows of active flow control cause different effects, but when combined provide the best results in the low angles of attack.

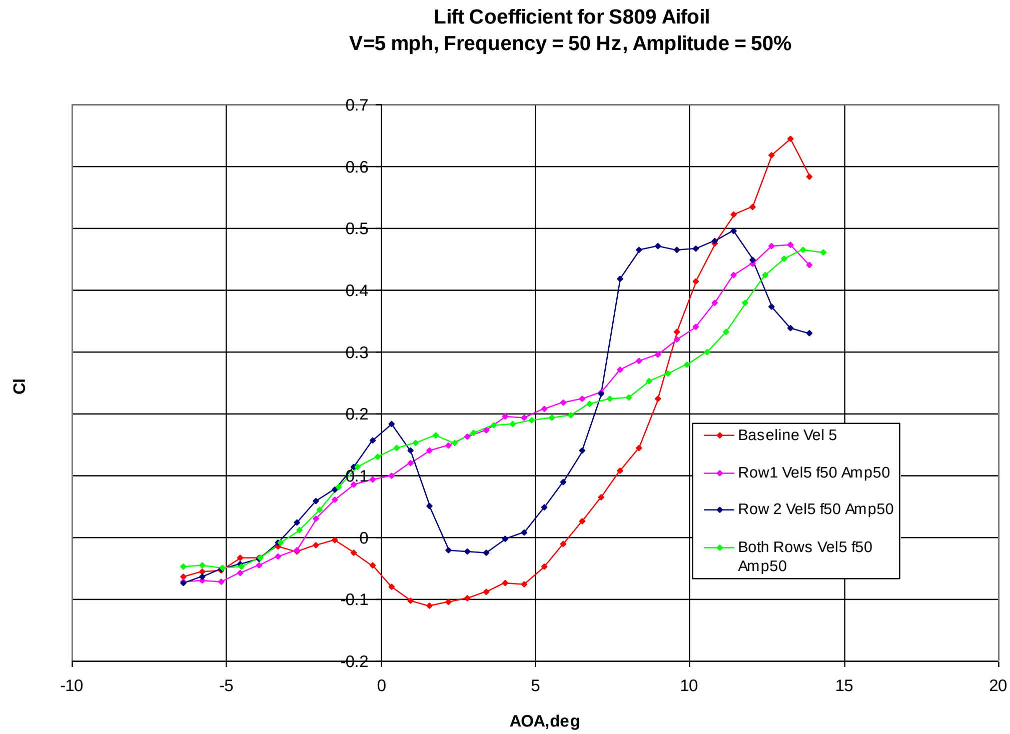

Figure 72- Cl vs. AOA for S809 Airfoil at 5 mph

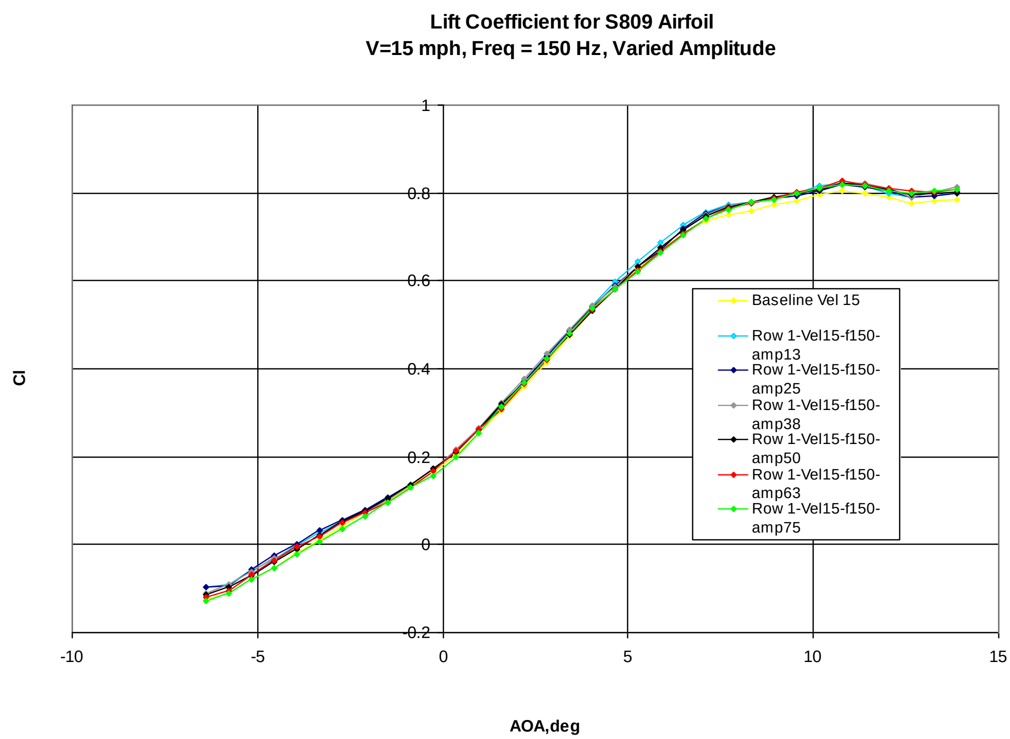

Figure 73 - Cl vs. AOA Vel 15 Varied Amplitude

In Figure 73 it is shown that the amplitude the active flow control is run at has little effect. It also shows that the best improvements for the high wind speeds happen at the larger angles of attack at around 8º to 10º. This trend continues all the way from 10 to 25 mph wind speeds.

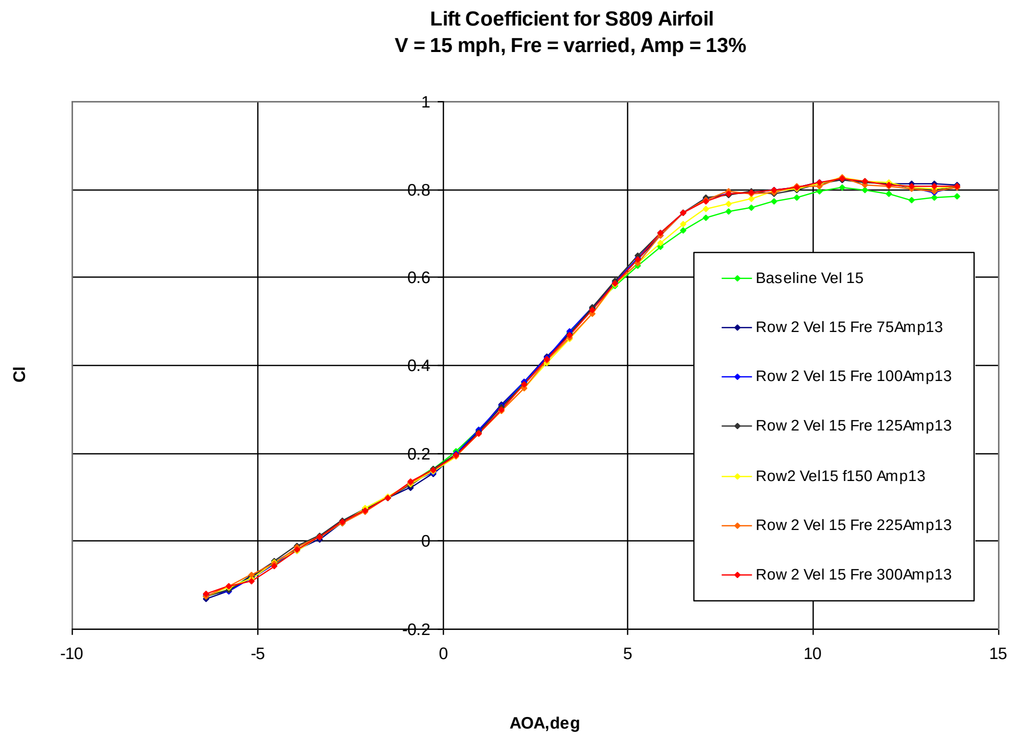

Figure 74 - Cl vs. AOA for V = 15mph, varied frequency

In Figure 74 it is shown that the frequency of the active flow control has similar effects at the higher wind speeds. No matter what frequency was used during these tests there was still a slight performance increase at the larger angles of attack.

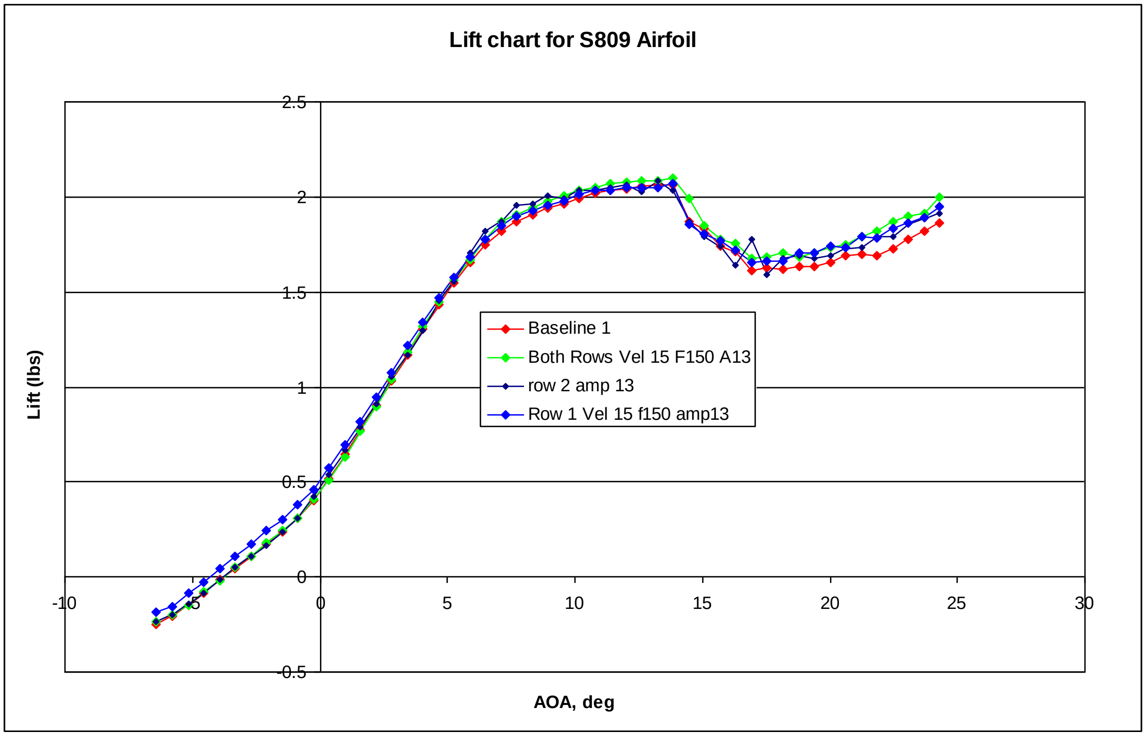

Figure 75 - Lift chart for different rows of AFC

In Figure 75 it is shown that the best results were achieved with both rows of active flow going engaged. This was an unexpected result that the team unintentionally was able to test. The primary purpose for putting two rows of active flow control in the wind tunnel model was to test for leading edge separation and trailing edge separation. Because the team had two rows built into the model, a decision was made to test both at the same time. Using two rows has not been researched very well. This led to the decision to use two rows in the prototype.

The project sponsor was concerned with the marginal performance increase with the active flow control, so it was decided that an alternative method of active flow be tested. The original wind tunnel model was modified to have plasma actuators attached at the same locations as the hole. With the plasma actuation this would ensure that a strong active flow control source was used that had been tested in other experiments and is known to work well. The results were actually worse than those of the loud speaker, but still maintained the marginal increase in performance over the baseline. The modified wind tunnel model is shown in Figure 76. The faint purple/blue lines you see is the plasma field during a wind tunnel run.

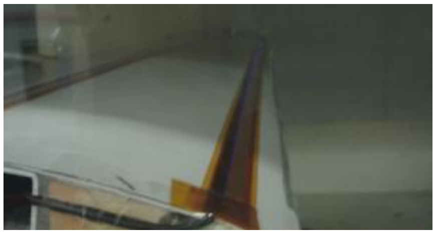

Figure 76 - Wind tunnel model modified for plasma actuation

B. Prototype Testing Results

Figure 77 - Full view of wind turbine

The prototype wind turbine, at the time writing, was unable to verify the wind tunnel results. The wind turbine is capable of spinning up to around 150 rpms and producing power. The amount of power varies widely, however, based on which load (resistance) was used in the circuit. Unfortunately, with the same loads and blade pitch, the difference in power generated by the turbine with active flow control turned on and off was undetectable.

An additional problem arose from the testing equipment. The arrays of fans used for lab testing were inadequate to test all the configurations and conditions originally planned. Ideally, tests would have been performed from the low wind speed range to the high wind speeds. The fans obtained for this project were capable of a maximum of 18 mph and could go to a minimum of 14 mph. This puts the only available range of wind speeds between the 10 and 20 mph speeds tested in the wind tunnel.

It was found in the wind tunnel testing that the best performance improvements could be found at the low wind speeds (approximately 5mph). Since the testing setup was unable to produce a consistent low speed wind for lab testing, the team could not verify these results with the prototype model.

For the wind speed ranges where testing was possible, the wind tunnel testing suggests that the performance increase would be marginal at best but there should be some slight improvement. Once again, the team was unable to verify that there was any improvement in performance when active flow control was used.

An additional cause of the active flow control having no effect was determined in late April. The arrays of fans use a propeller spinning at high rpms to produce the desired airflow. Propellers cause the airflow through them to swirl and create many small vortexes in the airflow. These vortexes and swirling would cause the active flow control to have no effect on the airflow over the blades. The active flow control is designed to be used with a consistent straight air flow which would be found where the wind turbine would be built at or even that an aircraft wing sees during flight. To simulate this flow in the laboratory a large air straightener would have been required. This proved to be out of the capabilities of this project as the materials and time could not be found to build one large enough to cover the area needed for testing.

It was thought that if there could be found a configuration where the wind turbine would not start unless active flow control was engaged, that this would show the usefulness of the technology. This was tested in two ways. Firstly, the wind turbine was pushed away from the fan array so that a slower wind speed would be seen by the turbine blades. This was found to be very inaccurate. The turbine would randomly start turning or stay stationary during all of the testing configurations, making it impossible to determine whether active flow control was causing the rotation or not. The airflow over the blades was very irregular and the vortices could be felt with the tester's hand. The second method was to find a blade pitch where the turbine would not start unless active flow control was engaged. This was also inaccurate. The flow was still plagued with vortices and swirling and additionally the angles of the blades were past the range of stalling for the airfoil used so the flow must have been separating before the active flow control could have any effect.

Other general notes found from testing involve the relationship between blade pitch and turbine performance. It was found that that there was a sweet spot from about 10° to 45° of pitch rotation where the wind turbine would spin the fastest. This was found to be the best combination of forces acting on the blade from the wind and forces generated by the airfoil with the common goal of causing the turbine to spin.

However, the best starting position was at 90°, where the blade was parallel to the ground. In this orientation the blade is basically a wing, with the wind blowing directly over it just like a plane's wing flies through the air. It is believed that in this position the lift performance increase found from the wind tunnel testing with active flow control could improve the start up wind speed of the turbine. This would require the ability to dynamically change blade pitch, because for the best performance the blade would start in the 90° configuration and transition to the 10° to 45° range.

XI. Conclusion

A. Suggestions for Improvement

While the Scaled Model Wind Turbine with Active Flow Control project was generally successful, there are still a number of ways in which the prototype turbine could be improved for the future. At this stage, the team has delivered a functional prototype to the project sponsor. However, the team was unable, for a number of reasons discussed earlier, to concretely verify the effects of Active Flow Control on the turbine's performance. As such, the bulk of these proposals are opportunities to improve upon the turbine's performance, or to improve the quality of the AFC test data.

The turbine's unexpectedly high start-up torque requirement was one issue that developed during testing. This increase in torque directly relates to an increase in the start-up wind speed for the turbine. Therefore, it is recommended that steps be taken to reduce this torque. There are several possibilities here. For example, the current WindBlue DC-520 "High Wind" generator could be swapped for the DC-540 "Low Wind" model. The DC-520 was selected because it was believed that the increase in rotational speed achieved by the gearbox would effectively raise the wind speed seen by the generator, and thus, a higher output generator could benefit fully from this. However, the DC-540 model likely has a lower start-up torque to accommodate the lower wind speeds for which it is designed. As such, this may in fact be a better choice to use in combination with a planetary gearbox, even if it lowers the maximum output of the turbine.

In addition, a variable-speed gearbox, such as a multi-gear planetary gearbox or continuously variable transmission (CVT) could help to reduce or eliminate this problem. A multi-speed transmission could use underdriven gears to get the generator started at low wind speeds, and once the generator has begun to turn, it could shift to a higher (overdriven) gear to maximize power output. The size and costs of such a system may become prohibitive, but a multi-gear transmission would provide the all-around best performance.

The turbine could also see a significant performance boost with a new set of blades. The NREL blades using the S809 airfoil were, of course, designed for a much larger turbine operating under much higher Reynolds numbers. A new turbine blade, specifically designed for the specific range of Reynolds numbers under which the scaled turbine operates, would likely net much higher rotational speeds and power production. This was considered as a possibility during the design of the original blade, but was rejected because the design of a new blade was far beyond the scope of the project. However, a design project whose aim is specifically to create an efficient small wind turbine blade may produce a much more effective component for the prototype turbine.

The testing equipment is another area of potential improvement. As noted in the results section, the results of the AFC testing on the prototype turbine were seriously affected by the fans used to produce artificial wind. Because these fans swirl the air flowing through them, they produce air currents which are not at all similar to those seen by a wind turbine in a natural environment, and additionally cause AFC to become almost entirely ineffective. The project sponsor recommended construction of flow straighteners to resolve this issue; but this was outside the scope of the project and was not completed due to time constraints. However, before any further AFC testing takes place, it is highly recommended that flow straighteners are constructed to reduce a serious influencing factor on the test data.

If, after the test equipment has been upgraded, AFC testing produces some of the results seen during wind tunnel testing, there are a number of future possibilities to expand the capabilities and output of the turbine by utilizing AFC. For example, an electronic control system could be added to the AFC circuit, which would modify the frequency, amplitude, or other parameters based on wind speed, blade rotation speed, blade pitch, and any number of other variables. Electronic control could further refine and enhance the efficiency gains provided by Active Flow Control. In addition, electronic control could be used to switch between rows of AFC holes positioned at different locations down the blade. The possibilities are limitless, but first, the turbine must be made to show solid performance gains under testing conditions.

B. Discussion of the Final Product

The prototype wind turbine described in this report is the culmination of nine months of careful design, analysis, construction, and testing. While not a complete success, this project did succeed in a number of key areas. Perhaps most importantly, wind tunnel testing of a scaled wind turbine airfoil showed the potential for promising gains as a result of using Active Flow Control. These gains were discovered for low wind speeds, but indicate a possible 500 percent increase in lift over a turbine without Active Flow Control. This has the potential to lower the start-up wind speed of wind turbines, allowing them to produce energy at times when they weren't before.

Additionally, the design team was able to deliver a complete, working prototype wind turbine, designed from scratch using off-the-shelf and custom components. The completed turbine fulfills all major functional requirements as laid out at the start of the project: its blades are geometrically scaled from a full-size research wind turbine, the blades are adjustable for pitch, the turbine contains a functional Active Flow Control system which may be switched on and off, it generates electrical power which may be used to operate the Active Flow Control system, and it visually indicates power production with a digital watt meter. These were the key metrics for delivering a robust prototype, and all of them were met.

The final functional requirement required that the turbine show an increase in efficiency while Active Flow Control is operational. For numerous reasons, this requirement has not yet been fulfilled. While the turbine has yet to show significant performance gains while using Active Flow Control, the undeniably positive wind tunnel results indicate that with some tweaks to the experimental equipment and procedure, those gains may yet be found. Therefore, while it has yet to reveal its full potential, the prototype turbine will undoubtedly provide a solid test bed for future Active Flow Control research. And while it is still uncertain what it may hold, that future looks bright indeed

XII. Acknowledgments

This project would not have been successful without the efforts of many individuals who contributed to this project. The team members would like to thank Dr. Hermann Fasel and Dr. Andreas Gross for sponsoring our project and guiding us throughout the year. Also, special thanks for the staff of ENGR498 for organizing the course and keeping the team up-to-date. Thanks to Bill Richards for the support and help with the blades. Thanks to Ventana Medical Systems for printing our blades on their rapid prototype machine, and for the significant discount on this process. Thanks to Joe Hartley for the enormous amount of help and effort put into the CNC machining of the hub and the help with all the other parts manufactured in AME's machine shop. Finally, thanks to the AME Department for giving us the opportunity, tools and environment to be creative and work on such a great project.

XIII. References

B.Goksel, I. Rechenberg. Active Flow Control by Surface Smooth Plasma Actuators. Berlin,Germany.

Bertorell, Pual, ed. The Aviation Consumer.

Bloxham, Matthew Jon. The effects of vortex generator jet frequency, Duty cycle and phase on seperation bubble dynamics. April 2007.

O. Stalnov, A. Kribus and A. Seifert. High-Performance wind turbines using active flow control . Tel Aviv .

P.B. Martin, C. Tung. Active Flow Control Measurments and CFD on a Transport Helicopter Fuselage. Mesa: US Army Research,Development and Engineering Command,Ames Research center.

Ronald D. Joslin, Lucas G. Horta and Fang-Jenq Chen. Transitioning Active Flow Control to Applications. Hampton,VA.

S. Schereck, M.Robinson. Wind Turbine Blade Flow Fields and Prospects for Active Aerodynamic Control. San Diego,CA, 2007.

S. Scott Collis, Ronald D. Joslin,Avi Seifert,Vassilis Theofilis. Issues in active flow control: theory, control,simulation and experiment. Albuquerque,NM.

XIX. Appendices

A. Xfoil Diagrams

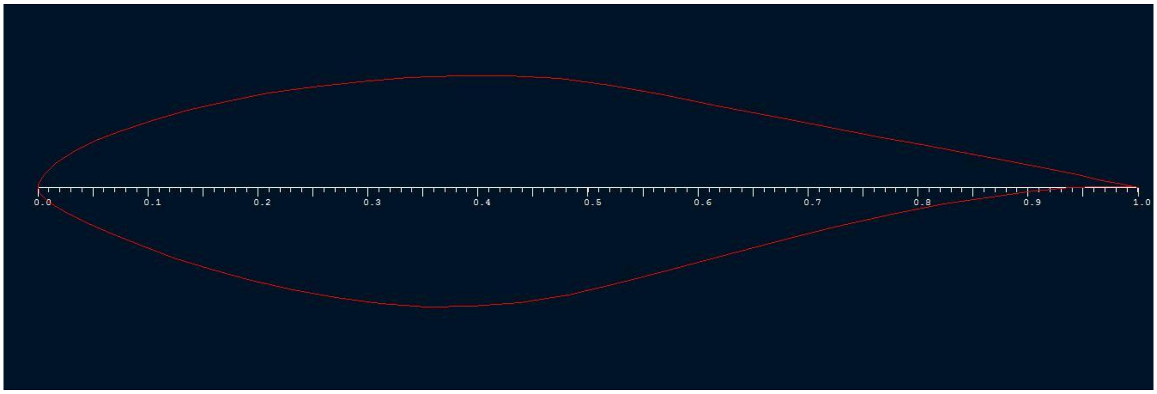

Figure 78 – S809 airfoil profile

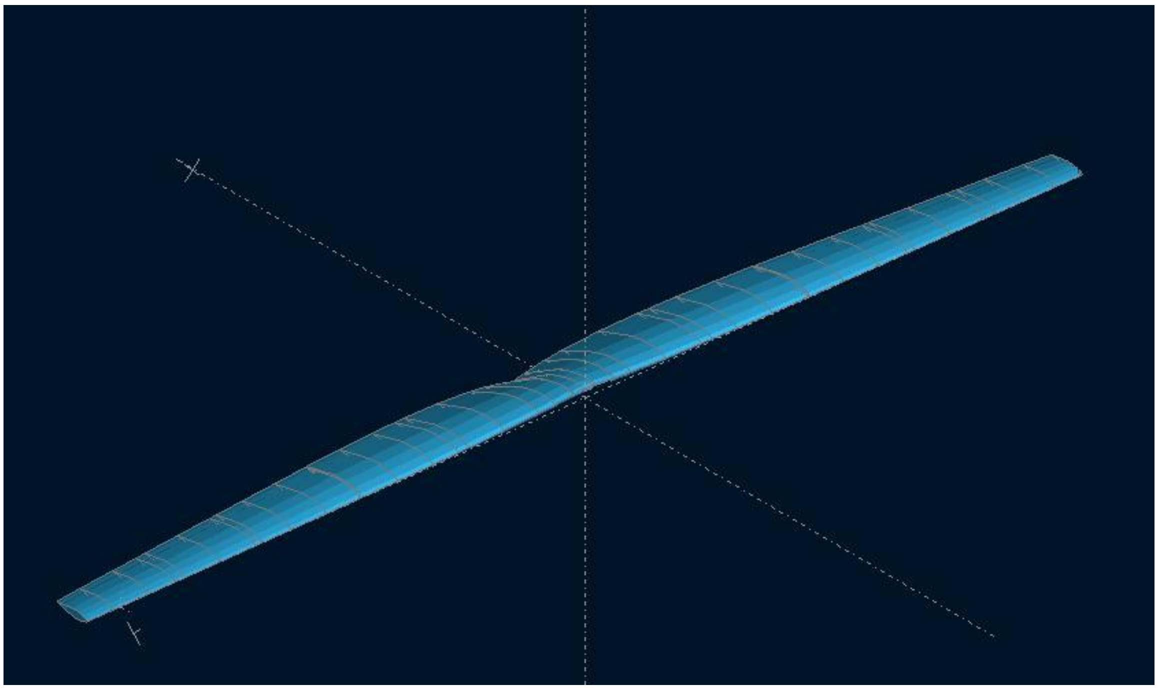

Figure 79 – Blades modeled in Xfoil

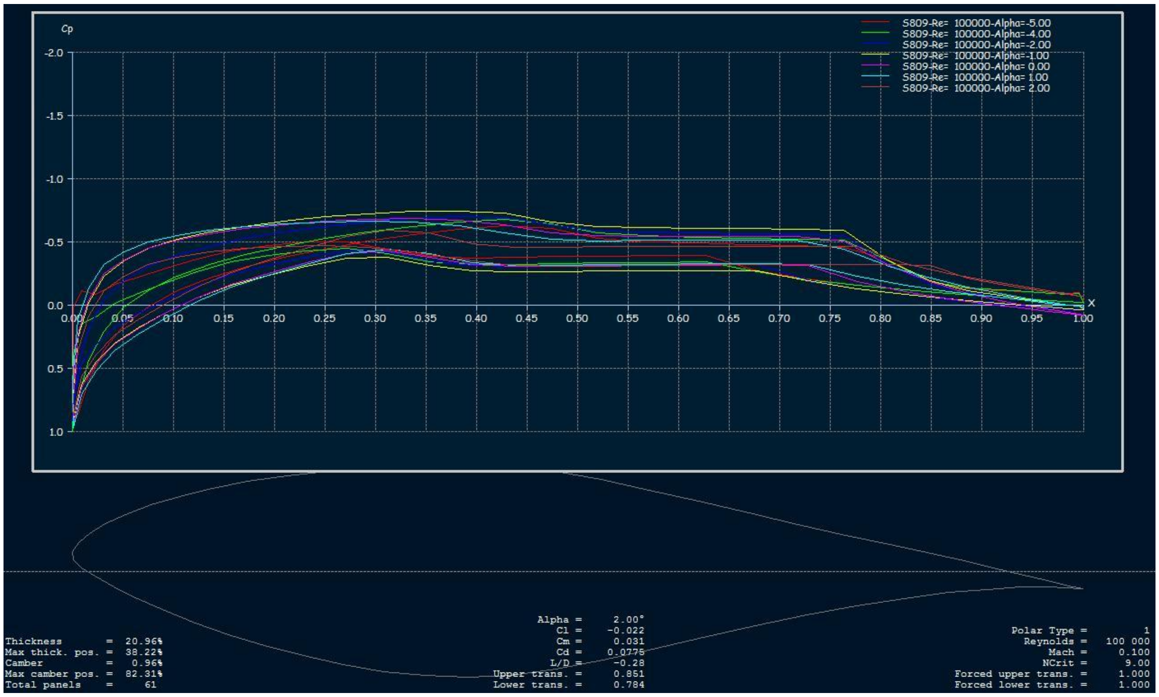

Figure 80 – Pressure distribution over airfoil section

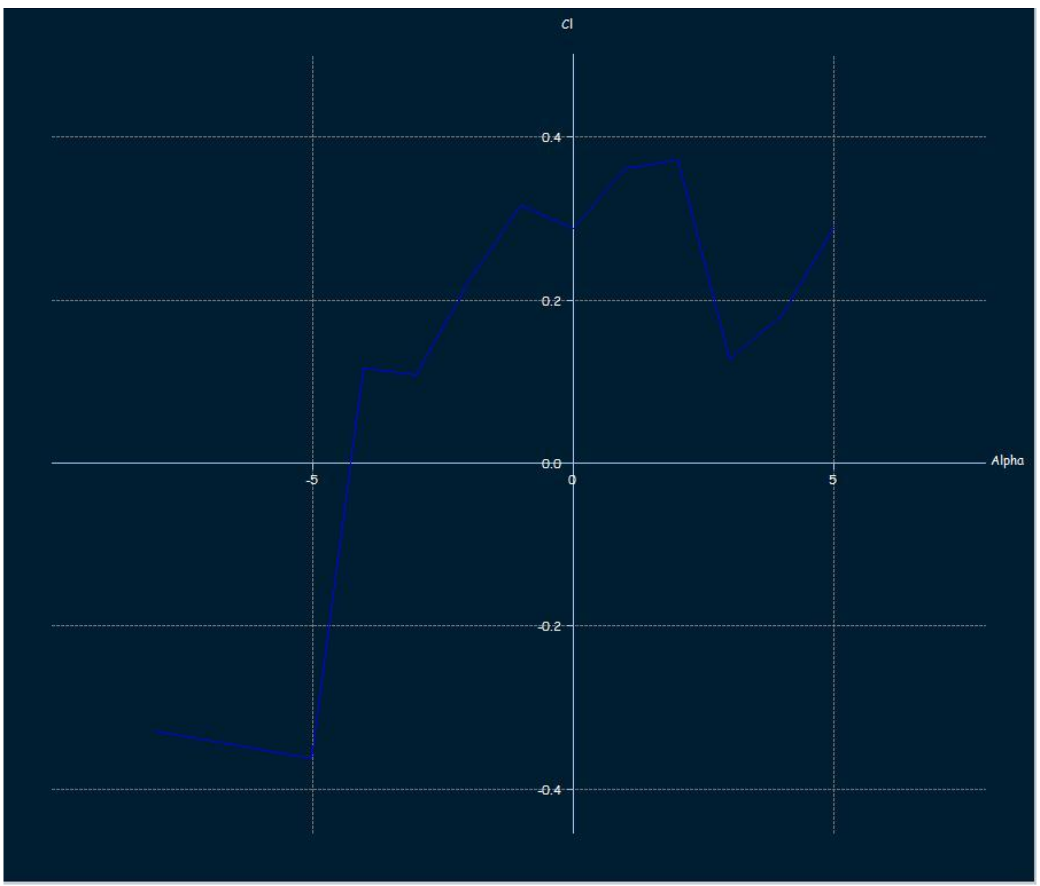

Figure 81 – C_L versus Alpha curve for S809 airfoil

B. Wind Turbine Scaling Excel Sheet

Wind Turbine - NREL

scaling: 1/5

	Turbine	Model
	kg/m/s	kg/m/s
Turbine Rotor Diameter	10.058	2
Blade Length	5.03	1.15
Blade Chord Average	0.50	0.10
Minimum Wind Speed	6.00	Unknown
Blade Mass	60.20	12.00

Froude Scaling		
RPM	80.00	178.89
Blade Tip Speed	42.13	21.54
Mid Blade Speed	20.94	9.37

Reynolds Numbers		
viscosity (kinematic)	0.00002076	0.00002076
Re # Max	744,225	148,845
Re # Min (from 1.257 and up)	373,847	74,769
Distance From Hub (m)	**Re #**	**Re #**
0	0	0
0.508	44,690	8,938
0.66	58,062	11,612
0.883	65,208	13,042
1.008	141,964	28,393
1.067	189,887	37,977
1.133	248,725	49,745
1.257	373,847	74,769
1.343	394,547	78,909
1.51	433,249	86,650
1.648	463,534	92,707
1.952	524,621	104,924
2.257	579,269	115,854
2.343	592,831	118,566
2.562	625,498	125,100
2.867	664,096	132,819
3.172	695,063	139,013
3.185	696,626	139,325
3.476	718,193	143,639
3.781	735,436	147,087
4.023	741,921	148,384

4.086	743,646	148,729
4.391	744,225	148,845
4.696	737,172	147,434
4.78	734,927	146,985
5	722,344	144,469
5.305	702,183	140,437
5.532	680,884	136,177

Table 13 – Scaling Sheet for Wind Turbine

C. NREL Blade Scaling Sheet

Radial Distance(m)	Span Station 1(r/5.532 m)	Span Station 1(r/5.029 m)	Chord Length(m)	Twist2 (degrees)	Thickness(m)	Thickness Calculated (m)	Twist Axis(% chord)	Scaled Radial Distance (m)	Scaled Chord Length (m)
0	0	0	0	hub	hub		hub	0.000	0.000
0.508	0.092	0.101	0.218	0	0.218	0.218	50	0.092	0.039
0.66	0.12	0.131	0.218	0	0.218	0.218	50	0.119	0.039
0.883	0.16	0.176	0.183	0	0.183	0.183	50	0.160	0.033
1.008	0.183	0.2	0.349	6.7	0.163	0.163	35.9	0.182	0.063
1.067	0.193	0.212	0.441	9.9	0.154	0.154	33.5	0.193	0.080
1.133	0.205	0.225	0.544	13.4	0.154	0.154	31.9	0.205	0.098
1.257	0.227	0.25	0.737	20.04	0.154	0.154	30	0.227	0.133
1.343	0.243	0.267	0.728	18.074	20.95%chord	0.153	30	0.243	0.132
1.51	0.273	0.3	0.711	14.292	20.95%chord	0.149	30	0.273	0.129
1.648	0.298	0.328	0.697	11.909	20.95%chord	0.146	30	0.298	0.126
1.952	0.353	0.388	0.666	7.979	20.95%chord	0.140	30	0.353	0.120
2.257	0.408	0.449	0.636	5.308	20.95%chord	0.133	30	0.408	0.115
2.343	0.424	0.466	0.627	4.715	20.95%chord	0.131	30	0.424	0.113
2.562	0.463	0.509	0.605	3.425	20.95%chord	0.127	30	0.463	0.109
2.867	0.518	0.57	0.574	2.083	20.95%chord	0.120	30	0.518	0.104
3.172	0.573	0.631	0.543	1.15	20.95%chord	0.114	30	0.573	0.098
3.185	0.576	0.633	0.542	1.115	20.95%chord	0.114	30	0.576	0.098
3.476	0.628	0.691	0.512	0.494	20.95%chord	0.107	30	0.628	0.093
3.781	0.683	0.752	0.482	-0.015	20.95%chord	0.101	30	0.684	0.087
4.023	0.727	0.8	0.457	-0.381	20.95%chord	0.096	30	0.727	0.083
4.086	0.739	0.812	0.451	-0.475	20.95%chord	0.094	30	0.739	0.082
4.391	0.794	0.873	0.42	-0.92	20.95%chord	0.088	30	0.794	0.076
4.696	0.849	0.934	0.389	-1.352	20.95%chord	0.081	30	0.849	0.070
4.78	0.864	0.95	0.381	-1.469	20.95%chord	0.080	30	0.864	0.069
5	0.904	0.994	0.358	-1.775	20.95%chord	0.075	30	0.904	0.065
5.305	0.959	1.055	0.328	-2.191	20.95%chord	0.069	30	0.959	0.059
5.532	1	1.1	0.305	-2.5	20.95%chord	0.064	30	1.000	0.055

Table 14 – NREL Blade data and Scaled data

D. Airfoil Scaling Excel Sheet

Note - All Units are meters		
Span Station:		0
NREL Chord Length:		0.711
30% Length		0.038557
Model Blade Radius:		1
Model Scale Factor:		18.08%
Model Section Coordinates		
X	Y	Z
0.12852	0.00000	0.00000
0.12804	0.00007	0.00000
0.12663	0.00031	0.00000
0.12441	0.00077	0.00000
0.12149	0.00142	0.00000
0.11794	0.00218	0.00000
0.11379	0.00300	0.00000
0.10906	0.00388	0.00000
0.10379	0.00483	0.00000
0.09808	0.00588	0.00000
0.09203	0.00702	0.00000
0.08575	0.00823	0.00000
0.07936	0.00948	0.00000
0.07300	0.01074	0.00000
0.06684	0.01187	0.00000
0.06090	0.01265	0.00000
0.05502	0.01298	0.00000
0.04913	0.01299	0.00000
0.04330	0.01277	0.00000
0.03761	0.01233	0.00000
0.03211	0.01171	0.00000
0.02689	0.01093	0.00000
0.02198	0.01001	0.00000
0.01745	0.00896	0.00000
0.01335	0.00782	0.00000
0.00973	0.00660	0.00000
0.00662	0.00532	0.00000
0.00406	0.00403	0.00000
0.00209	0.00274	0.00000

0.00074	0.00150	0.00000
0.00005	0.00035	0.00000
0.00018	-0.00064	0.00000
0.00120	-0.00163	0.00000
0.00298	-0.00278	0.00000
0.00543	-0.00404	0.00000
0.00846	-0.00540	0.00000
0.01198	-0.00681	0.00000
0.01593	-0.00824	0.00000
0.02025	-0.00960	0.00000
0.02489	-0.01086	0.00000
0.02979	-0.01199	0.00000
0.03487	-0.01293	0.00000
0.04008	-0.01361	0.00000
0.04541	-0.01397	0.00000
0.05082	-0.01393	0.00000
0.05634	-0.01347	0.00000
0.06199	-0.01254	0.00000
0.06791	-0.01118	0.00000
0.07411	-0.00956	0.00000
0.08052	-0.00786	0.00000
0.08702	-0.00616	0.00000
0.09350	-0.00457	0.00000
0.09982	-0.00317	0.00000
0.10584	-0.00200	0.00000
0.11140	-0.00110	0.00000
0.11637	-0.00048	0.00000
0.12062	-0.00010	0.00000
0.12404	0.00007	0.00000
0.12653	0.00008	0.00000
0.12803	0.00003	0.00000
0.12852	0.00000	0.00000

Table 15 – Airfoil scaling sheet

E. Structural Analysis

In various parts of the wind turbine design calculations relating to structural strengths were required to be performed. Here is a list of the calculations used:

Moment of Inertia of a hollow circle. Where (*D*) is the outer diameter and (*d*) is the inner diameter.

$$Ix = Iy = \frac{\pi}{64}(D^4 - d^4)$$ **(Equation 5)**

Area of a hollow circle. Where (D) is the outer diameter and (d) is the inner diameter.

$$A = \frac{\pi}{4}(D^2 - d^2)$$ **(Equation 6)**

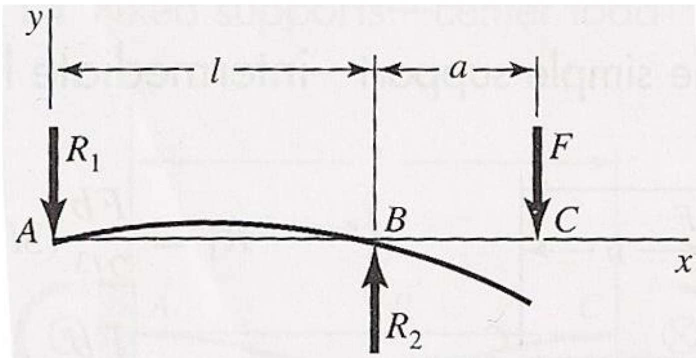

Figure 82 – Beam loading representing main shaft

For a beam modeled as in Figure 82. The following equations were used:

Moment equation where (F) is the force, (a) is the distance between point B and C, (l) is the distance between point A and B and (x) is the distance from point A.

$$M_{AB} = \frac{-Fax}{l}$$ **(Equation 7)**

Shear (V) equation uses same variables as Equation 3.

$$V_{AB} = \frac{-Fa}{l}$$ **(Equation 8)**

$$V_{BC} = F$$ **(Equation 9)**

Maximum Deflection where (E) is the Modulus of Elasticity of the materials and (I) is the Moment of Inertia of the beam.

$$y_C = -\frac{Fa^2}{3EI}(l + a)$$ **(Equation 10)**

Maximum principle stress where (M) is the maximum moment on the beam, (y) is the position up the cross section of the beam and (I) is the Moment of Inertia.

$$\sigma_{\max} = \frac{My}{I}$$ **(Equation 11)**

Maximum Shear Stress where (V) is the maximum shear force on the beam and (A) is the cross sectional area of the beam.

$$\tau_{\max} = \frac{3V}{2A}$$ **(Equation 12)**

Safety Factor equation where (*Sy*) is the yield strength of the material and (*n*) is the safety factor.

$$n = \frac{.5S_y}{\sigma_{\max}}$$ **(Equation 13)**

F. Main Shaft Bending Excel Sheet

Shaft Geometry		**Calculations**		**Materials Information**	
D	0.75	Force (lb)	50	Name:	AISI 52100 Steel
d	0.44	Moment (lb-in)	150	E	30500000
l (length between bearings)	6	V Shear (lb)	25	Sy (psi)	204527.87
a (over hang length)	3	Inertia (lb^4)	0.0137		
		Area (in^2)	0.2897		
		σmax (psi)	4108.3		
		τmax (psi)	129.43		
		yc (in)	**-0.003**		
		n	790.11		
		B1 (pound)	25		
		B2 (pound)	75		

Table 16 – Main Shaft loading calculations

G. Speaker and PVC Tube Experiment Excel Sheet

Table 17 – Speaker and PVC tube experiment sheets

Test 1		Test 2		Test 3	
Tube Length:	1.37m	Tube Length:	1.028m	Tube Length:	.8625 m
Speaker Size:	10 in sub	Speaker Size:	6 in	Speaker Size:	6 in

			Cabinet:	Unsealed		Cabinet:	sealed
Volume Settings: (small amp - sub amp)	3/8 - 1/2	1/4 -1/2	Volume Settings:	3/4 -	1/2 -	Volume Settings:	3/4 -
Frequency (Hz)	Distance (in)	Distance (in)	Frequency (Hz)	Distance	Distance	Frequency (Hz)	Distance (in)
120	Surface		140	3		160	2
100	3		120	4		140	3
80	4	Surface	100	5		120	4
70	7		90	6		110	6
65	8		86	9		105	6
63	8	0.5	84	16	4	100	7
60	8		80	8		96	6
55	5.5		70	6		85	4
30	4		60	5		70	3
20	2		30	2		60	2

H. Bill of Materials

Housing							
Item	Price	Quantity	Total Cost	Unit of Measurement	Part no.	Manufacturer	Source
Gearbox, Planetary, 1:5	$209.00	1	$209.00	Each	GBPH-0601-CS-005-AA231-500	Anaheim Automation	Anaheim Automation
Shaft	$54.53	1	$54.53	Each	6007K45	various	McMASTER
Generator	$250.00	1	$250.00	Each	DC-520	WindBlue Power	WindBlue Power
Slip Ring	$148.00	1	$148.00	Each	LPT019-0210	Jinpat Electronics	Jinpat Electronics
Bearing, Double-Sealed	$35.10	2	$70.20	Each	6361K11	various	McMASTER
Amplifier	$69.00	1	$69.00	Each	5065 Gen 2 T-Amp	Sonic Impact	Parts-Express

Frequency Generator	$0.00	1	$0.00	Each	Software	NCH	Internet
Watt Meter	$80.00	1	$80.00	Each	HB404	Annex Depot	Annex Depot
Battery, 12V	$41.00	1	$41.00	Each	YT6.5L	Scorpion	Batterystuff.com
Charge Controller	$105.00	1	$105.00	Each	NC25A	Flexcharge	WindBlue Power
Shaft Coupler	$9.66	2	$19.32	Each	8974K161	Custom/In-house	McMASTER (Raw Mat'l)
Bracket, Generator Mount	$35.27	1	$35.27	Each	4459T61	Custom/In-house	McMASTER (Raw Mat'l)
Bracket, Gearbox Mount	$24.23	1	$24.23	Each	4459T11	Custom/In-house	McMASTER (Raw Mat'l)
Tube, Steel	$24.56	2	$49.12	Each	6527K31	Custom	McMASTER
Mount, Electronics	$15.00	1	$15.00	Each	N/A	Custom/In-house	Home Depot (Raw Mat'l)
Hardware	$55.00	1	$55.00	Each	Estimated	Estimated	McMASTER
Total			$1,224.67				

Blade							
Item	Price Per	Quantity	Total Cost	Unit of Measurement	Part no.	Manufacturer	Source
Carbon Spar	$13.33	6	$80.00	ft	Various	Various	Internet
ABS Plastic	$250.00	1	$250.00	Spool	340-2000	PADT	PADT
Aluminum Pipe	$13.28	1	$13.28	Each	9056K773	various	McMASTER
Total			$343.28				

Hub							
Item	Price	Quantity	Total Cost	Unit of Measurment	Part no.	Manufacture	Source
Speaker	$90.00	1	$90.00	Each	W6-1721	Tangband	Parts-Express
Aluminum Block	$237.93	1	$237.93	Each	Custom	various	Online-metals.com

Aluminum Pipe	$11.29	1	$11.29	Each	9056K291	various	McMASTER
Sound Insulator	$20.00	1	$20.00	Each	260-530	various	Parts-Express
Total			$359.22				

Tower / Shell							
Item	Price	Quantity	Total Cost	Unit of Measurment	Part no.	Manufacture	Source
Tube, Aluminum	$197.03	1	$197.03	Each	9056K556	Custom / In-house	McMASTER (Raw Mat'l)
Bracket, Frame Support	$17.45	4	$69.80	Each	89215K349	Custom / In-house	McMASTER (Raw Mat'l)
Base	$10.00	4	$40.00	Each	N/A	Custom / In-house	Home Depot (Raw Mat'l)
Shell	$450.00	1	$450.00	Each	Estimated	Estimated	Estimated
Total			$756.83				

Table 18 – Bill of Materials

Grand Total	$2684.00

I. Responses to PDR and CDR Questions

PDR Questions:

Have you thought about induction coupling?
Yes, there were two ways of induction coupling that we thought of to transfer the electrical energy: The slip rings and coils.

Did we research patents on AFC?
Yes, although there weren't many patents the present a wind turbine with AFC incorporated in it but we found a few.

How is the stream attached to the blade in the Plasma Actuators?
Plasma actuators has two electrodes that are opposite in charge separated by a dielectric layer. These two electrodes are connected to a high voltage source the produces 10-20KV.As soon as the AC amplitude is high enough the air ionizes in the region of the

electrode that will delay the separation time of the stream lines so the stream lines will be attached for a longer period.

CDR Questions

Has your Sponsor approved your design?

Our Sponsor, Dr. Fasel of the AME Department, has approved the majority of our design. The main outstanding issue is the determination of the lift and drag forces acting on the turbine blades. These figures will determine everything from the maximum horizontal force on the tower to the operating RPM of the turbine at a given wind speed. Once these figures have been calculated (currently underway), the design can be re-optimized for the resulting loads. Following this, the design group should be able to obtain final approval of the design.

Has your team considered the resonance frequency of the blade, with respect to its length?

This has been considered, and is discussed in detail in Section IX.

How will the resonance frequency scale to a full-size wind turbine?

The resonance frequency can easily scale to a longer blade length. For example, a tuned chamber of length 0.8625m (see Section IX) may be scaled to a blade of length 80m, simply by selecting a higher order harmonic. In this case, selecting the 91^{st} order harmonic (n=91) will result in a tuned chamber of length 78.5m, which will resonate at the same frequency as the 0.8625m chamber.

Does the frequency of AFC depend upon wind speed or turbine rotation rate?

The frequency required by AFC does vary slightly with wind speed and turbine rotation rate. However, the AFC frequency is not defined by a single specific frequency, but rather a range of frequencies. Therefore, as long as the AFC is operating at a frequency within the range, it will continue to function if the wind speed or rotation rate moves up or down slightly. In a full-size, production wind turbine, the AFC frequency could be computer-controlled, and varied based on wind speed and rotation rate to maintain an optimal frequency.

Has your team considered the possibility of using two smaller loudspeakers, each generating different frequencies, which will combine to create a single, lower-frequency wave?

Our team did not consider this possibility, primarily because none of the members were aware that the possibility existed. However, we do not foresee any issues with our current speaker configuration.

Do the air perturbations generated by the speaker have a constant magnitude as they travel down the blade?

Our testing found that the amount of air pulsed by the speaker did not vary along the length of the blade.

What determines the spacing of the holes on the blade?

The spacing of the holes is determined by the size of the hole itself. The spacing should be about 2-3 times the diameter of the hole (e.x., 1mm-diameter holes should be spaced 2-3mm apart).

J. FMEA

Team 3679 - Scaled Model Wind Turbine with Active Flow Control Technology

Design FMEA Summary

Subsystem	Component	Function	Failure Mode	Consequence	Cause	Mitigation
Powertrain	Bearing	Support Shaft	Minor cracking	Decreased longevity / No effect	Defective part from manufacturer	Manufacturer QA
					Excessive loading / Fatigue	Bearing strength much greater than design loads / Product lifespan not expected to exceed fatigue life
			Major fracture	Shaft misalignment - increased vibration / decreased turbine efficiency	Defective part from manufacturer	Manufacturer QA
					Excessive loading / Fatigue	Bearing strength much greater than design loads / Product lifespan not expected to exceed fatigue life
				Shaft unsupported	Defective part from manufacturer	Manufacturer QA
					Excessive loading / Fatigue	Bearing strength much greater than design loads / Product lifespan not expected to exceed fatigue life
		Allow Shaft to rotate freely	Increased friction / Sticking	Decreased turbine efficiency	Improperly greased bearings	Regular maintenance
					Contamination	Double-sealed bearing reduces foreign particle intrusion
			Jamming	Shaft does not rotate - no power produced	Improperly greased bearings	Regular maintenance
					Contamination	Double-sealed bearing reduces foreign particle intrusion
					Excessive wear	Product lifespan not expected to exceed bearing life
Powertrain	Shaft, Drive	Transmit torque to Gearbox Coupler	Minor cracking	Shaft does not rotate smoothly - decreased turbine efficiency	Excessive loading / Fatigue	Shaft strength much greater than design loads / Product lifespan no expected to exceed fatigue life

			Major fracture	Torque not transmitted	Excessive loading / Fatigue	Shaft strength much greater than design loads / Product lifespan no expected to exceed fatigue life
			Failure of Hub / Coupler mounts	Torque not transmitted	Improper installation	Post-installation inspection
					Excessive loading / Fatigue	Mount strength much greater than design loads / Product lifespan not expected to exceed fatigue life
		Support Hub Assembly	Major fracture	Hub Assembly not supported / Damage to Hub	Excessive loading / Fatigue	Shaft strength much greater than design loads / Product lifespan no expected to exceed fatigue life
			Failure of Hub mounts	Hub Assembly not supported / Damage to Hub	Improper installation	Post-installation inspection
					Excessive loading / Fatigue	Fastener strength much greater than design loads / Product lifespan not expected to exceed fatigue life
		Provide Mounting for Slip Ring	Failure of Slip Ring mounts	Electrical signal not transmitted to Speaker	Improper installation	Post-installation inspection
Powertrain	Coupler, Gearbox	Transmit torque to Gearbox	Minor cracking	Decreased longevity / No effect	Improper installation	Post-installation inspection
					Excessive loading / Fatigue	Coupler strength much greater than design loads / Product lifespan not expected to exceed fatigue life
			Major fracture	Torque not transmitted	Improper installation	Post-installation inspection
					Excessive loading / Fatigue	Coupler strength much greater than design loads / Product lifespan not expected to exceed fatigue life
Powertrain	Gearbox, Planetary, 1:5 Ratio	Transmit torque to Generator Coupler	Major fracture of input / output shafts	Torque not transmitted	Improper installation	Post-installation inspection
					Excessive loading / Fatigue	Coupler strength much greater than design loads / Product lifespan not expected to exceed fatigue life

			Internal gear failure	Torque not transmitted	Defective part from manufacturer	Manufacturer QA
					Excessive wear	Product lifespan not expected to exceed fatigue life
			Binding	Torque not transmitted / damage to other powertrain components	Defective part from manufacturer	Manufacturer QA
					Excessive wear	Product lifespan not expected to exceed fatigue life
		Increase speed of output shaft with respect to input shaft	Fails to increase shaft speed	Electrical power output reduced	No credible cause determined	None
Powertrain	Coupler, Generator	Transmit torque to Generator	Minor cracking	Decreased longevity / No effect	Improper installation	Post-installation inspection
					Excessive loading / Fatigue	Coupler strength much greater than design loads / Product lifespan not expected to exceed fatigue life
			Major fracture	Torque not transmitted	Improper installation	Post-installation inspection
					Excessive loading / Fatigue	Coupler strength much greater than design loads / Product lifespan not expected to exceed fatigue life
Powertrain	Generator, Permanent Magnet	Convert mechanical power to electrical power	Stripping of threads on input shaft	Coupler not attached - Power not generated	Improper installation	Post-installation inspection / Ensure coupler is installed to rated torque
			Internal generator failure	Power not generated	Defective part from manufacturer	Manufacturer QA
					Insufficient cooling of generator	Ports on exterior of housing allow convective cooling
					Excessive wear	Product lifespan not expected to exceed generator life
			Binding of generator	Power not generated / Damage to powertrain components and/or Hub Assembly	Shorting of output wires	Ensure wires are properly separated, soldered, and insulated at installation
Blade	Air Tube	Transfer air pulse from speaker to airfoil	Crack	Air leakage/ reduced performance of AFC	Excessive loading / Fatigue	Ensure Blade Spar is strong enough to support blade during all loads

		surface	Clog	Air blockage preventing airflow, shuts down AFC	External materials clogging up small holes on air foil surface	Take care in blade transportation and storage, check holes periodically and remove any clogs seen
Blade	Composite Skin	Creates Blade shape and provides structural support	Crack	Blade could start to bend, breaking other internal parts	Excessive loading / Fatigue/ Collision with external object	Composite skin strength designed to be much greater than expected loadings
					Improper manufacturing	Manufacturer QA
			Major Failure	Blade would be destroyed during high loading	Excessive loading / Fatigue/ Collision with external object	Composite skin strength designed to be much greater than expected loadings
					Improper manufacturing	Manufacturer QA
Blade	Spar	Main structural support for blade	Crack	Blade could start to bend, breaking other parts	Excessive loading / Fatigue	Spar strength designed to handle much more than expected loading
			Major Failure	Blade would be destroyed during high loading	Excessive loading / Fatigue	Spar strength designed to handle much more than expected loading
Blade	Hub Adaptor	Connect blade to hub support structure	Major Failure	Blade would no longer stay attached to hub/ massive unbalance	Excessive loading/ Fatigue	Adaptor's strength designed to be much larger than expected loading
					Manufacturing Defect	Manufacturer QA
			Slip	Blades pitch will no longer be able to be set	Excessive loading/ Fatigue	Grooves cut into side of adaptor to prevent any slipping
					Improper installation	Post-installation inspection
			Deform	Blade would no longer be capable of being installed onto hub	Excessive loading/ Fatigue	Adaptor's strength designed to be much larger than expected loading
					Improper installation	Post-installation inspection
					Extensive wear	Proper installation techniques and material selection with high wear resistance
Blade	Set Screws	Keep hub adaptor attached to hub	Major Failure	Blade would come apart from hub during operation	Excessive loading/ Fatigue	Set screw strength designed to be much larger than expected values
					Manufacturing	Manufacturer QA

					Defect	
			Slip	Blade would come apart from hub during operation	Excessive loading/ Fatigue	Set screw strength designed to be much larger than expected values
					Improper installation	Post-installation inspection
			Deform	Blade would no longer be able to be removed from hub	Excessive loading/ Fatigue	Set screw strength designed to be much larger than expected values
		Set pitch angle of blade	Major Failure	Blades pitch will no longer be able to be set	Excessive loading/ Fatigue	Set screw strength designed to be much larger than expected values
					Manufacturing Defect	Manufacturer QA
			Slip	Blades would rotate and ruin test	Excessive loading/ Fatigue	Set screw strength designed to be much larger than expected values
					Improper installation	Post-installation inspection
			Deform	Blades would rotate and ruin test	Excessive loading/ Fatigue	Set screw strength designed to be much larger than expected values
					Manufacturing Defect	Manufacturer QA
Hub	Main Hub	Support Hub Assembly	Minor cracking	Decreased longevity/ AFC interference due to air pulse leak and sound wave leak	Excessive loading/ Fatigue	Main hub design and material selected to withstand much more loading then expected during use
					Manufacturing Defect	Manufacturer QA
			Major Failure	Hub assembly breaks apart, massive wind turbine failure, large unbalance	Excessive loading/ Fatigue	Main hub design and material selected to withstand much more loading then expected during use
					Manufacturing Defect	Manufacturer QA
			Deformation	Unbalance	Excessive loading/ Fatigue	Main hub design and material selected to withstand much more loading then expected during use
					Manufacturing	Manufacturer QA

					Defect	
		Transfer torque generated by blades to main drive shaft	Minor cracking	Decreased longevity/ No effect	Excessive loading/ Fatigue	Main hub design and material selected to withstand much more loading then expected during use
					Manufacturing Defect	Manufacturer QA
			Major Failure	Hub spins freely around shaft	Excessive loading/ Fatigue	Main hub design and material selected to withstand much more loading then expected during use
					Manufacturing Defect	Manufacturer QA
					Improper installation	Post-installation inspection
				Hub comes apart from main shaft	Excessive loading/ Fatigue	Main hub design and material selected to withstand much more loading then expected during use
					Manufacturing Defect	Manufacturer QA
					Improper installation	Post-installation inspection
		Support Blades	Minor cracking	Decreased longevity/ AFC interference due to air pulse leak and sound wave leak	Excessive loading/ Fatigue	Main hub design and material selected to withstand much more loading then expected during use
					Manufacturing Defect	Manufacturer QA
			Major Failure	Blades break apart from hub	Excessive loading/ Fatigue	Main hub design and material selected to withstand much more loading then expected during use
					Manufacturing Defect	Manufacturer QA
			Deformation	Blades misalign and cause massive unbalance	Excessive loading/ Fatigue	Main hub design and material selected to withstand much more loading then expected during use

					Manufacturing Defect	Manufacturer QA
Hub	Hub Cap	Supports Speaker	Minor cracking	Speaker looses effectiveness	Fatigue	Hub cap construction designed to withstand higher loading than expected during use
Hub	Hub Cap	Supports Speaker	Minor cracking	Speaker looses effectiveness	Manufacturing Defect	Manufacturer QA
Hub	Hub Cap	Supports Speaker	Major Failure	Speaker breaks loose and AFC no longer functions properly	Fatigue	Hub cap construction designed to withstand higher loading than expected during use
Hub	Hub Cap	Supports Speaker	Major Failure	Speaker breaks loose and AFC no longer functions properly	Manufacturing Defect	Manufacturer QA
Hub	Hub Cap	Supports Speaker	Major Failure	Speaker breaks loose and AFC no longer functions properly	Improper installation	Post-installation inspection
Hub	Hub Cap	Aerodynamic Shape for controlling air flow around turbine housing	Major Failure	Cap falls off or pieces of cap falls off creating stagnation and reducing the effective streamlining of the wind turbine	Excessive loading/ Fatigue	Hub cap construction designed to withstand higher loading than expected during use
Hub	Hub Cap	Aerodynamic Shape for controlling air flow around turbine housing	Major Failure	Cap falls off or pieces of cap falls off creating stagnation and reducing the effective streamlining of the wind turbine	Manufacturing Defect	Manufacturer QA
Hub	Hub Cap	Aerodynamic Shape for controlling air flow around turbine housing	Deformation	Flow over deformed areas result in unpredictable effects	Excessive loading/ Fatigue	Hub cap construction designed to withstand higher loading than expected during use
Hub	Hub Cap	Aerodynamic Shape for controlling air flow around turbine housing	Deformation	Flow over deformed areas result in unpredictable effects	Manufacturing Defect	Manufacturer QA
Hub	Speaker	Creates sound waves and air pulses used in AFC	Mounts Breaking	Speaker no longer will be mounted correctly and causes AFC to lose effectiveness	Fatigue	Speaker is designed for high loading/ Product lifespan not expected to exceed fatigue life
Hub	Speaker	Creates sound waves and air pulses used in AFC	Mounts Breaking	Speaker no longer will be mounted correctly and causes AFC to lose effectiveness	Manufacturing Defect	Manufacturer QA
Hub	Speaker	Creates sound waves and air pulses used in AFC	Diaphragm Breaking	Speaker is no longer to produce sound waves and air pulses, AFC is stopped	Fatigue	Speaker is designed for high loading/ Product lifespan not expected to exceed fatigue life

					Improper operation	Proper testing of frequency and amplitude controllers before operation begins
			Electrical Connection Fails	Speaker is no longer to produce sound waves and air pulses, AFC is stopped	Fatigue	Speaker is designed for high loading/ Product lifespan not expected to exceed fatigue life
					Improper installation	Post-installation inspection
AFC Electronics	Amp	Increases the amplitude of a signal	failure to maintain temp	Decrease of woofer efficiency	Long term use	Periodic Maintenance
						Higher product life span
					Defective part from manufacturer	Manufacturer QA
			Insufficient amplification	Decrease of woofer efficiency	Not enough power	Battery
			Generates too large an amplitude	Malfunction of device/ Damage of the speaker	Excessive Power	Use of fuses
AFC Electronics	Frequency Gen	Generate electrical waveforms	Fails to Generate continuous waves	Decrease of woofer efficiency	Defective part from manufacturer	Manufacturer QA
					Over heat	cooling vents
AFC Electronics	Charge controller	Prevents Overcharge	Failure to regulate charge	Reduction Battery Performance/lifespan/	Defective part from manufacturer	
				Over charge	Improper connection	
				Deep discharging	AFC not working	
AFC Electronics	Battery	supply power	Failure to maintain temp	Malfunction of device	Overheat	
				Loss of original charge	Improper positioning	
			Failure to get charged	Failure to start generating power	Defective part from manufacturer	
AFC Electronics	Wattmeter	measure the electric power	Failure to measure electric power	No effect		
AFC Electronics	Slip ring	Electrical connector to a rotating assembly	Failure to transfer electricity to hub	No electrical power transferred to hub	Defective part from manufacturer	
					High voltage	
Tower / Housing	Shell	contain mechanical and electrical	Minor cracking	Decreased longevity / No effect	Fiber glass not molded correctly	ensure the perfection of the molding process
				malfunction of	Liquids getting into	Seal Shell/ Liquids

		component s		electronics	electronics	could cause electronics to stop working
			Major Fracture	Shaft misalignment - increased vibration / decreased turbine efficiency	Excessive load on the Shell	ensure bearing support of the shaft / Vibration of the shaft will cause a major fracture in the shell
					liquids getting into electronics	ensure the perfection of the molding process/Liquids could cause electronics to stop working
Tower / Housing	Angle Bracket	Support shell	Minor cracking	Shaft misalignment - increased vibration / decreased turbine efficiency	Excessive load	Thicker angle brackets/ Making angle brackets thicker will help in holding unexpected loads
			Major Fracture	Shaft misalignment - increased vibration / decreased turbine efficiency	Excessive load	Thicker angle brackets/Making angle brackets thicker will help in holding unexpected loads
Tower / Housing	Tower	Support shell component s/blades	Vibration of tower	Shaft misalignment - increased vibration / decreased turbine efficiency	Excessive loading on tower	foot that will support tower
			Failure of mounting hole	Vibration of shell	Defective part from the manufacture	Manufacturer QA
					Excessive loading	Thicker angle brackets
				Shaft misalignment	Excessive load on the Shell	Thicker angle brackets
					Crack in the shell	Seal Shell/ Liquids could cause electronics to stop working
					Defective part from the manufacture	Manufacturer QA
Tower / Housing	Tower foot	Support tower against forces	Tower Vibration	Fracture and misalignment of the shaft	Big Forces	four foot that are made of plywood/ plywood will support the tower against forces from any direction

K. Slip Ring Data

See attached page

L. Drawings

See attached pages

M. Gantt Chart

Below is a sample of the Gantt chart, which was completed in Microsoft Project. Because Project files are not easily printed on small-size paper, the complete Gantt chart is provided as an electronic attachment to this report.

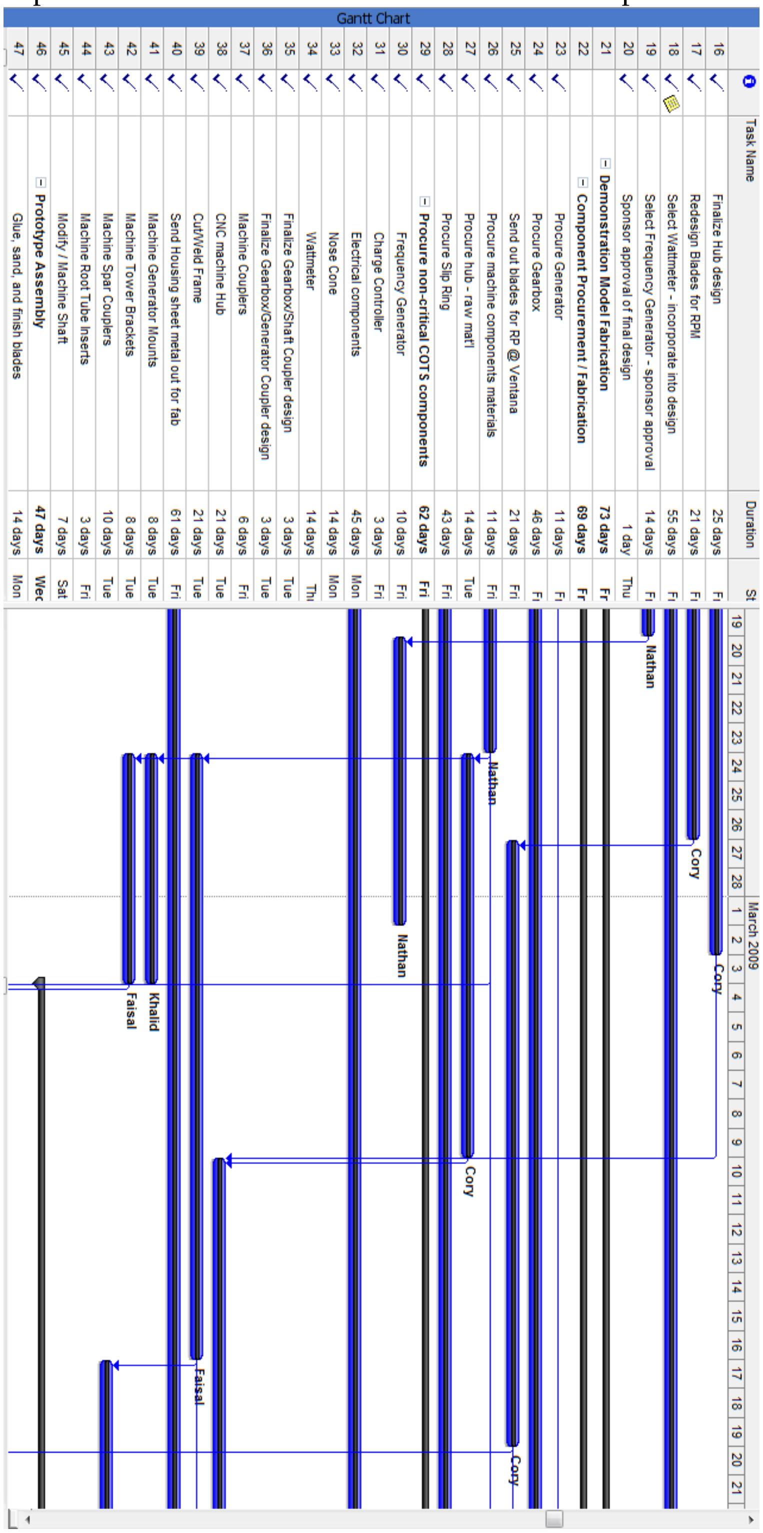

N. Electrical Design

NOTES, UNLESS OTHERWISE SPECIFIED.

1. MATERIAL: ALUMINUM ALLOY 2024 PER AMS-QQ-A-250/5 OR EQUIVALENT.
2. FINISH: NONE.
3. BREAK ALL SHARP EDGES, R.03 MAX.
4. PART IS TO BE FREE FROM BURRS, SHARP EDGES, AND OTHER VISUAL DEFECTS.
5. DIMENSIONS IN ( ) ARE FOR REFERENCE ONLY.

REVISIONS		
REV.	DESCRIPTION	DATE
1	INITIAL ENGINEERING RELEASE	02/26/2009

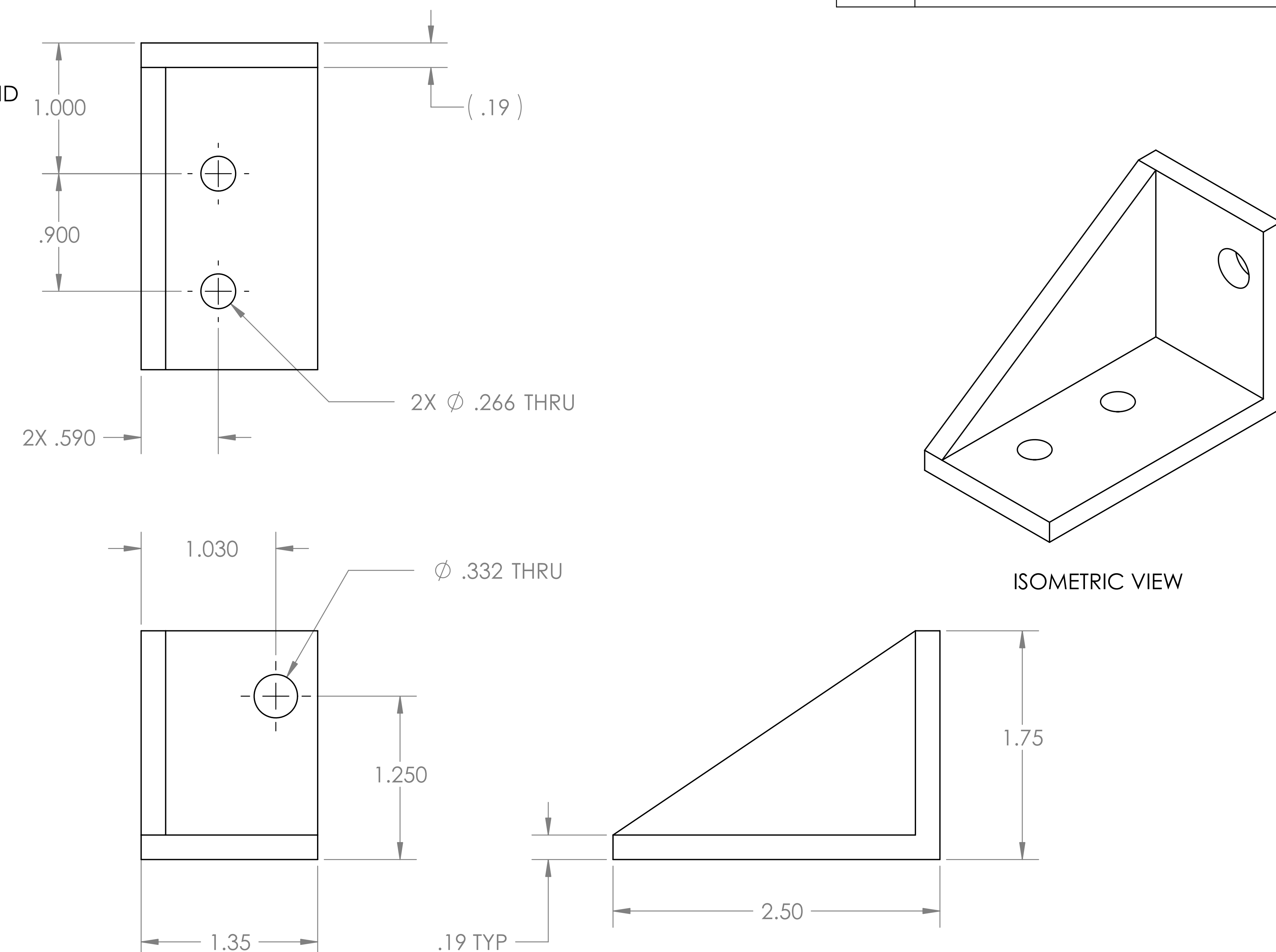

ISOMETRIC VIEW

UNLESS OTHERWISE SPECIFIED:		NAME	DATE
DIMENSIONS ARE IN INCHES TOLERANCES: ANGULAR: X°±1° X.X±0.5° TWO PLACE DECIMAL ±.010" THREE PLACE DECIMAL ±.005" INTERPRET DRAWING IAWASME Y14.5M-1994 OR LATER.	DRAWN	N.W.	02/23/09
	CHECKED	F.A.M.	02/26/09
	ENG APPR.		
	MFG APPR.		
	Q.A.		
DO NOT SCALE DRAWING	COMMENTS:		

TITLE:

MOUNT, GENERATOR, PORT SIDE

SIZE	DWG. NO.	REV
B	3679-0002	1
SCALE: 1:1		SHEET 1 OF 1

NOTES, UNLESS OTHERWISE SPECIFIED.

1. MATERIAL: ALUMINUM ALLOY 2024 PER AMS-QQ-A-250/5 OR EQUIVALENT.
2. FINISH: NONE.
3. BREAK ALL SHARP EDGES, R.03 MAX.
4. PART IS TO BE FREE FROM BURRS, SHARP EDGES, AND OTHER VISUAL DEFECTS.
5. DIMENSIONS IN ( ) ARE FOR REFERENCE ONLY.

REVISIONS		
REV.	DESCRIPTION	DATE
1	INITIAL ENGINEERING RELEASE	02/26/2009

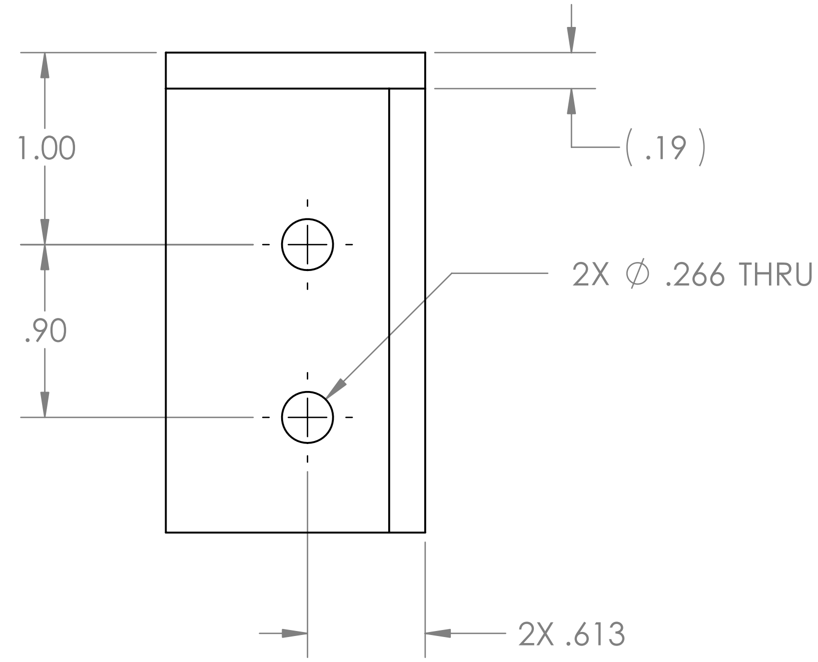

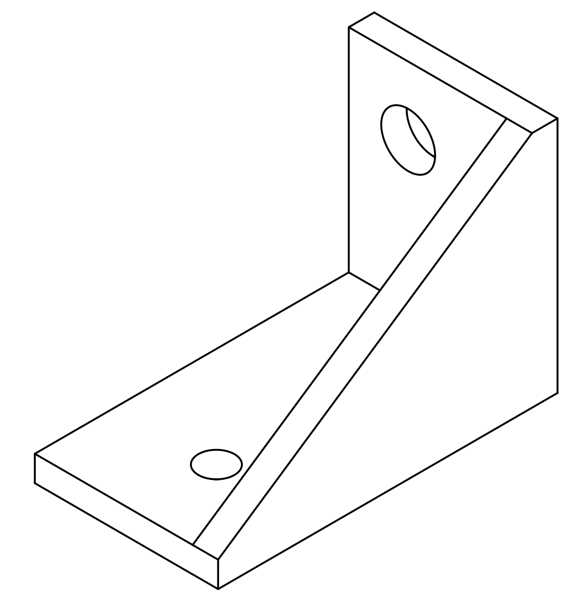
ISOMETRIC VIEW

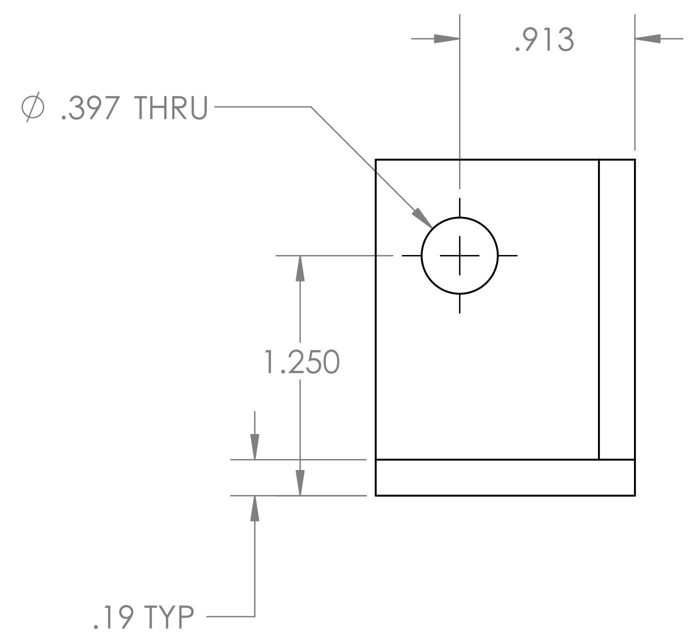

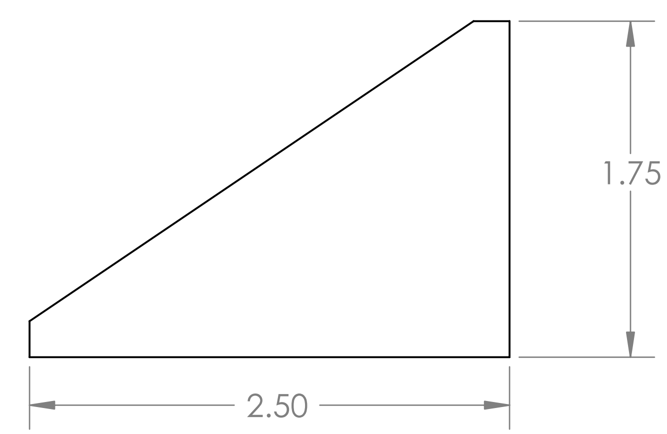

PROPRIETARY AND CONFIDENTIAL

THE INFORMATION CONTAINED IN THIS DRAWING IS THE SOLE PROPERTY OF THE UNIVERSITY OF ARIZONA. ANY REPRODUCTION IN PART OR AS A WHOLE WITHOUT THE WRITTEN PERMISSION OF THE UNIVERSITY OF ARIZONA IS PROHIBITED.

UNLESS OTHERWISE SPECIFIED:

DIMENSIONS ARE IN INCHES
TOLERANCES:
ANGULAR: X°±1° X.X±0.5°
TWO PLACE DECIMAL ±.010"
THREE PLACE DECIMAL ±.005"

INTERPRET DRAWING IAWASME Y14.5M-1994 OR LATER.

DO NOT SCALE DRAWING

	NAME	DATE
DRAWN	N.W.	02/23/09
CHECKED	K.M.	02/26/09
ENG APPR.		
MFG APPR.		
Q.A.		

COMMENTS:

TITLE:

MOUNT, GENERATOR, STRBRD

SIZE	DWG. NO.	REV
B	3679-0003	1

SCALE: 1:1 SHEET 1 OF 1

NOTES, UNLESS OTHERWISE SPECIFIED.

1. MATERIAL: 5052-H32 ALUMINUM SHEET PER AMS-QQ-A-250-8, 0.040" THICK.
2. FINISH: 100% WHITE POWDER COAT EXTERIOR SURFACES AS INDICATED BY FLAGNOTE 6.
3. PART IS TO BE FREE FROM BURRS, SHARP EDGES, AND OTHER VISUAL DEFECTS.
4. THROUGH HOLE CENTERLINES ARE SPACED AT THE ANGLES INDICATED. IF HOLES ARE DRILLED IN FLAT PATTERN, HOLE ELONGATION POST-BENDING IS PERMISSIBLE.
5. STEP BENDS PERMISSIBLE FOR THE RADIUS INDICATED.
6. COMPLETELY POWDER COAT SURFACES INDICATED. OVERSPRAY NOT PERMISSIBLE ON INTERIOR SURFACES.
7. PART IS SYMMETRIC ABOUT CENTERLINE.
8. DIMENSIONS IN ( ) ARE FOR REFERENCE ONLY.

REVISIONS		
REV.	DESCRIPTION	DATE
1	INITIAL ENGINEERING RELEASE	03/05/09

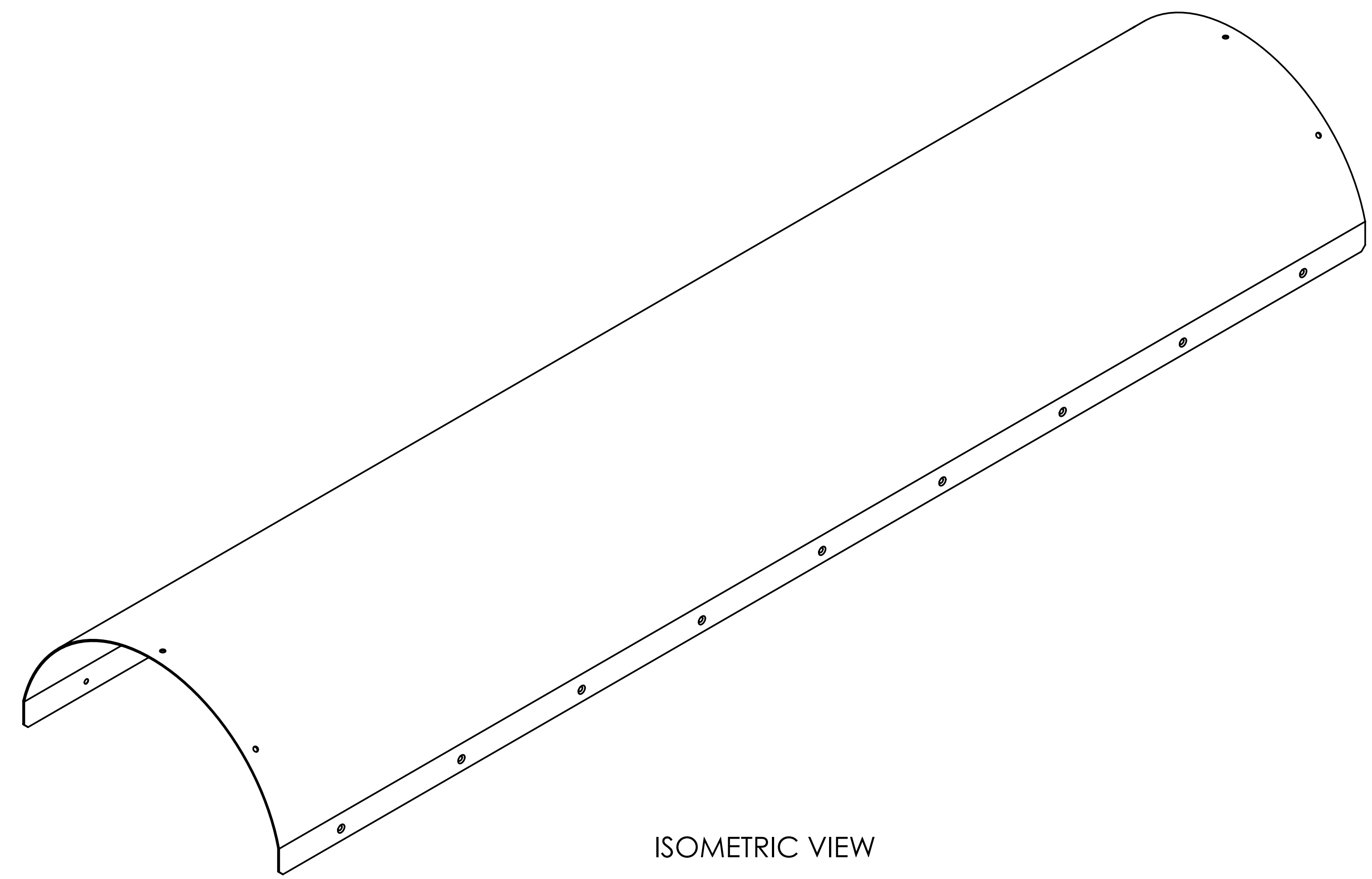

ISOMETRIC VIEW

UNLESS OTHERWISE SPECIFIED:

DIMENSIONS ARE IN INCHES
TOLERANCES:
ANGULAR: X°±1° X.X±0.5°
TWO PLACE DECIMAL ±.010"
THREE PLACE DECIMAL ±.005"

INTERPRET DRAWING IAWASME Y14.5M-1994 OR LATER.

DO NOT SCALE DRAWING

	NAME	DATE
DRAWN	NW	090303
CHECKED	CB	090304
ENG APPR.		
MFG APPR.		
Q.A.		

COMMENTS:

TITLE: SHELL, TOP

SIZE	DWG. NO.	REV
B	3679-0004	1

SCALE: 1:4 | SHEET 1 OF 3

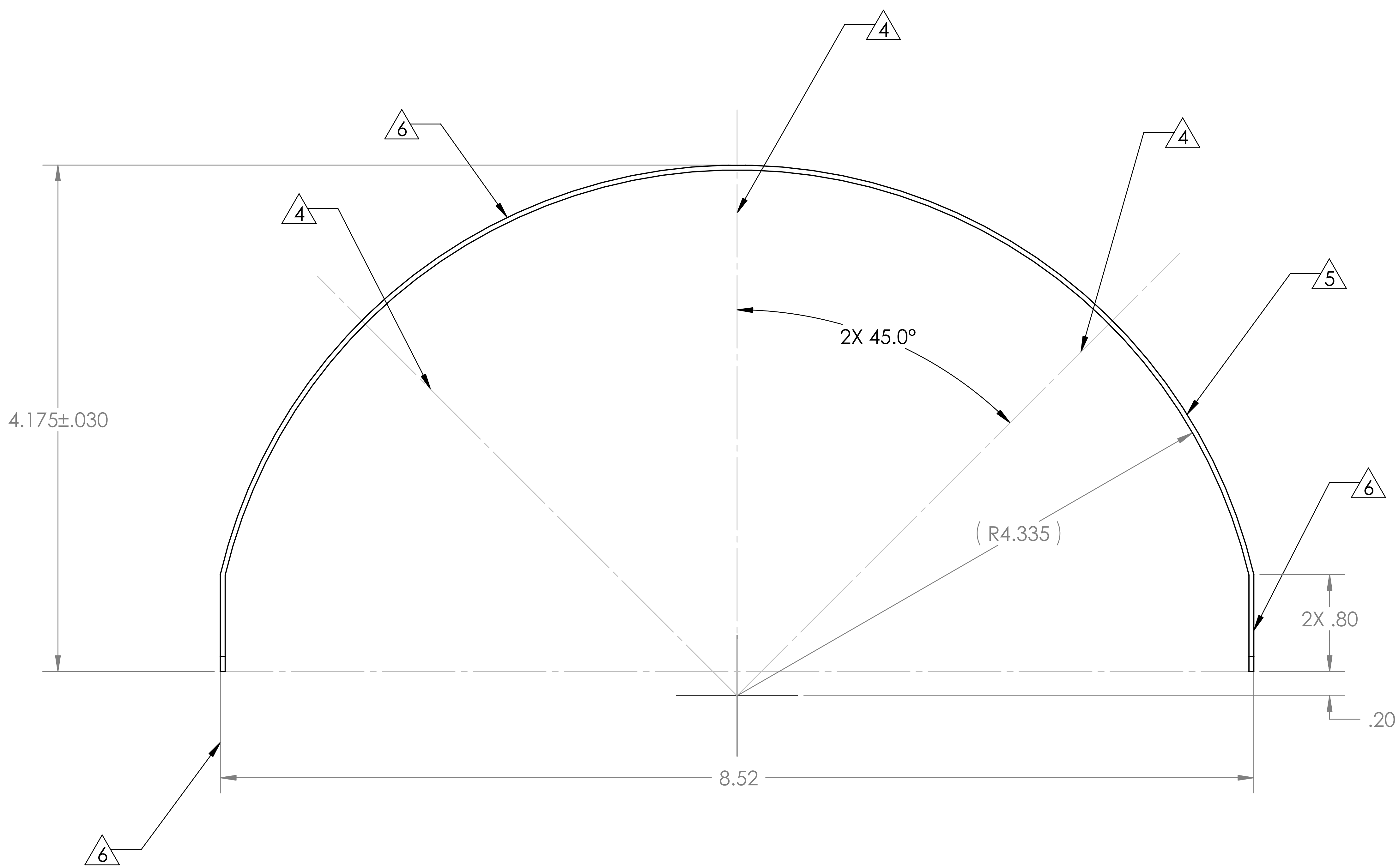

PROPRIETARY AND CONFIDENTIAL

THE INFORMATION CONTAINED IN THIS DRAWING IS THE SOLE PROPERTY OF THE UNIVERSITY OF ARIZONA. ANY REPRODUCTION IN PART OR AS A WHOLE WITHOUT THE WRITTEN PERMISSION OF THE UNIVERSITY OF ARIZONA IS PROHIBITED.

DO NOT SCALE DRAWING

TITLE: SHELL, TOP

SIZE	DWG. NO.	REV
B	3679-0004	1
SCALE: 1:1		SHEET 2 OF 3

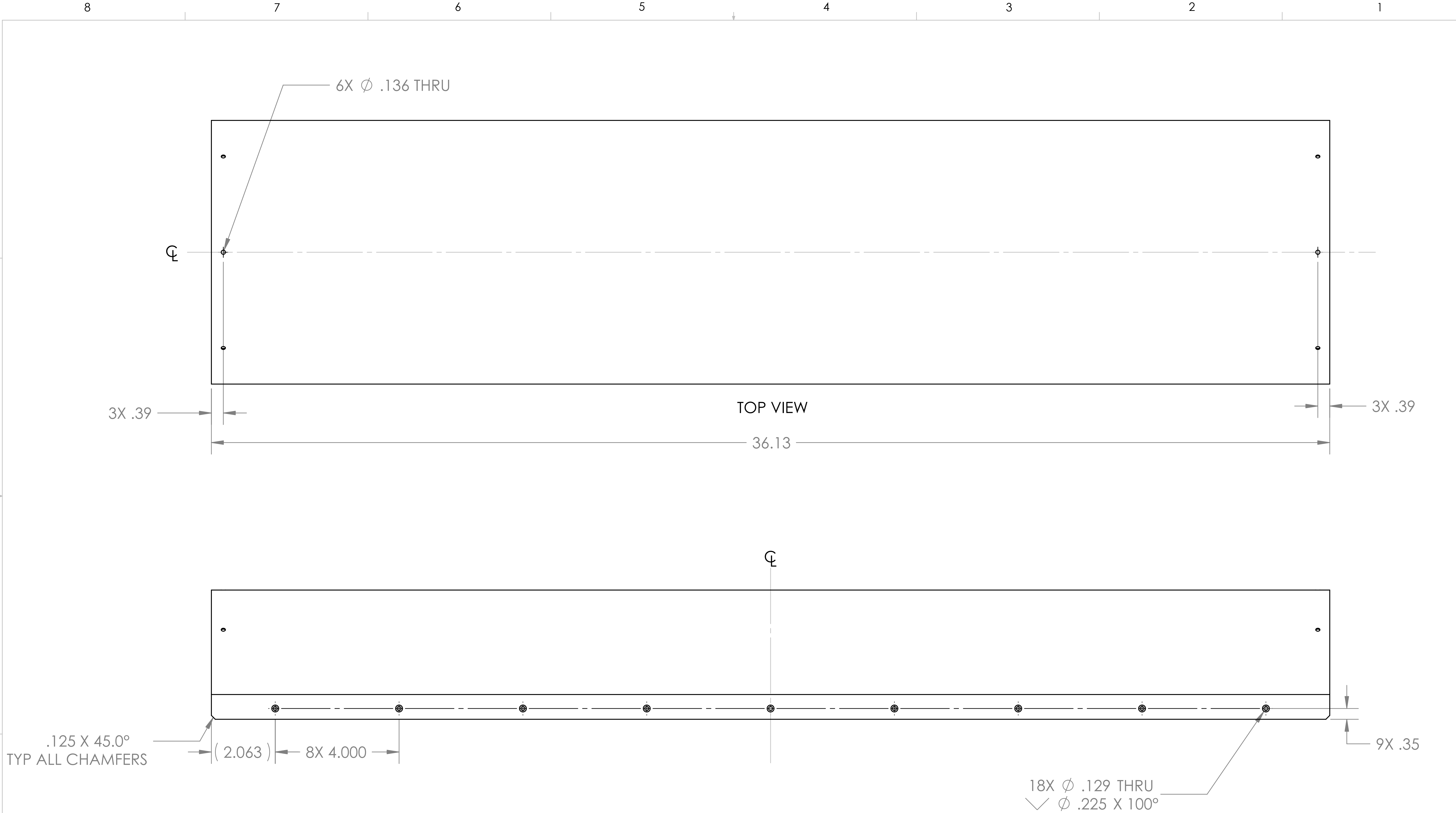

DO NOT SCALE DRAWING

TITLE:		
SHELL, TOP		
SIZE B	DWG. NO. 3679-0004	REV 1
SCALE: 1:3		SHEET 3 OF 3

NOTES, UNLESS OTHERWISE SPECIFIED.

1. MATERIAL:
   BASE: ALUMINUM ALLOY 6061 PER AMS-QQ-A-225/8, 0.25 IN THICK.
   TUBE: ALUMINUM ALLOY 6061 PER AMS-QQ-A-225/8, 4.00 IN ID, 4.5 IN OD.
2. FINISH: NONE.
3. BREAK ALL SHARP EDGES, R.03 MAX.
4. PART IS TO BE FREE FROM BURRS, SHARP EDGES, AND OTHER VISUAL DEFECTS.
5. WELD TUBE EDGE INDICATED TO BASE SUCH THAT TUBE CENTER AXIS COINCIDES WITH BASE CENTER POINT. GMAW WELDS MAY BE SUBSTITUTED FOR GTAW WELDS WHERE DEEMED NECESSARY.
6. TUBE HOLE CENTERLINES ARE ORIENTED AS SHOWN. PERMISSIBLE TO WELD TUBE SUCH THAT HOLES ARE ROTATED 90° FROM ORIENTATION SHOWN IN ISOMETRIC VIEW.
7. PART IS SYMMETRIC ABOUT CENTERLINE.
8. DIMENSIONS IN ( ) ARE FOR REFERENCE ONLY.

REVISIONS		
REV.	DESCRIPTION	DATE
1	INITIAL ENGINEERING RELEASE	03/24/09

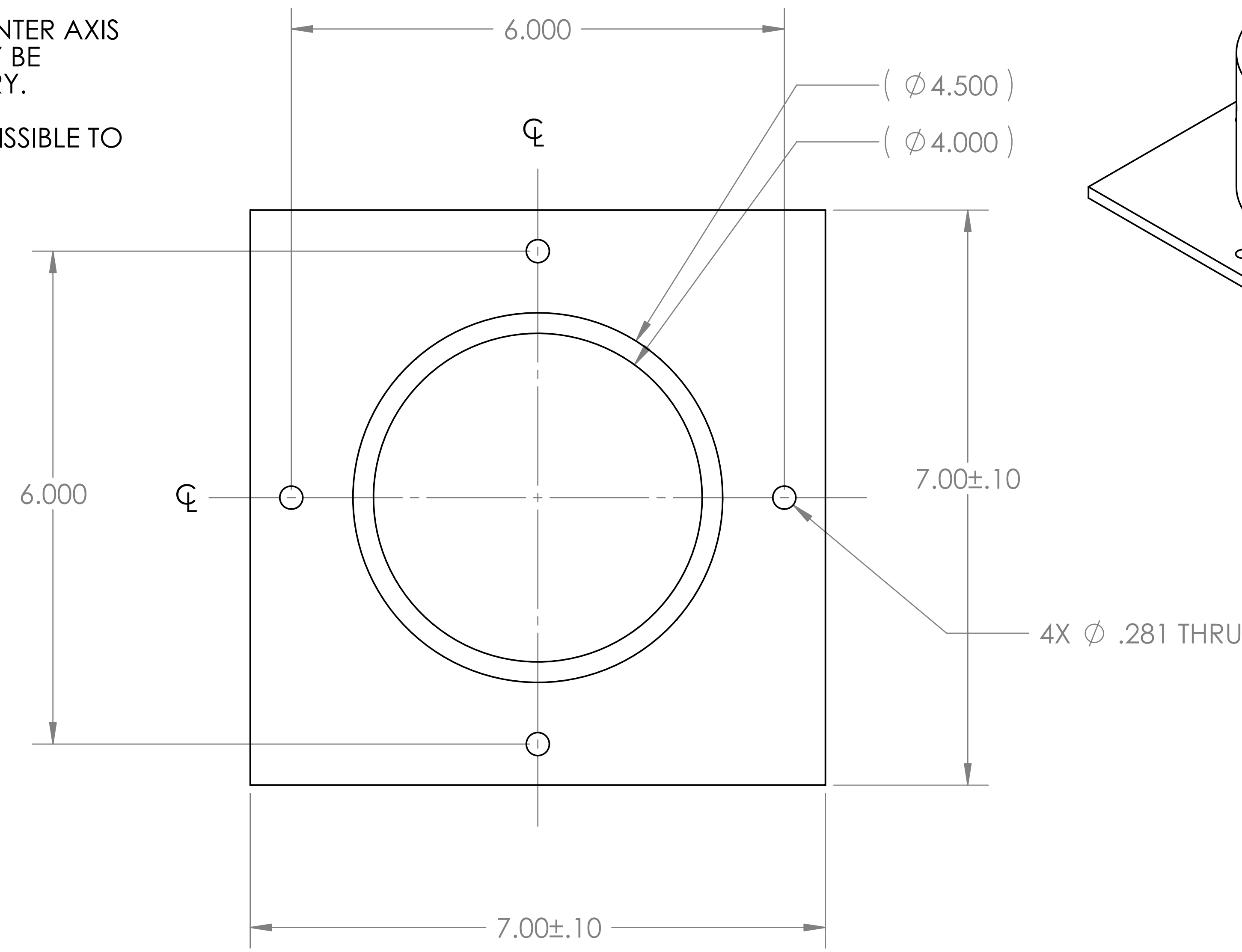

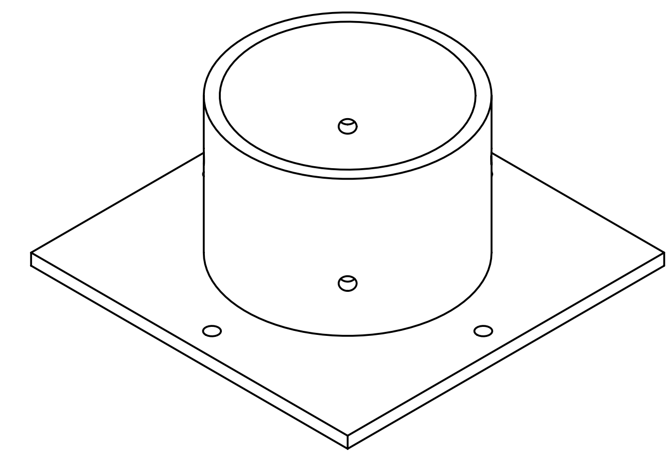

ISOMETRIC VIEW
SCALE 1:3

UNLESS OTHERWISE SPECIFIED:

DIMENSIONS ARE IN INCHES
TOLERANCES:
ANGULAR: X°±1° X.X±0.5°
TWO PLACE DECIMAL ±.010"
THREE PLACE DECIMAL ±.005"

INTERPRET DRAWING IAWASME Y14.5M-1994 OR LATER.

DO NOT SCALE DRAWING

	NAME	DATE
DRAWN	N.W.	03/23/09
CHECKED	F.A.M.	03/24/09
ENG APPR.		
MFG APPR.		
Q.A.		

COMMENTS:

TITLE:

BRACKET, TOWER MOUNT

SIZE	DWG. NO.	REV
B	3679-0005	1

SCALE: 1:2

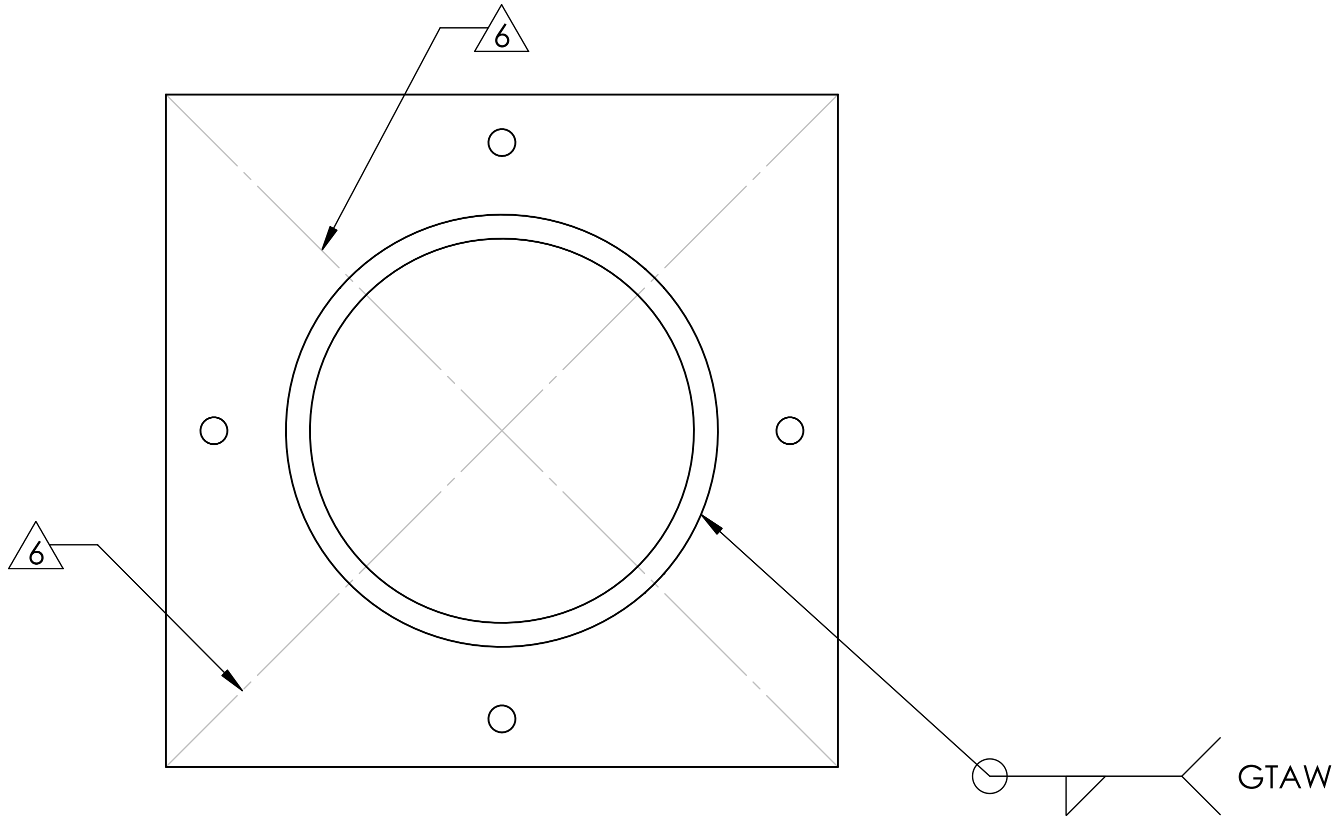

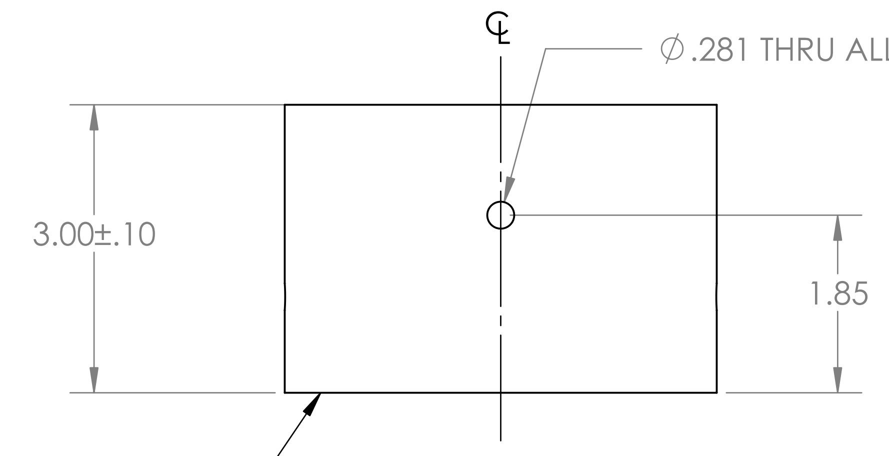

DETAIL A
TUBE FRONT VIEW

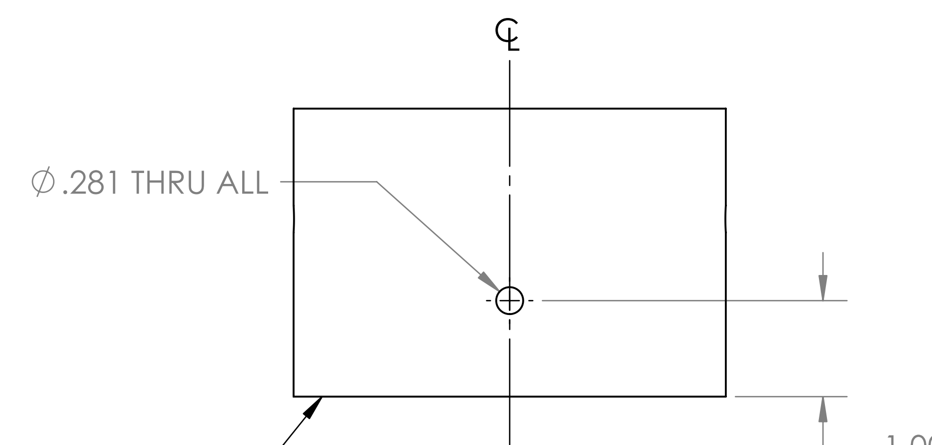

DETAIL B
TUBE RIGHT SIDE VIEW

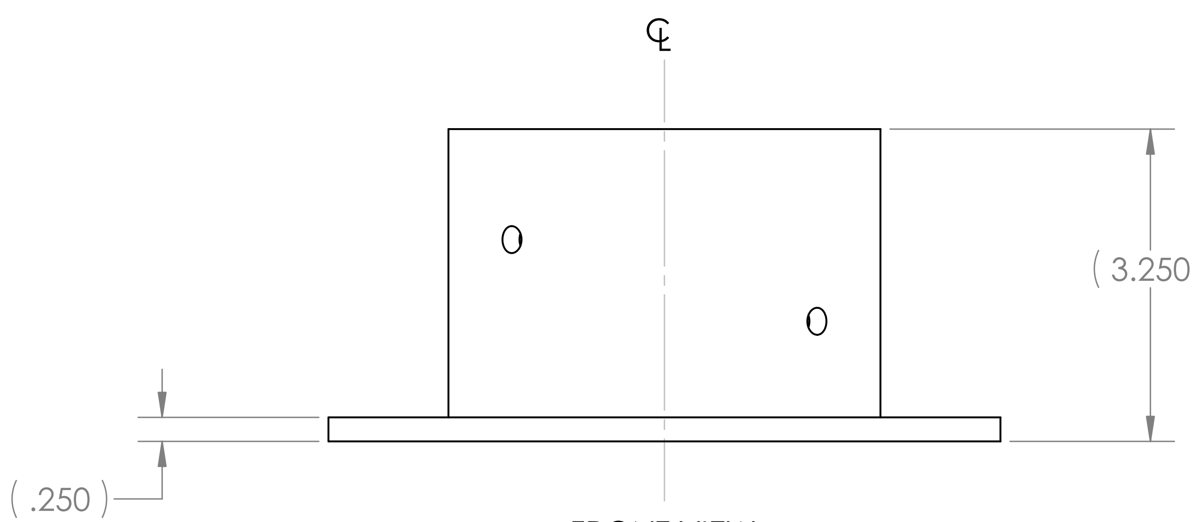

FRONT VIEW

TITLE: BRACKET, TOWER MOUNT		
SIZE **B**	DWG. NO. 3679-0005	REV 1
SCALE: 1:2		SHEET 2 OF 2

NOTES, UNLESS OTHERWISE SPECIFIED.

1. MATERIAL: TUBES: AISI 1008 LOW-CARBON STEEL, 1" X 1" SQUARE CROSS SECTION, 0.12" WALL THICKNESS. MAKE FROM MCMASTER-CARR P/N 6527K31 OR EQUIVALENT.
2. FINISH: NONE.
3. SEE TABLE 1 FOR TUBE CUT LENGTHS AND CORRESPONDING SEQUENCE NUMBERS. TUBE LENGTHS ARE FINISHED LENGTHS AND DO NOT INCLUDE WELD THICKNESSES.
4. WELD ALL TUBE JOINTS USING MGAW OR MTAW PROCESSES AS APPROPRIATE. WELD ALL AROUND EACH JOINT. GRIND WELDS ON TOP AND BOTTOM SURFACES OF ASSEMBLY FLAT WITHIN 0.025" WHERE POSSIBLE.
5. WELD GEARBOX MOUNT PLATE (P/N 3679-0007) TO FRAME AS SHOWN. ENSURE CENTERPOINT OF HOLE INDICATED COINCIDES WITH ASSEMBLY CENTERLINE.
6. ASSEMBLY AND TUBES ARE SYMMETRIC ABOUT CENTERLINES.
7. DIMENSIONS IN ( ) ARE FOR REFERENCE ONLY.

REVISIONS		
REV.	DESCRIPTION	DATE
1	INITIAL ENGINEERING RELEASE	03/05/09

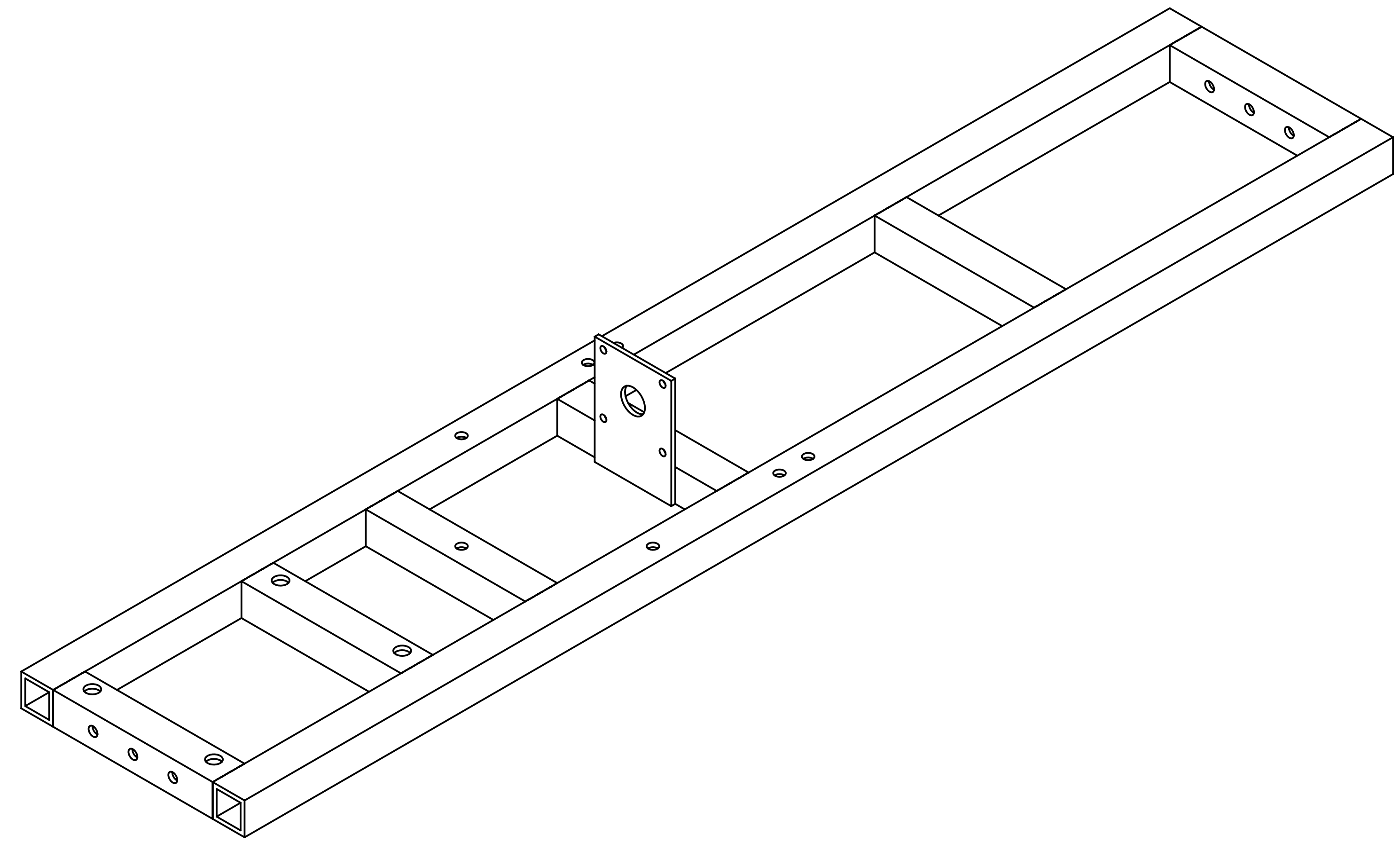

ISOMETRIC VIEW

SEQ. NO.	QTY.	LENGTH (IN.)	REFERENCE DETAIL
010	2	36.0	A
020	1	5.0	B1-B2
030	1	5.0	C
040	2	5.0	D
050	1	5.0	E
060	1	5.0	F

TABLE 1. TUBE CUT LENGTHS

UNLESS OTHERWISE SPECIFIED:
DIMENSIONS ARE IN INCHES
TOLERANCES:
ANGULAR: X°±1° X.X±0.5°
TWO PLACE DECIMAL ±.010"
THREE PLACE DECIMAL ±.005"
INTERPRET DRAWING IAWASME Y14.5M-1994 OR LATER.
DO NOT SCALE DRAWING

	NAME	DATE
DRAWN	N.W.	03/01/09
CHECKED	K.M.	03/05/09
ENG APPR.		
MFG APPR.		
Q.A.		
COMMENTS:		

TITLE:
ASSEMBLY, FRAME

SIZE B | DWG. NO. 3679-0006 | REV 1

SCALE: 1:4 | SHEET 1 OF 4

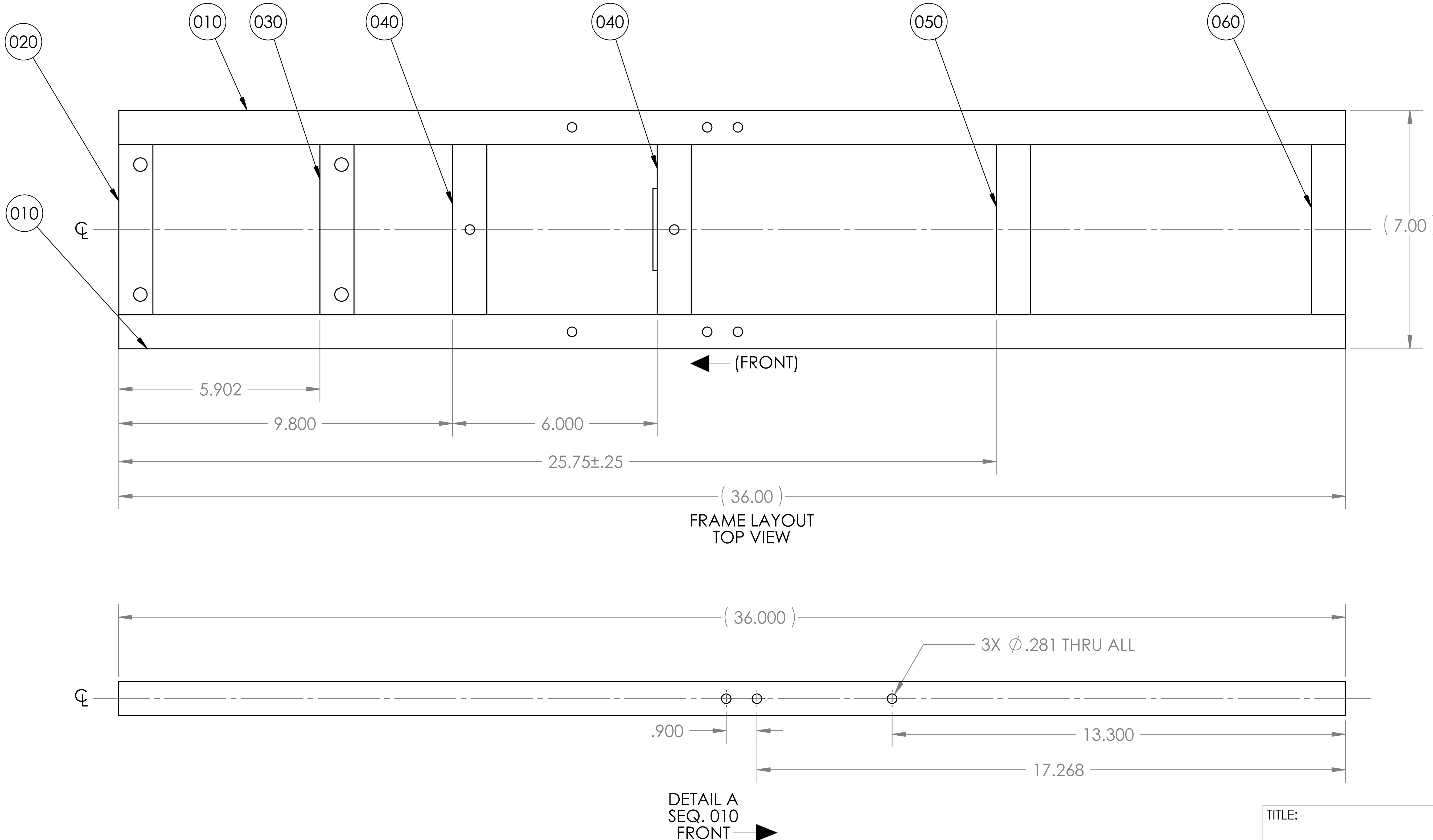

DO NOT SCALE DRAWING

TITLE: ASSEMBLY, FRAME

SIZE	DWG. NO.	REV
B	3679-0006	1

SCALE: 1:3

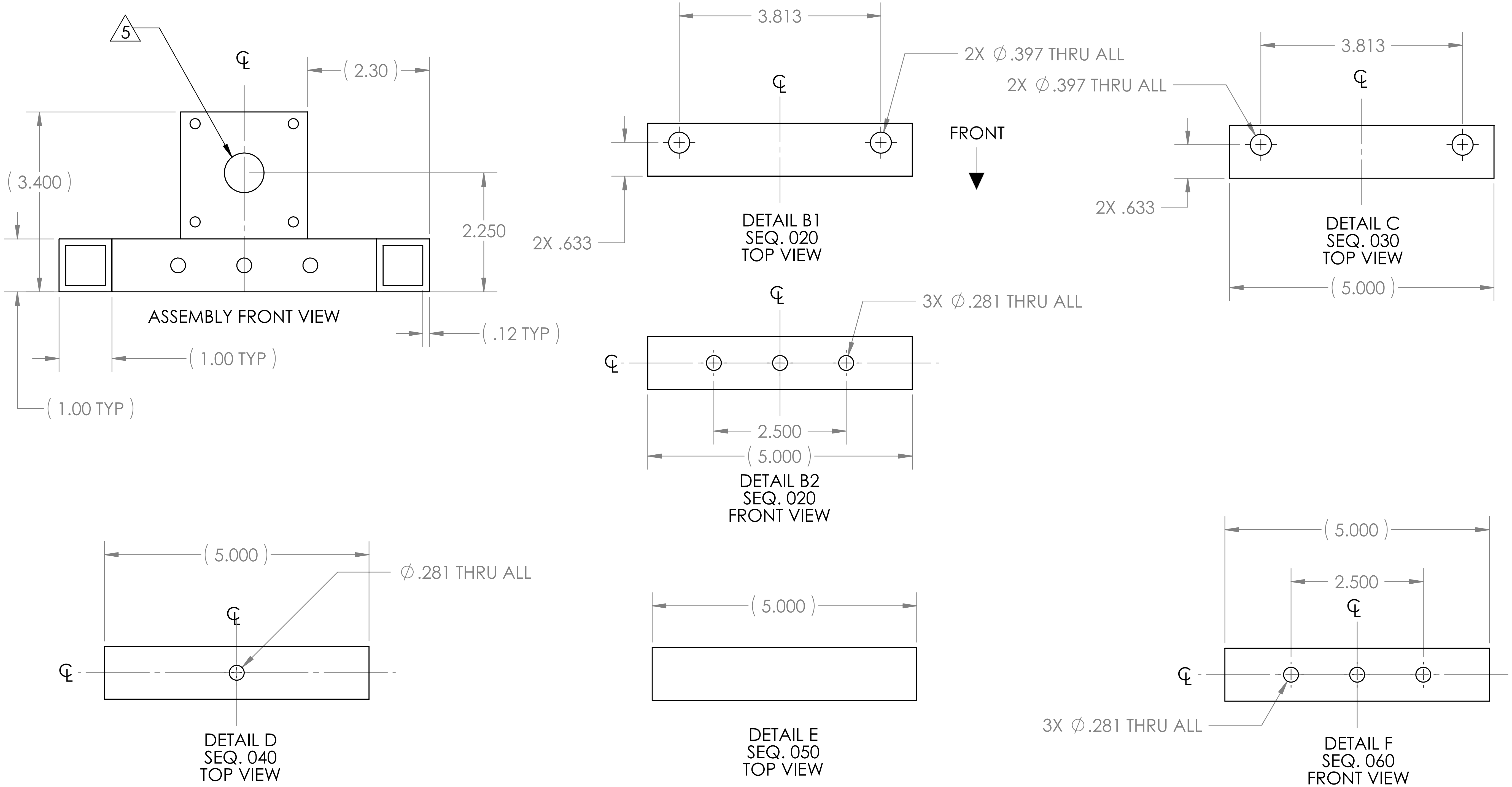

TITLE:		
ASSEMBLY, FRAME		
SIZE B	DWG. NO. 3679-0006	REV 1
SCALE: 1:2		SHEET 3 OF 4

NOTES, UNLESS OTHERWISE SPECIFIED.

1. MATERIAL: AISI 4130 ALLOY STEEL, 0.125" THICK. MAKE FROM MCMASTER-CARR P/N 4459T11 OR EQUIVALENT.
2. FINISH: NONE.
3. BREAK SHARP EDGES, R.03 MAX.
4. PART IS TO BE FREE FROM BURRS, SHARP EDGES, AND OTHER VISUAL DEFECTS.
5. PART IS SYMMETRIC ABOUT CENTERLINE.
6. DIMENSIONS IN ( ) ARE FOR REFERENCE ONLY.

REVISIONS		
REV.	DESCRIPTION	DATE
1	INITIAL ENGINEERING RELEASE	02/28/09

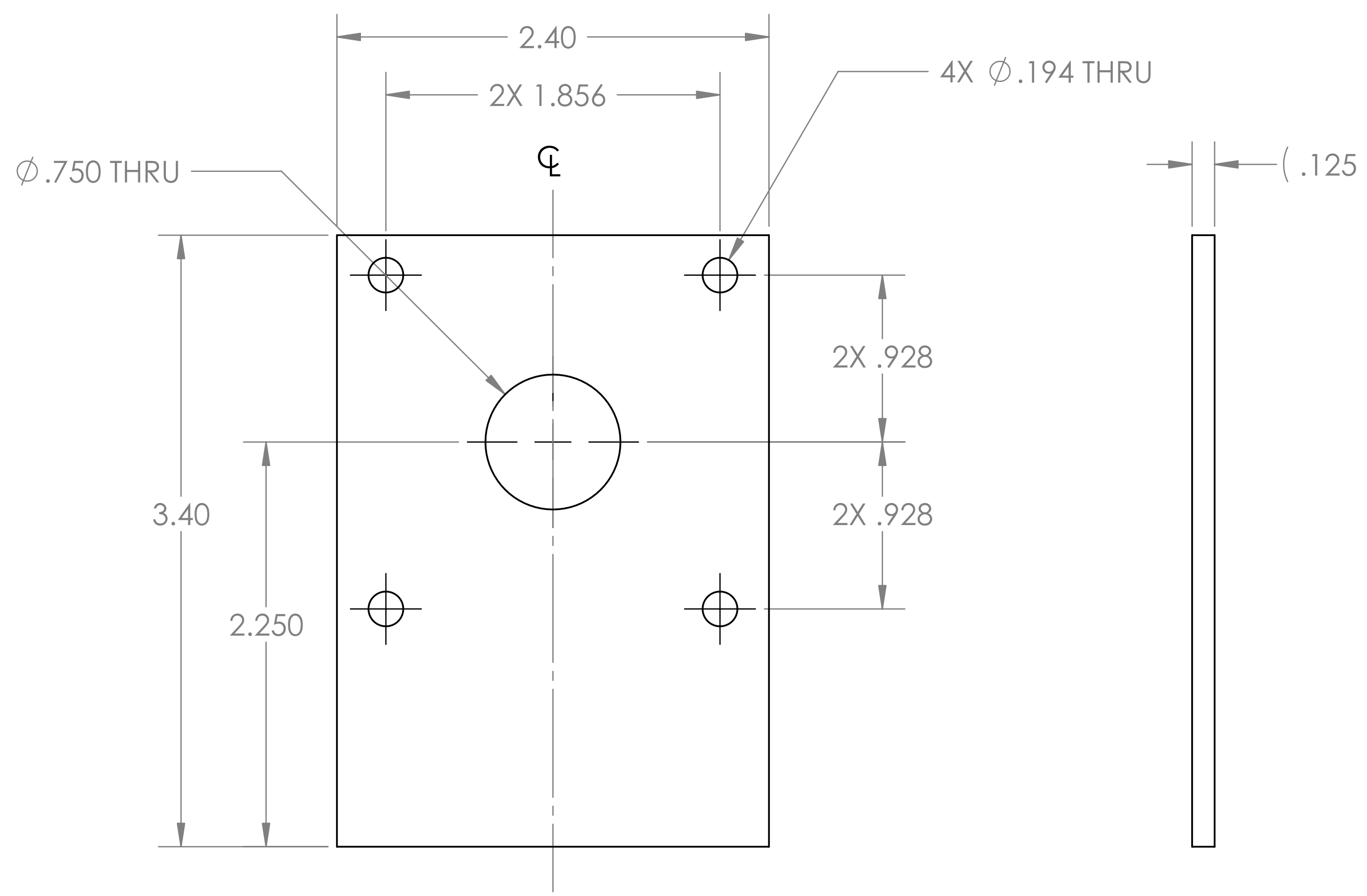

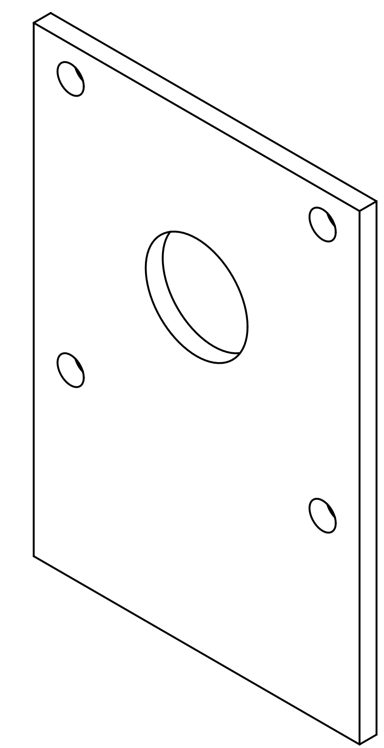

ISOMETRIC VIEW

PROPRIETARY AND CONFIDENTIAL

THE INFORMATION CONTAINED IN THIS DRAWING IS THE SOLE PROPERTY OF THE UNIVERSITY OF ARIZONA. ANY REPRODUCTION IN PART OR AS A WHOLE WITHOUT THE WRITTEN PERMISSION OF THE UNIVERSITY OF ARIZONA IS PROHIBITED.

UNLESS OTHERWISE SPECIFIED:

DIMENSIONS ARE IN INCHES
TOLERANCES:
ANGULAR: X°±1° X.X±0.5°
TWO PLACE DECIMAL ±.010"
THREE PLACE DECIMAL ±.005"

INTERPRET DRAWING IAWASME Y14.5M-1994 OR LATER.

DO NOT SCALE DRAWING

	NAME	DATE
DRAWN	N.W.	02/26/09
CHECKED	K.M.	02/28/09
ENG APPR.		
MFG APPR.		
Q.A.		

COMMENTS:

TITLE:

BRACKET, GEARBOX MOUNT

SIZE	DWG. NO.	REV
B	3679-0007	1

SCALE: 1:1 SHEET 1 OF 1

NOTES, UNLESS OTHERWISE SPECIFIED.

1. MATERIAL: 5052-H32 ALUMINUM SHEET PER AMS-QQ-A-250-8, 0.040" THICK.
2. FINISH: 100% WHITE POWDER COAT EXTERIOR SURFACES AS INDICATED BY FLAGNOTE 7.
3. PART IS TO BE FREE FROM BURRS, SHARP EDGES, AND OTHER VISUAL DEFECTS.
4. THROUGH HOLE CENTERLINES ARE SPACED AT THE ANGLES INDICATED. IF HOLES ARE DRILLED IN FLAT PATTERN, HOLE ELONGATION POST-BENDING IS PERMISSIBLE.
5. STEP BENDS PERMISSIBLE FOR THE RADIUS INDICATED.
6. INSTALL PEM P/N LAC-440-1MD PER PEM SPECIFICATIONS WHERE INDICATED.
7. COMPLETELY POWDER COAT INDICATED SURFACES. NO PAINT ALLOWED IN THREADS. NO OVERSPRAY PERMISSIBLE ON INTERIOR SURFACES.
8. FILLET RADIUS IS 0.25". POST-BENDING FILLET ELONGATION IS PERMISSIBLE.
9. PART IS SYMMETRIC ABOUT CENTERLINE.
10. DIMENSIONS IN ( ) ARE FOR REFERENCE ONLY.

REVISIONS

REV.	DESCRIPTION	DATE
1	INITIAL ENGINEERING RELEASE	03/05/09

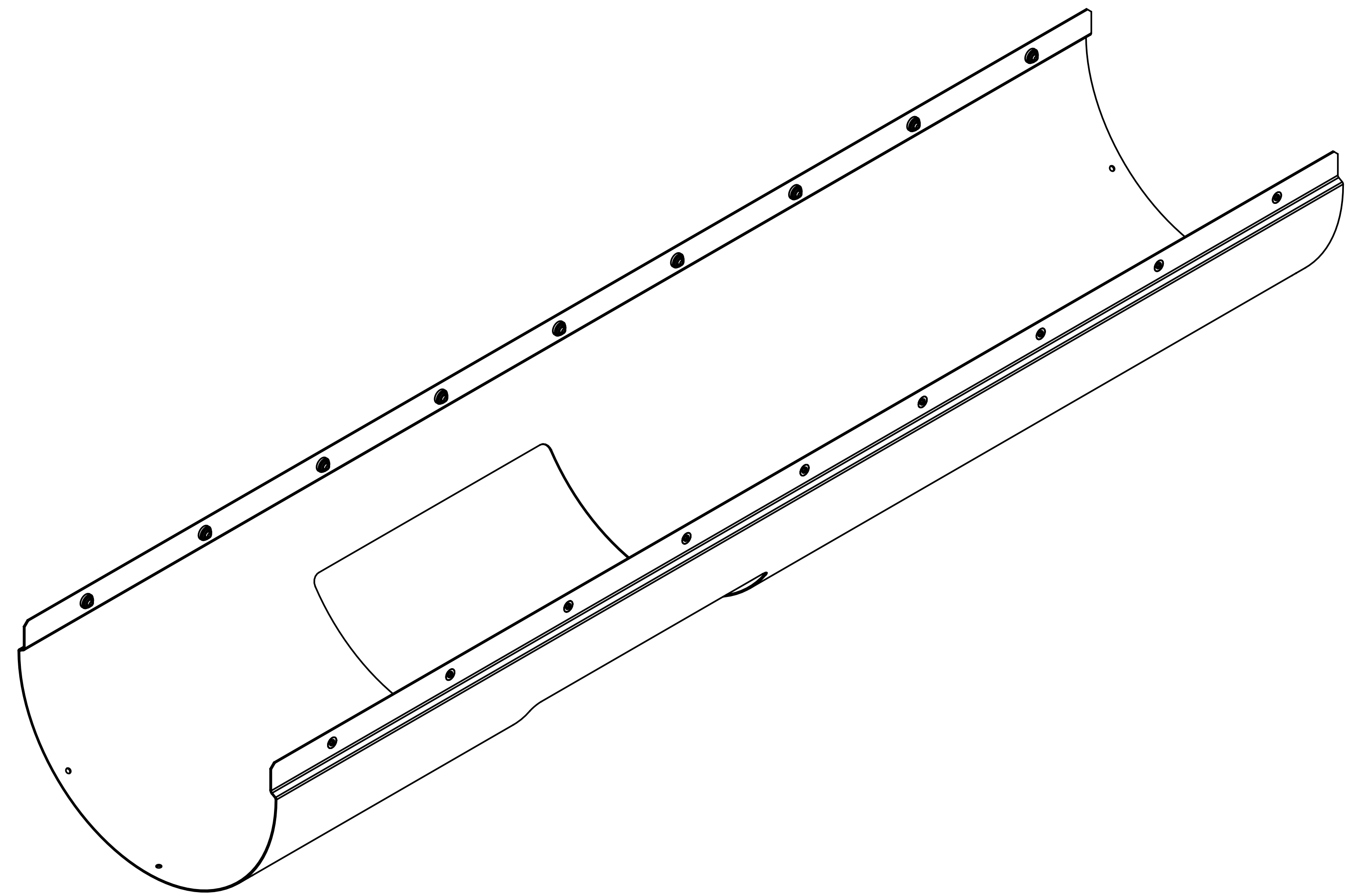

ISOMETRIC VIEW

UNLESS OTHERWISE SPECIFIED:

DIMENSIONS ARE IN INCHES
TOLERANCES:
ANGULAR: X°±1° X.X±0.5°
TWO PLACE DECIMAL ±.010"
THREE PLACE DECIMAL ±.005"

INTERPRET DRAWING IAWASME Y14.5M-1994 OR LATER.

DO NOT SCALE DRAWING

	NAME	DATE
DRAWN	NW	090303
CHECKED	CB	090304
ENG APPR.		
MFG APPR.		
Q.A.		

COMMENTS:

TITLE:

SHELL, BOTTOM

SIZE	DWG. NO.	REV
B	3679-0008	1

SCALE: 1:4

SHEET 1 OF 3

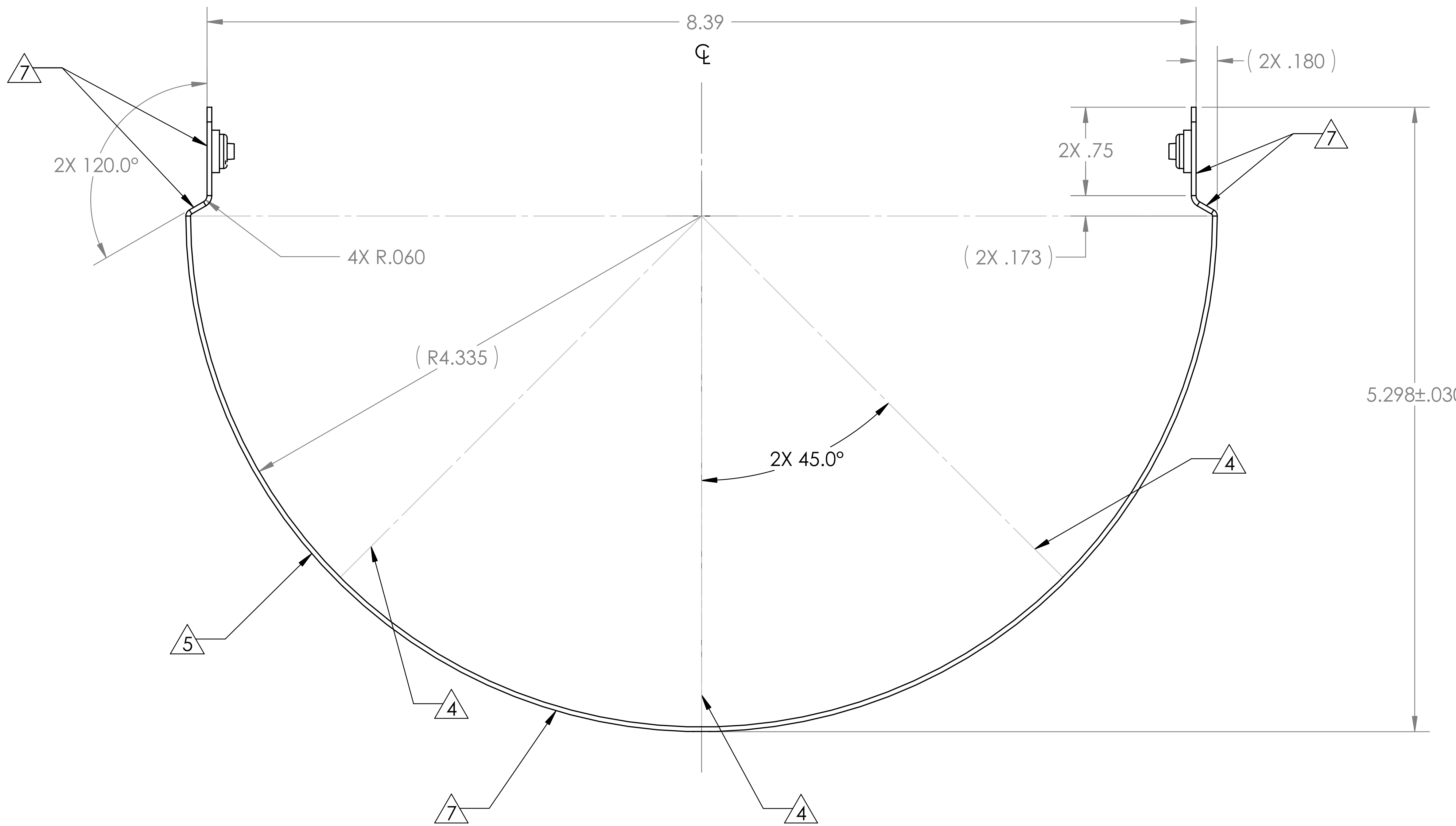

PROPRIETARY AND CONFIDENTIAL

DO NOT SCALE DRAWING

TITLE:

SHELL, BOTTOM

SIZE **B** DWG. NO. 3679-0008 REV 1

SCALE: 1:1 SHEET 2 OF 3

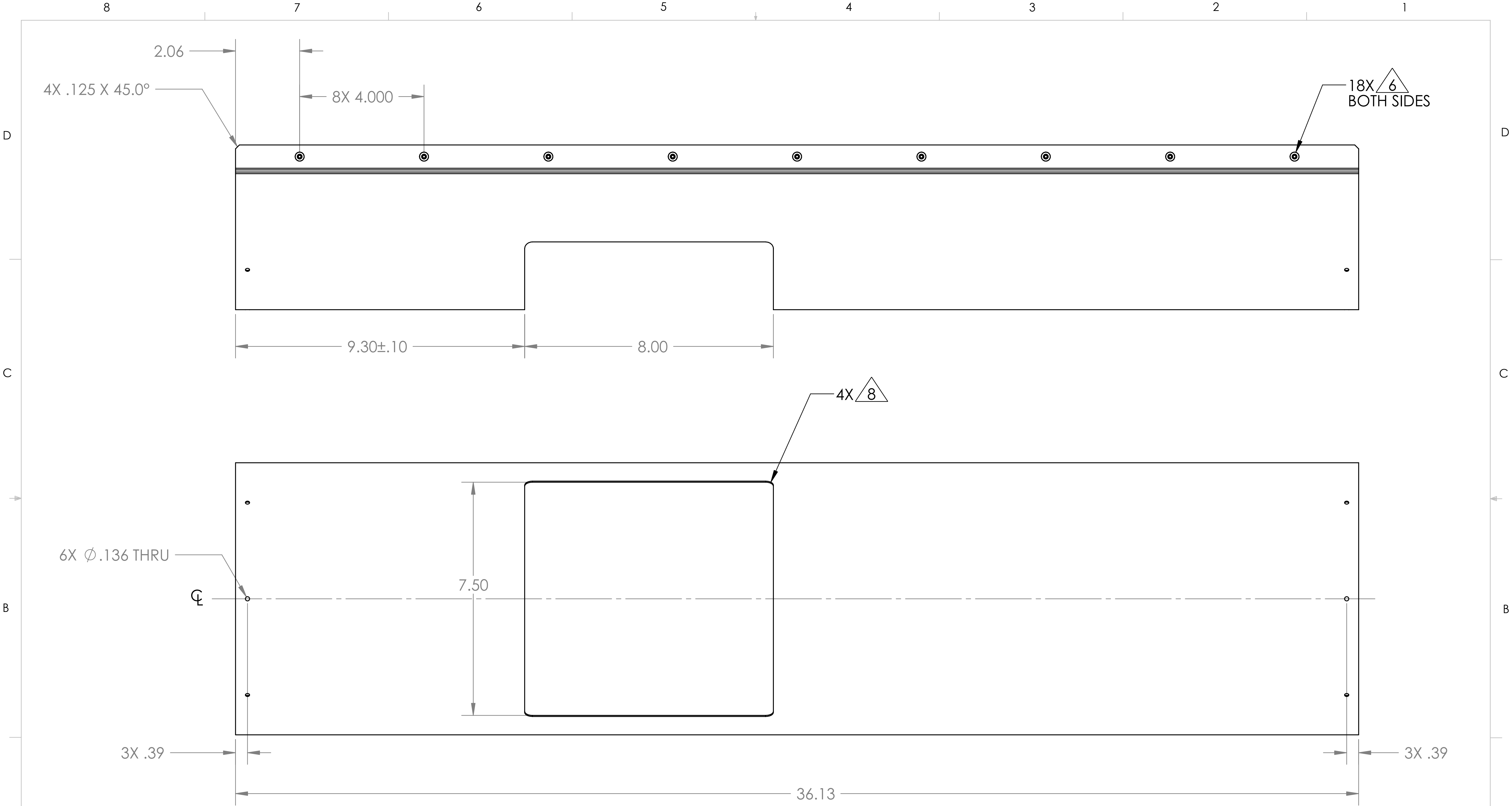

PROPRIETARY AND CONFIDENTIAL

THE INFORMATION CONTAINED IN THIS DRAWING IS THE SOLE PROPERTY OF THE UNIVERSITY OF ARIZONA. ANY REPRODUCTION IN PART OR AS A WHOLE WITHOUT THE WRITTEN PERMISSION OF THE UNIVERSITY OF ARIZONA IS PROHIBITED.

DO NOT SCALE DRAWING

TITLE: SHELL, BOTTOM

SIZE	DWG. NO.	REV
B	3679-0008	1

SCALE: 1:3 | SHEET 3 OF 3

NOTES, UNLESS OTHERWISE SPECIFIED.

1. MATERIAL: 5052-H32 ALUMINUM SHEET PER AMS-QQ-A-250-8, 0.040" THICK.
2. FINISH: 100% WHITE POWDER COAT ENTIRE PART. NO PAINT ALLOWED IN THREADS.
3. BENDS: R.06 X 90° TYPICAL.
4. PART IS TO BE FREE FROM BURRS, SHARP EDGES, AND OTHER VISUAL DEFECTS.
5. INSTALL PEM P/N LAC-440-1MD PER PEM SPECIFICATIONS WHERE INDICATED.
6. TAB CENTERLINES ARE SPACED AT THE ANGLES INDICATED.
7. BEND RELIEFS SHOWN ARE FOR REFERENCE ONLY. ALL RELIEFS SHALL BE RECTANGULAR IN SHAPE AND 0.05" WIDE, MAX.
8. PART IS SYMMETRIC ABOUT CENTERLINE.
9. DIMENSIONS IN ( ) ARE FOR REFERENCE ONLY.

REVISIONS		
REV.	DESCRIPTION	DATE
1	INITIAL ENGINEERING RELEASE	03/05/09

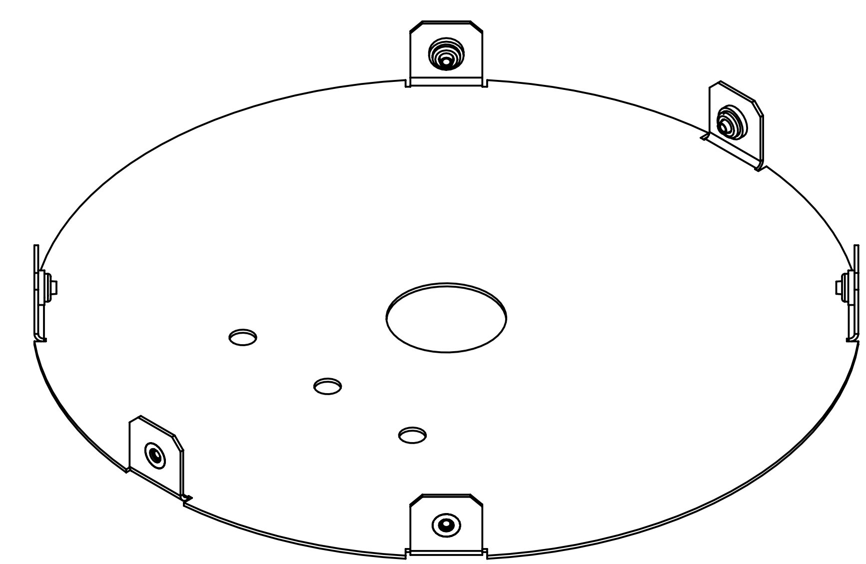

ISOMETRIC VIEW

UNLESS OTHERWISE SPECIFIED:

DIMENSIONS ARE IN INCHES
TOLERANCES:
ANGULAR: X°±1° X.X±0.5°
TWO PLACE DECIMAL ±.010"
THREE PLACE DECIMAL ±.005"

INTERPRET DRAWING IAWASME Y14.5M-1994 OR LATER.

DO NOT SCALE DRAWING

	NAME	DATE
DRAWN	NW	090303
CHECKED	CB	090304
ENG APPR.		
MFG APPR.		
Q.A.		

COMMENTS:

TITLE:

SHELL, FRONT

SIZE B | DWG. NO. 3679-0009 | REV 1

SCALE: 1:2 | SHEET 1 OF 2

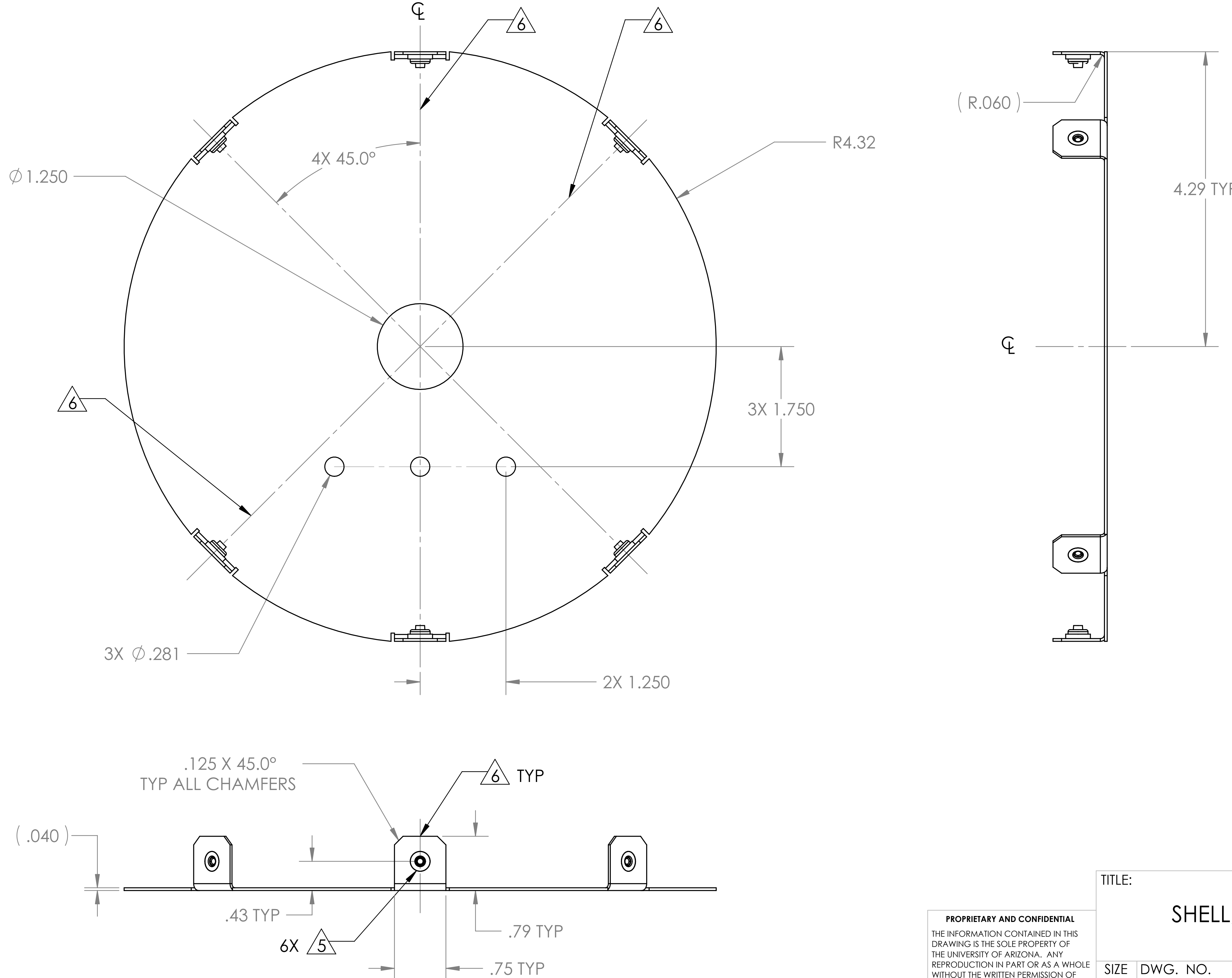

PROPRIETARY AND CONFIDENTIAL

THE INFORMATION CONTAINED IN THIS DRAWING IS THE SOLE PROPERTY OF THE UNIVERSITY OF ARIZONA. ANY REPRODUCTION IN PART OR AS A WHOLE WITHOUT THE WRITTEN PERMISSION OF THE UNIVERSITY OF ARIZONA IS PROHIBITED.

DO NOT SCALE DRAWING

TITLE: SHELL, FRONT

SIZE	DWG. NO.	REV
B	3679-0009	1
SCALE: 2:3		SHEET 2 OF 2

NOTES, UNLESS OTHERWISE SPECIFIED.

1. MATERIAL: 5052-H32 ALUMINUM SHEET PER AMS-QQ-A-250-8, 0.040" THICK.
2. FINISH: 100% WHITE POWDER COAT ENTIRE PART. NO PAINT ALLOWED IN THREADS.
3. BENDS: R.06 X 90° TYPICAL.
4. PART IS TO BE FREE FROM BURRS, SHARP EDGES, AND OTHER VISUAL DEFECTS.
5. INSTALL PEM P/N LAC-440-1MD PER PEM SPECIFICATIONS WHERE INDICATED.
6. TAB CENTERLINES ARE SPACED AT THE ANGLES INDICATED.
7. BEND RELIEFS SHOWN ARE FOR REFERENCE ONLY. ALL RELIEFS SHALL BE RECTANGULAR IN SHAPE AND 0.05" WIDE, MAX.
8. PART IS SYMMETRIC ABOUT CENTERLINE.
9. DIMENSIONS IN ( ) ARE FOR REFERENCE ONLY.

REVISIONS		
REV.	DESCRIPTION	DATE
1	INITIAL ENGINEERING RELEASE	03/05/09

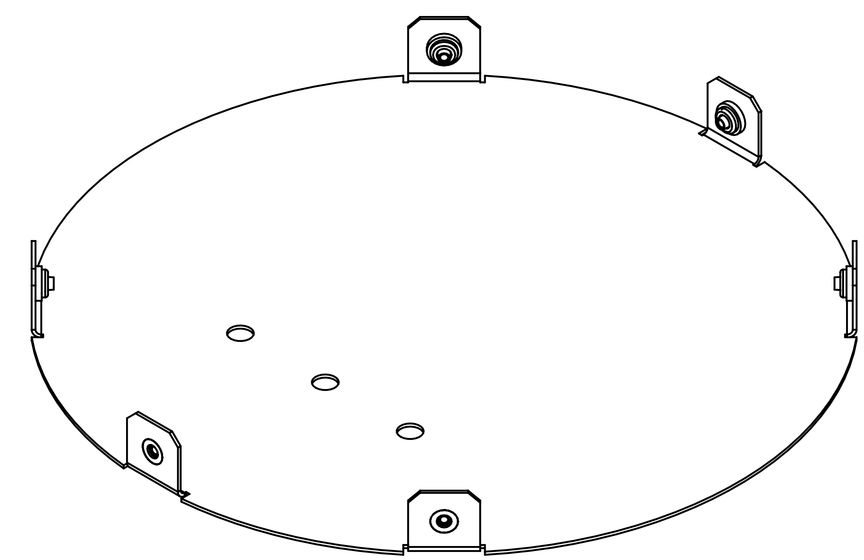

ISOMETRIC VIEW

UNLESS OTHERWISE SPECIFIED:

DIMENSIONS ARE IN INCHES
TOLERANCES:
ANGULAR: X°±1° X.X±0.5°
TWO PLACE DECIMAL ±.010"
THREE PLACE DECIMAL ±.005"

INTERPRET DRAWING IAWASME Y14.5M-1994 OR LATER.

DO NOT SCALE DRAWING

	NAME	DATE
DRAWN	NW	090303
CHECKED	CB	090304
ENG APPR.		
MFG APPR.		
Q.A.		

COMMENTS:

TITLE:

SHELL, REAR

SIZE	DWG. NO.	REV
B	3679-0010	1

SCALE: 1:2 SHEET 1 OF 2

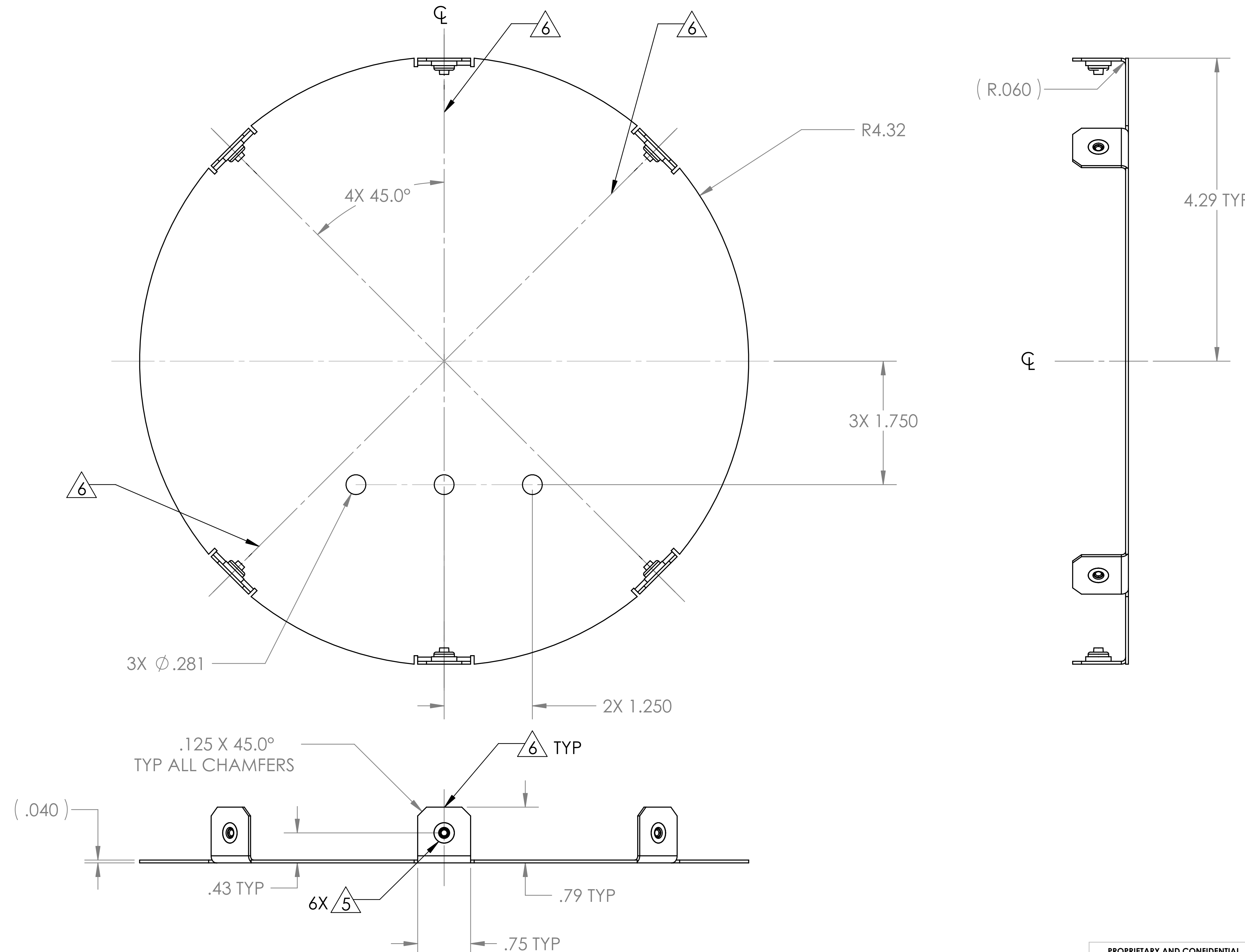

PROPRIETARY AND CONFIDENTIAL

THE INFORMATION CONTAINED IN THIS DRAWING IS THE SOLE PROPERTY OF THE UNIVERSITY OF ARIZONA. ANY REPRODUCTION IN PART OR AS A WHOLE WITHOUT THE WRITTEN PERMISSION OF THE UNIVERSITY OF ARIZONA IS PROHIBITED.

DO NOT SCALE DRAWING

TITLE: SHELL, REAR		
SIZE: B	DWG. NO. 3679-0010	REV 1
SCALE: 2:3		SHEET 2 OF 2

NOTES, UNLESS OTHERWISE SPECIFIED.

1. MATERIAL:
   BASE: ALUMINUM ALLOY 6061 PER AMS-QQ-A-225/8, 0.25 IN THICK.
   TUBE: ALUMINUM ALLOY 6061 PER AMS-QQ-A-225/8, 4.5 IN OD.
2. FINISH: NONE.
3. BREAK ALL SHARP EDGES, R.03 MAX.
4. PART IS TO BE FREE FROM BURRS, SHARP EDGES, AND OTHER VISUAL DEFECTS.
5. WELD TUBE EDGE INDICATED TO BASE SUCH THAT TUBE CENTER AXIS COINCIDES WITH BASE CENTER POINT. GMAW WELDS MAY BE SUBSTITUTED FOR GTAW WELDS WHERE DEEMED NECESSARY.
6. TUBE HOLE CENTERLINES ARE ORIENTED AS SHOWN. PERMISSIBLE TO WELD TUBE SUCH THAT HOLES ARE ROTATED 90° FROM ORIENTATION SHOWN IN ISOMETRIC VIEW.
7. PART IS SYMMETRIC ABOUT CENTERLINE.
8. DIMENSIONS IN ( ) ARE FOR REFERENCE ONLY.

REVISIONS		
REV.	DESCRIPTION	DATE
1	INITIAL ENGINEERING RELEASE	03/24/09

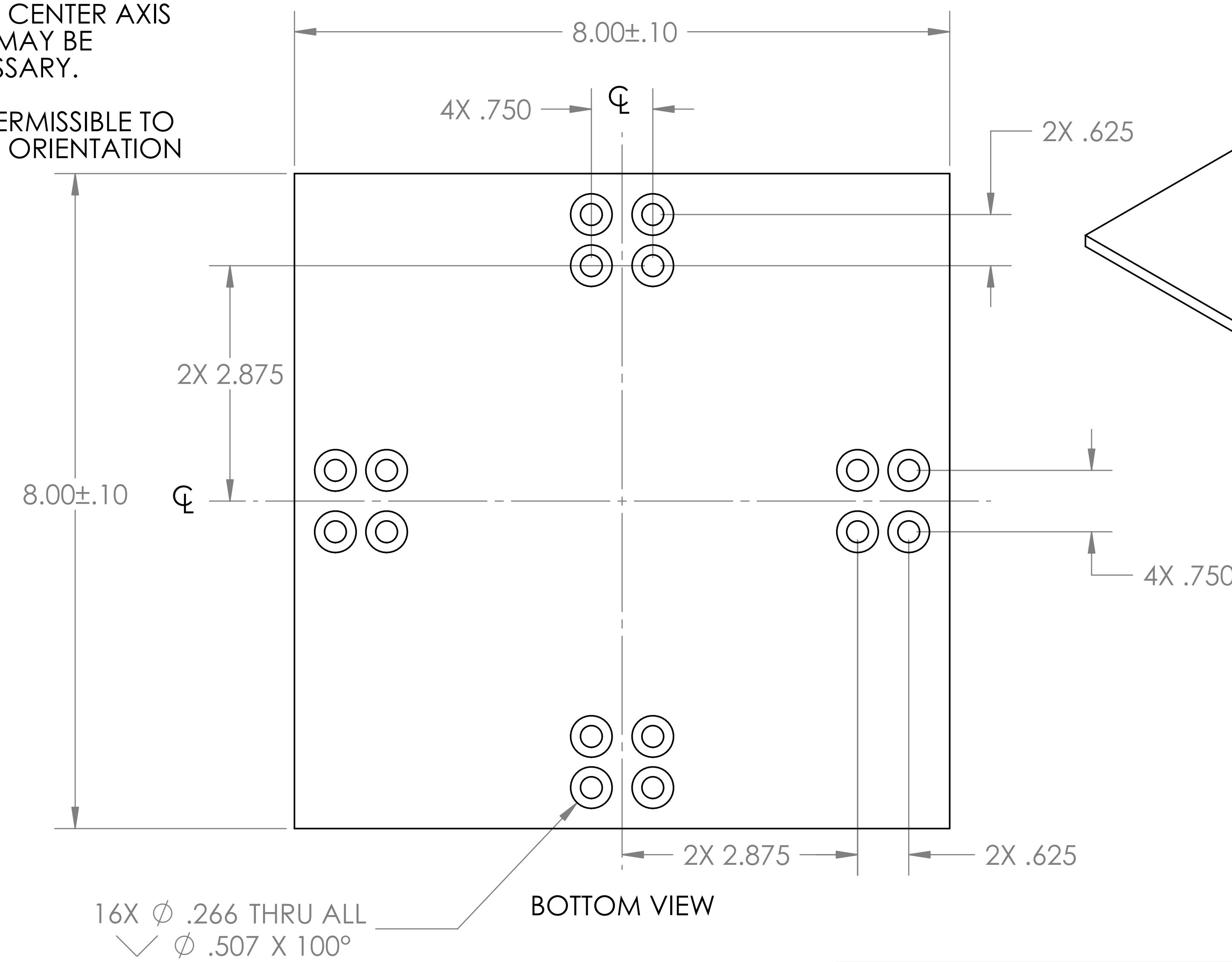

BOTTOM VIEW

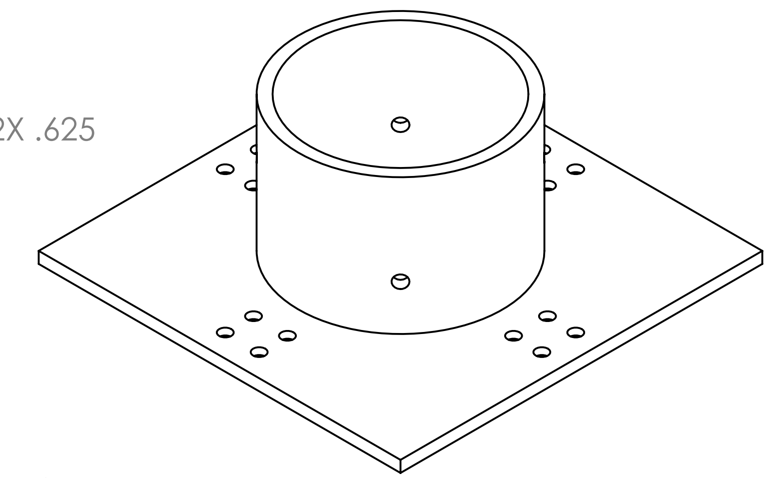

ISOMETRIC VIEW
SCALE 1:3

UNLESS OTHERWISE SPECIFIED:		NAME	DATE
DIMENSIONS ARE IN INCHES TOLERANCES: ANGULAR: X°±1° X.X±0.5° TWO PLACE DECIMAL ±.010" THREE PLACE DECIMAL ±.005"	DRAWN	N.W.	03/23/09
	CHECKED	F.A.M.	03/24/09
	ENG APPR.		
INTERPRET DRAWING IAWASME Y14.5M-1994 OR LATER.	MFG APPR.		
	Q.A.		
DO NOT SCALE DRAWING	COMMENTS:		

TITLE: BRACKET, BASE

SIZE	DWG. NO.	REV
B	3679-0011	1
SCALE: 1:2		SHEET 1 OF 2

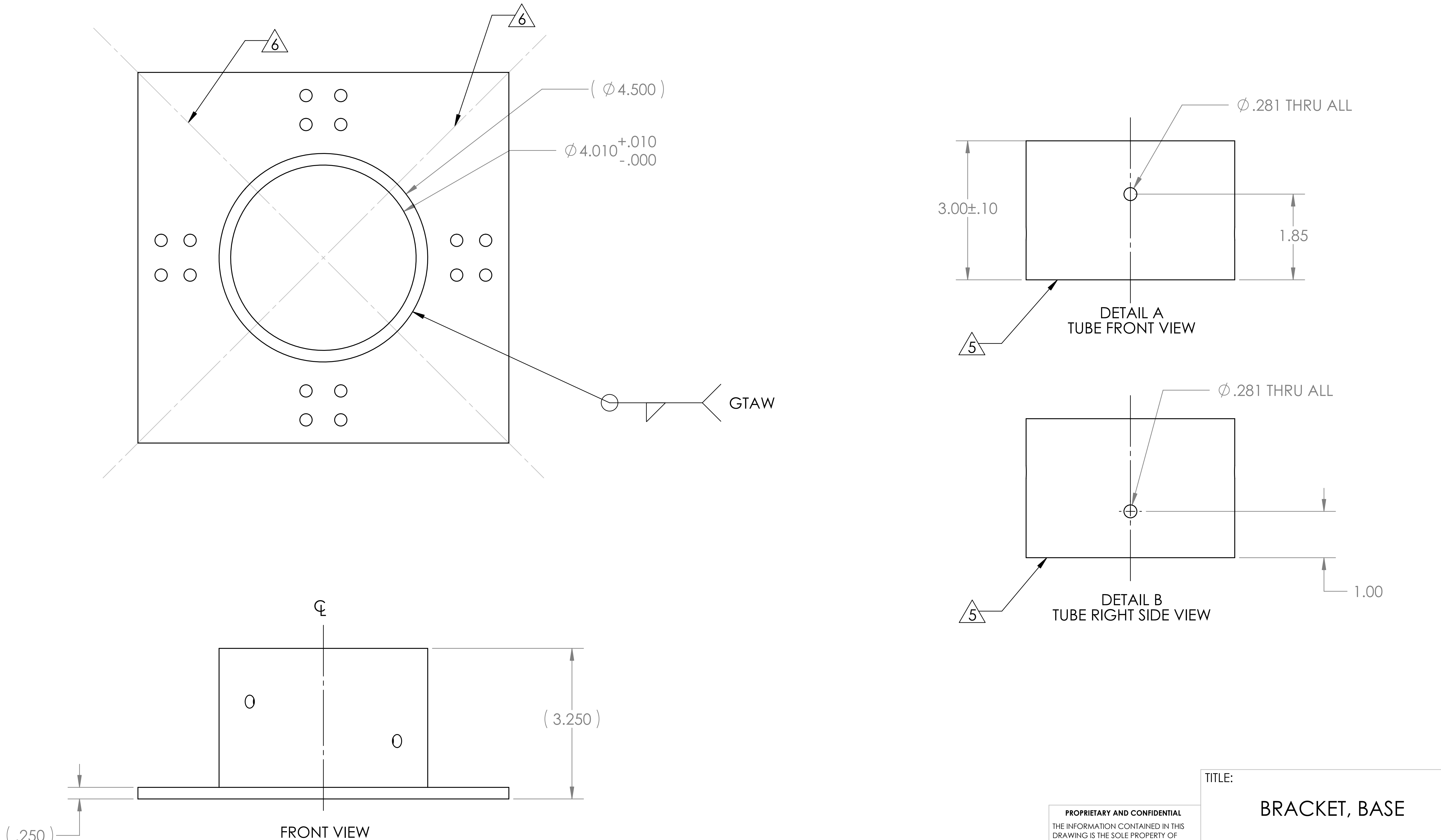

PROPRIETARY AND CONFIDENTIAL

THE INFORMATION CONTAINED IN THIS DRAWING IS THE SOLE PROPERTY OF THE UNIVERSITY OF ARIZONA. ANY REPRODUCTION IN PART OR AS A WHOLE WITHOUT THE WRITTEN PERMISSION OF THE UNIVERSITY OF ARIZONA IS PROHIBITED.

DO NOT SCALE DRAWING

TITLE: BRACKET, BASE		
SIZE **B**	DWG. NO. 3679-0011	REV 1
SCALE: 1:2		SHEET 2 OF 2

NOTES, UNLESS OTHERWISE SPECIFIED.

1. MATERIAL: ALUMINUM ALLOY 6061 PER AMS-QQ-A-250/11 OR EQUIVALENT.
2. FINISH: NONE.
3. PART IS TO BE FREE FROM BURRS, SHARP EDGES, OR OTHER VISUAL DEFECTS.
4. PART IS SYMMETRIC ABOUT CENTERLINES.
5. DIMENSIONS IN ( ) ARE FOR REFERENCE ONLY.

REVISIONS		
REV.	DESCRIPTION	DATE
1	INITIAL ENGINEERING RELEASE	03/05/09

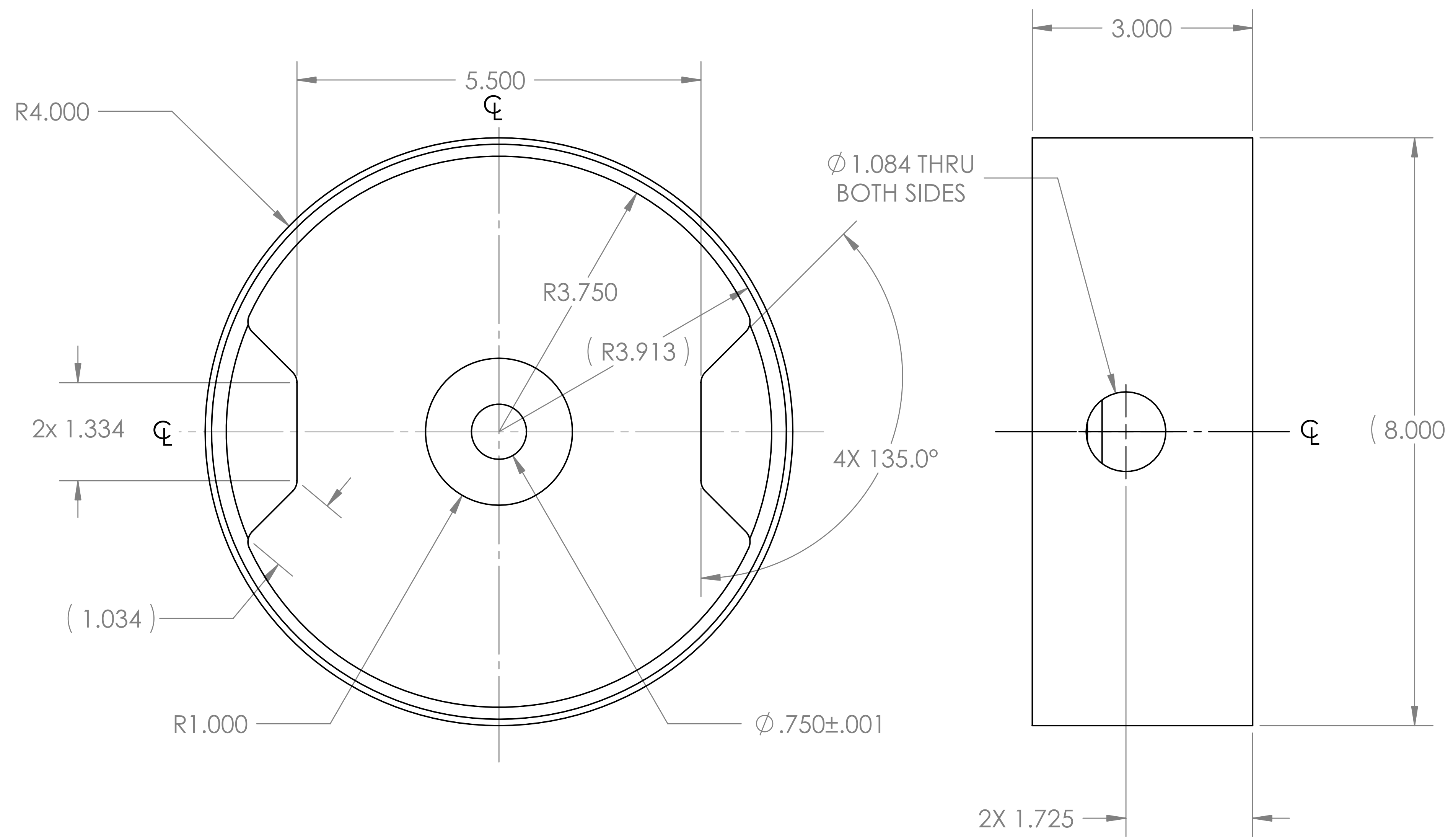

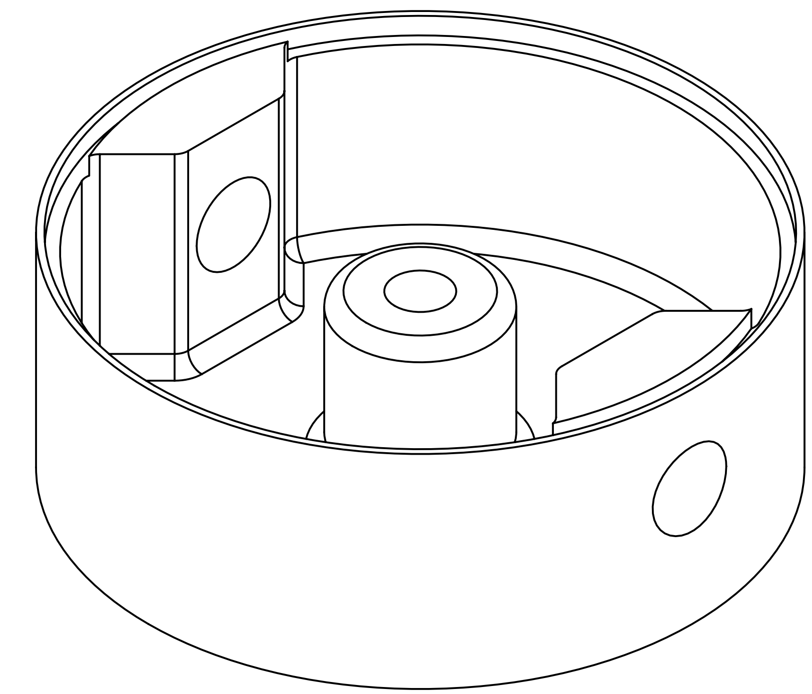

ISOMETRIC VIEW

PROPRIETARY AND CONFIDENTIAL

THE INFORMATION CONTAINED IN THIS DRAWING IS THE SOLE PROPERTY OF THE UNIVERSITY OF ARIZONA. ANY REPRODUCTION IN PART OR AS A WHOLE WITHOUT THE WRITTEN PERMISSION OF THE UNIVERSITY OF ARIZONA IS PROHIBITED.

UNLESS OTHERWISE SPECIFIED:

DIMENSIONS ARE IN INCHES
TOLERANCES:
ANGULAR: X°±1° X.X±0.5°
TWO PLACE DECIMAL ±.010"
THREE PLACE DECIMAL ±.005"

INTERPRET DRAWING IAWASME Y14.5M-1994 OR LATER.

DO NOT SCALE DRAWING

	NAME	DATE
DRAWN	CP	090303
CHECKED	NW	090304
ENG APPR.		
MFG APPR.		
Q.A.		

COMMENTS:

TITLE:

HUB, MAIN

SIZE	DWG. NO.	REV
B	3679-0012	1

SCALE: 1:2 SHEET 1 OF 2

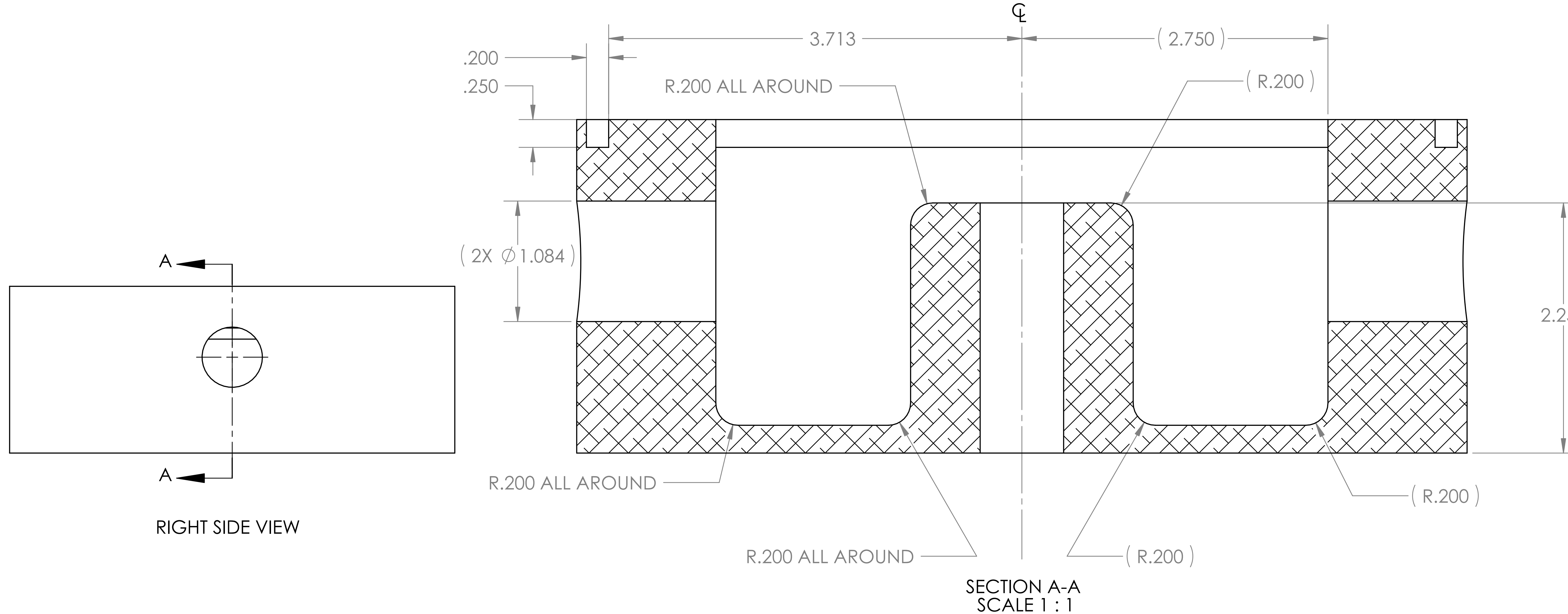

TITLE: HUB, MAIN

SIZE	DWG. NO.	REV
B	3679-0012	1

SCALE: 1:2 | SHEET 2 OF 2

NOTES, UNLESS OTHERWISE SPECIFIED.

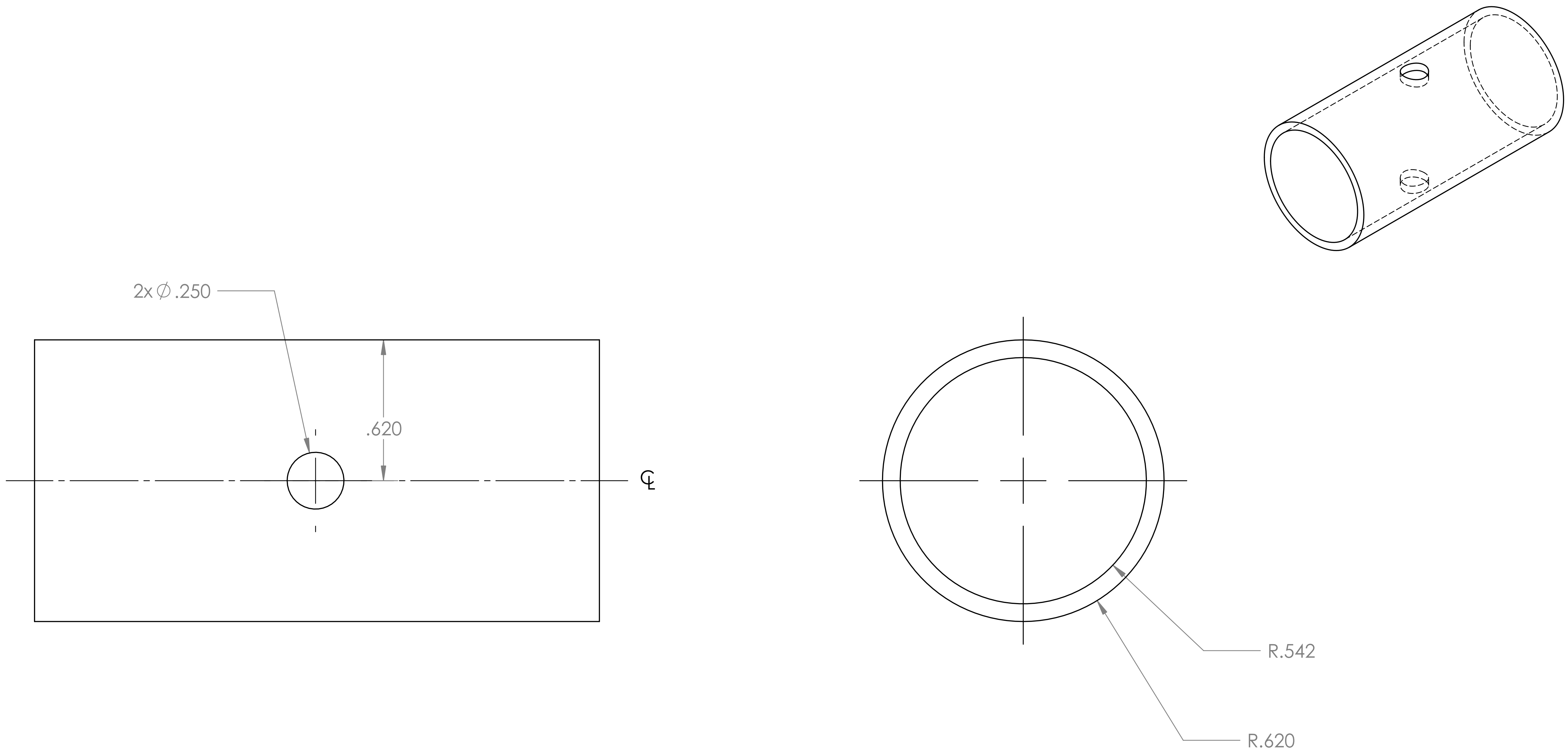

PROPRIETARY AND CONFIDENTIAL

THE INFORMATION CONTAINED IN THIS DRAWING IS THE SOLE PROPERTY OF THE UNIVERSITY OF ARIZONA. ANY REPRODUCTION IN PART OR AS A WHOLE WITHOUT THE WRITTEN PERMISSION OF THE UNIVERSITY OF ARIZONA IS PROHIBITED.

UNLESS OTHERWISE SPECIFIED:

DIMENSIONS ARE IN INCHES
TOLERANCES:
ANGULAR: X°±1° X.X±0.5°
TWO PLACE DECIMAL ±.010"
THREE PLACE DECIMAL ±.005"

INTERPRET DRAWING IAWASME Y14.5M-1994 OR LATER.

DO NOT SCALE DRAWING

	NAME	DATE
DRAWN		
CHECKED		
ENG APPR.		
MFG APPR.		
Q.A.		

COMMENTS:

TITLE:

Root Tube

SIZE	DWG. NO.	REV
B	3679-0022	

SCALE: 1:1 SHEET 1 OF 1

NOTES, UNLESS OTHERWISE SPECIFIED.

1. MATERIAL: ALUMINUM ALLOY 6061 PER AMS-QQ-A-250/11 OR EQUIVALENT.
2. FINISH: NONE.
3. PART IS TO BE FREE FROM BURRS, SHARP EDGES, OR OTHER VISUAL DEFECTS.
4. PART IS SYMMETRIC ABOUT CENTERLINES.
5. DIMENSIONS IN ( ) ARE FOR REFERENCE ONLY.

REVISIONS		
REV.	DESCRIPTION	DATE
1	INITIAL ENGINEERING RELEASE	03/24/09

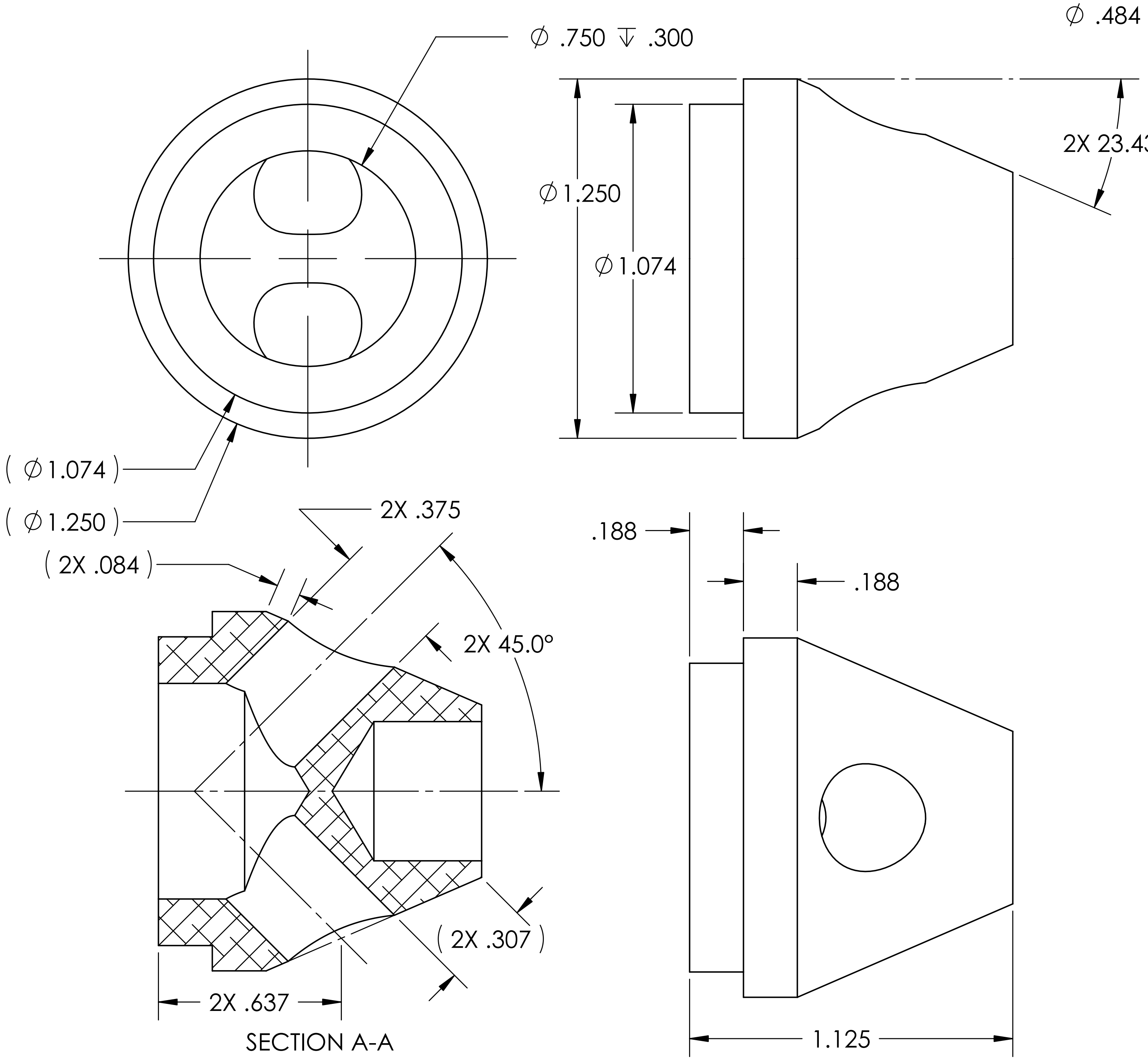

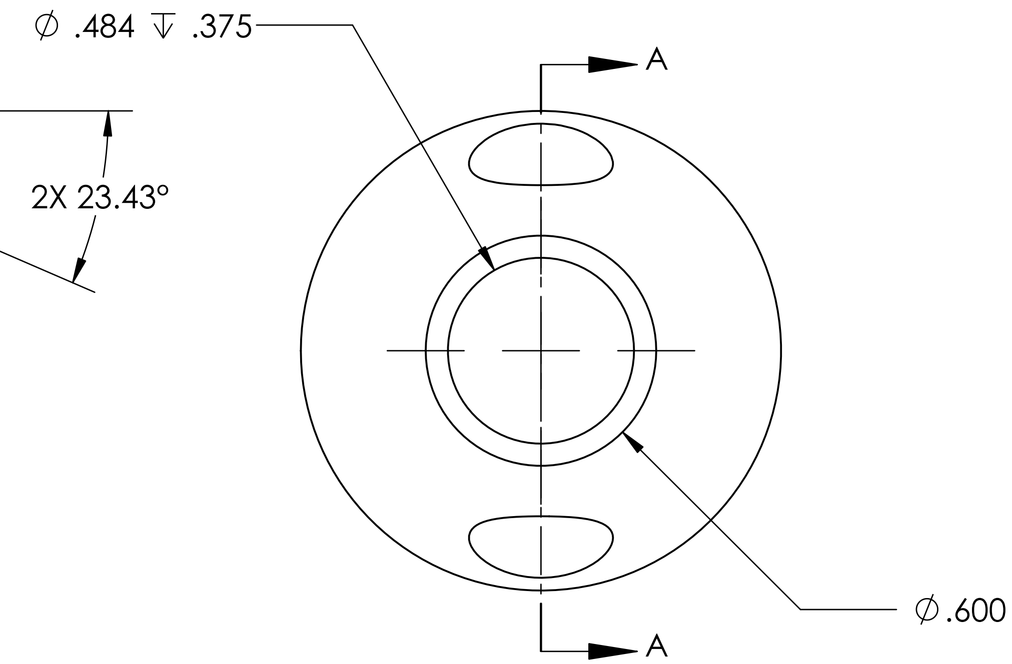

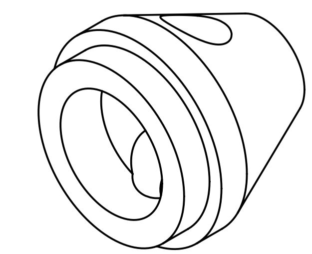

ISOMETRIC VIEW
SCALE 1:1

UNLESS OTHERWISE SPECIFIED:		NAME	DATE
DIMENSIONS ARE IN INCHES TOLERANCES: ANGULAR: X°±1° X.X±0.5° TWO PLACE DECIMAL ±.010" THREE PLACE DECIMAL ±.005" INTERPRET DRAWING IAWASME Y14.5M-1994 OR LATER.	DRAWN	C.P.	03/03/09
	CHECKED	N.W.	03/24/09
	ENG APPR.		
	MFG APPR.		
	Q.A.		
DO NOT SCALE DRAWING	COMMENTS:		

TITLE:

COUPLER, SPAR

SIZE	DWG. NO.	REV
B	3679-0014	1
SCALE: 2:1		SHEET 1 OF 1

NOTES, UNLESS OTHERWISE SPECIFIED.

1. MATERIAL: LOW-CARBON STEEL TUBE PER ASTM A513 OR EQUIVALENT, 4.0" OD, 3.76" ID. PERMISSIBLE TO MAKE FROM MCMASTER-CARR P/N 7767T49.
2. FINISH: NONE.
3. PART IS TO BE FREE FROM BURRS, SHARP EDGES, AND OTHER VISUAL DEFECTS.
4. PART IS SYMMETRIC ABOUT CENTERLINES.
5. DIMENSIONS IN ( ) ARE FOR REFERENCE ONLY.

REVISIONS		
REV.	DESCRIPTION	DATE
1	INITIAL ENGINEERING RELEASE	03/07/09

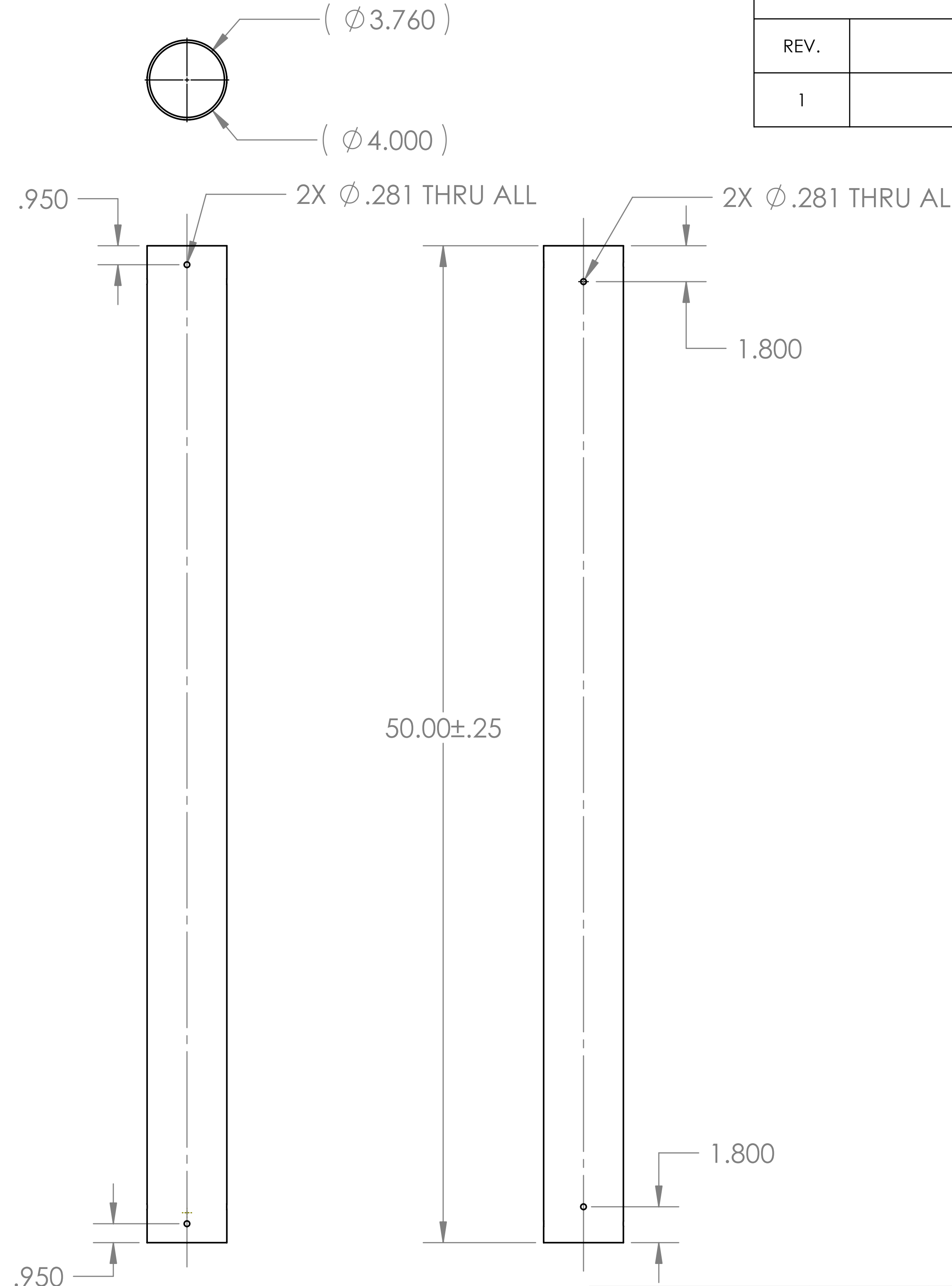

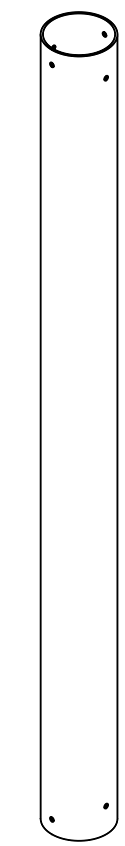

ISOMETRIC VIEW
SCALE 1:10

UNLESS OTHERWISE SPECIFIED:

DIMENSIONS ARE IN INCHES
TOLERANCES:
ANGULAR: X°±1° X.X±0.5°
TWO PLACE DECIMAL ±.010"
THREE PLACE DECIMAL ±.005"

INTERPRET DRAWING IAWASME Y14.5M-1994 OR LATER.

DO NOT SCALE DRAWING

	NAME	DATE
DRAWN	N.W.	03/05/09
CHECKED	F.A.M.	03/07/09
ENG APPR.		
MFG APPR.		
Q.A.		

COMMENTS:

TITLE:

TUBE, TOWER

SIZE	DWG. NO.	REV
B	3679-0015	1

SCALE: 1:8

SHEET 1 OF 1

NOTES, UNLESS OTHERWISE SPECIFIED.

1. MATERIAL: ALUMINUM ALLOY 6061 OR EQUIVALENT.
2. FINISH: NONE.
3. PART IS TO BE FREE FROM BURRS, SHARP EDGES, OR OTHER VISUAL DEFECTS.
4. BREAK SHARP EDGES, R.03 MAX.
5. DIMENSIONS IN ( ) ARE FOR REFERENCE ONLY.

REVISIONS		
REV.	DESCRIPTION	DATE
1	INITIAL ENGINEERING RELEASE	03/24/09

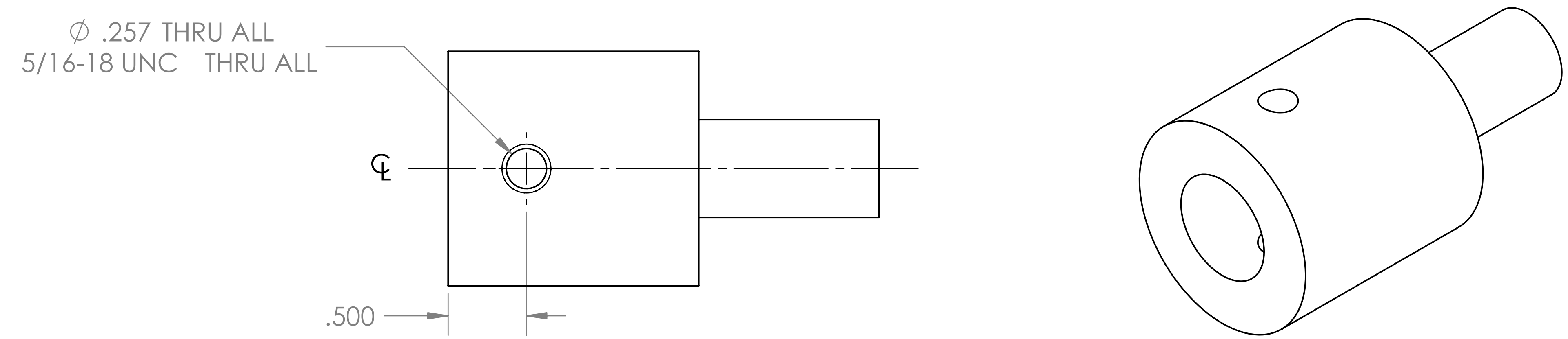

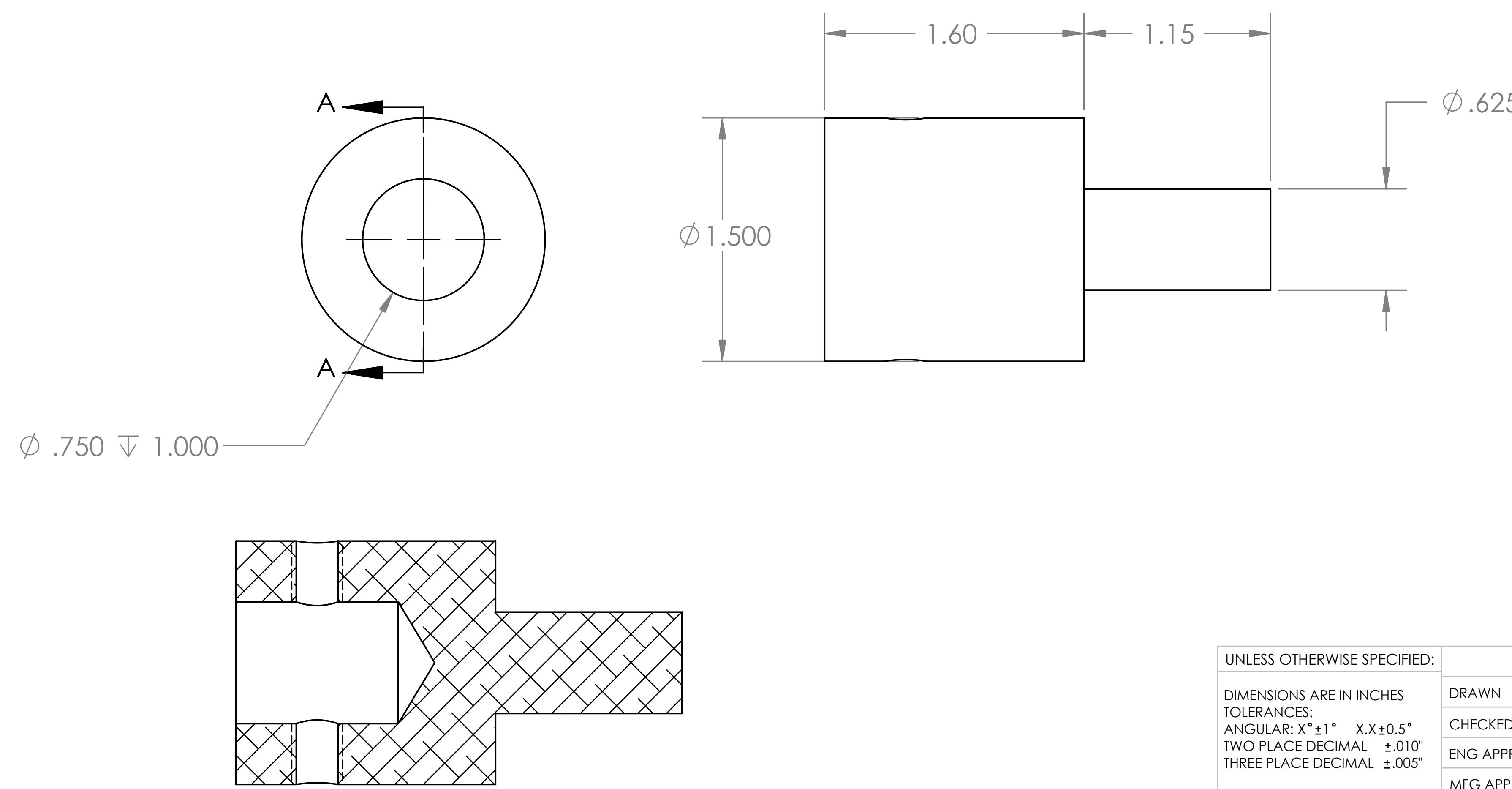

SECTION A-A

PROPRIETARY AND CONFIDENTIAL

THE INFORMATION CONTAINED IN THIS DRAWING IS THE SOLE PROPERTY OF THE UNIVERSITY OF ARIZONA. ANY REPRODUCTION IN PART OR AS A WHOLE WITHOUT THE WRITTEN PERMISSION OF THE UNIVERSITY OF ARIZONA IS PROHIBITED.

UNLESS OTHERWISE SPECIFIED:

DIMENSIONS ARE IN INCHES
TOLERANCES:
ANGULAR: X°±1° X.X±0.5°
TWO PLACE DECIMAL ±.010"
THREE PLACE DECIMAL ±.005"

INTERPRET DRAWING IAWASME Y14.5M-1994 OR LATER.

DO NOT SCALE DRAWING

	NAME	DATE
DRAWN	N.W.	03/23/09
CHECKED	F.A.M.	03/24/09
ENG APPR.		
MFG APPR.		
Q.A.		
COMMENTS:		

TITLE:

COUPLER, GBS

SIZE	DWG. NO.	REV
B	3679-0016	1

SCALE: 1:1 SHEET 1 OF 1

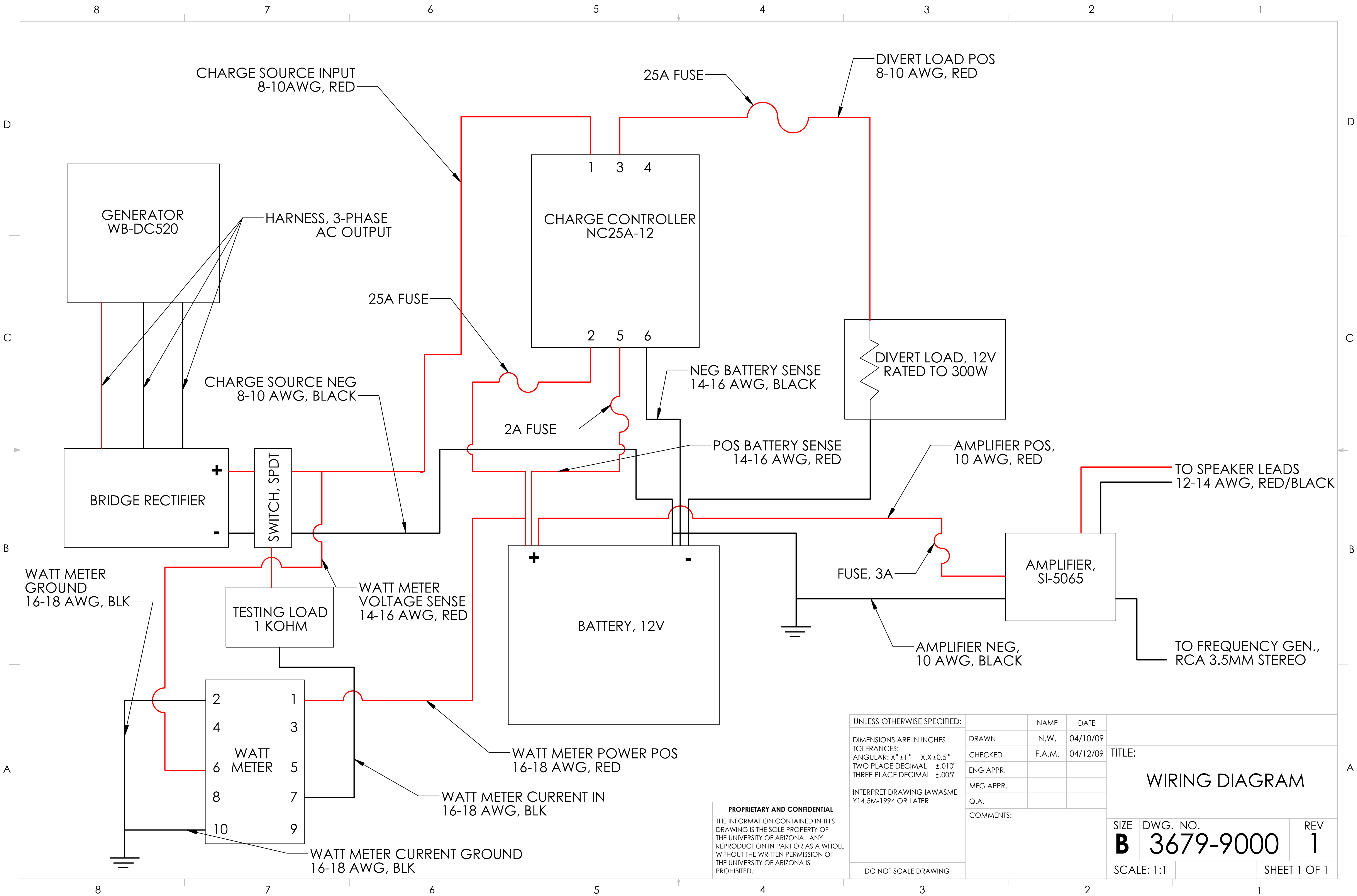

PROPRIETARY AND CONFIDENTIAL

UNLESS OTHERWISE SPECIFIED:

DIMENSIONS ARE IN INCHES
TOLERANCES:
ANGULAR: X°±1° X.X±0.5°
TWO PLACE DECIMAL ±.010"
THREE PLACE DECIMAL ±.005"

INTERPRET DRAWING IAWASME Y14.5M-1994 OR LATER.

DO NOT SCALE DRAWING

	NAME	DATE
DRAWN	N.W.	04/10/09
CHECKED	F.A.M.	04/12/09
ENG APPR.		
MFG APPR.		
Q.A.		

COMMENTS:

TITLE:

WIRING DIAGRAM

SIZE	DWG. NO.	REV
B	3679-9000	1

SCALE: 1:1 SHEET 1 OF 1